Stony Brook University

Role of *tolC* homologs in the virulence of *Francisella tularensis*

A Dissertation Presented

by

Gabrielle Platz

to

The Graduate School

in Partial Fulfillment of the

Requirements for the Degree of

Doctor of Philosophy

in

Genetics

Stony Brook University

August 2009

Stony Brook University
The Graduate School

Gabrielle Platz

We, the dissertation committee for the above candidate for the Doctor of Philosophy Degree, hereby recommend acceptance of this dissertation.

Dr. David G. Thanassi- Dissertation Advisor
Associate Professor, Department of Molecular Genetics and Microbiology

Dr. Jorge Benach- Chairperson of Defense
Professor and Chair, Department of Molecular Genetics and Microbiology
Director, Center for Infectious Disease

Dr. Martha B. Furie
Professor, Department of Pathology

Dr. James B. Bliska
Professor, Department of Molecular Genetics and Microbiology

Dr. Raymond J. Dattwyler
Professor of Medicine and Microbiology and Immunology,
New York Medical College, Valhalla, NY

This Dissertation is accepted by the Graduate School

Lawrence Martin
Dean of Graduate School

Abstract of the Dissertation

Role of *tolC* homologs in the virulence of *Francisella tularensis*

by

Gabrielle Platz

Doctor of Philosophy

in

Genetics

Stony Brook University

2009

Francisella tularensis is the causative agent of tularemia. There are five subspecies of *F. tularensis,* three that are pathogenic to humans. *F. tularensis* subsp. *tularensis* is extremely pathogenic and sometimes fatal. *F. tularensis* subsp. *holarctica* causes a less severe disease. The live vaccine strain (LVS) is derived from a *holarctica* strain and retains virulence in the mouse. *F. tularensis* subsp. *novicida* causes disease in immunocompromised persons. *F. tularensis* is classified as a Category A agent of

bioterrorism by the Centers for Disease Control due to its low infectious dose, ease of aerosol dissemination and capacity to cause high morbidity and mortality.

F. tularensis is a Gram-negative, intracellular pathogen. Gram-negative bacteria have two cellular membranes, making it necessary for the development of highly sophisticated secretion systems. One such pathway is the type I section system (TISS), which functions in both drug efflux and protein secretion. The TISS consists of three proteins: an inner membrane protein, often containing an ATP binding cassette (ABC), a periplasmic protein, and an outer membrane protein (OMP). The TolC protein of *Escherichia coli* represents the canonical T1SS OMP. Genomic evidence supporting the existence of a TISS in *F. tularensis* includes two orthologs of the *E. coli tolC* gene, termed *tolC* and *ftlC*, and 15 putative ABC proteins.

In this dissertation, I constructed *tolC* and *ftlC* deletion mutations in the LVS and investigated the role these genes play in survival and virulence. Antibiotic sensitivity assays revealed that both TolC and FtlC function in drug efflux. However, only TolC was determined to be an essential virulence determinant, as the *tolC* mutant was avirulent in the mouse model and defective in colonizing organs. In vitro analysis revealed that *F. tularensis* actively inhibits host cell death and secretion of proinflammatory cytokines in a TolC-dependent manner. Based on these results, we propose that in the absence of TolC *F. tularensis* induces rapid host cell death and a large proinflammatory response. This causes the bacteria to lose its intracellular replicative niche, and with insufficient bacterial numbers the pathogen is cleared by the increased innate immune response of the host.

Table of Contents

List of Figures and Tables

Acknowledgements

My journey to earning a Ph. D. has not always been easy, nor has it always been straightforward. However, I did get here and now I would like to thank those individuals who made this achievement possible. Most importantly, I would like to thank my advisor Dr. David G. Thanassi. I hope all who read this acknowledgement have had the chance to meet him, but for those of you who have not, let me offer you a short description; David is kind, knowledgeable, patient, supportive and positive. He has guided this work by suggesting great research ideas, and by being supportive of my ideas. In short, David is the type of person who always sees the glass as half full and I thank him from the bottom of my heart for his mentorship over these past five years.

I am also indebted to the wonderful people who work in the Thanassi laboratory. Nadine Henderson and Ken-Michael Bayle have made much of this work possible by the sheer fact that they kept me and the lab well stocked with reagents and equipment. Horacio Gil, the post-doc under who I began this project, taught me so much about experimental technique, time management and the productive side to having more than one experiment going at any given time. Horacio also planned and designed many of the experiments described in Chapter Three, and performed the initial analysis of the TolC homologs and the intradermal mouse infections. To past lab members, Stephane Shu kin So and Lisa Runco, I thank you for all your help and support with the various experimental questions I may have had and for being such good friends. To new lab members, Matt Hatkoff, William McCaig, and Chris Doyle, you've all made the past years fun and I'm sure you'll all do great things in the future, thank you. To my lab-mate

Qin Yuan Li, I want to thank you for your loyal ear, advice, support, and most importantly, your friendship; because of you, I got through some of the more difficult times and I'll never forget your kindness.

I would like to thank DeAnna Bublitz for her contributions to this paper, which include the quantification of chemokines released by human host cells in Chapter Four. I would also like to thank Gloria Monslave for her help in creating the anti-TolC and anti-FtlC antibodies.

I am very excited about moving onto the next chapter in my life but I am equally sad to be leaving the Center for Infectious Diseases, which has been an unbelievably great place to work and where I have met some unbelievable friends. To the entire CID, thank you so much! To my thesis committee, Dr. Jorge Benach, Dr. Martha Furie, Dr. James Bliska and Dr. Dattwayler, I offer my sincerest appreciation for all your time, thoughts, and suggestions.

To my family…Well, this section can go on forever because I owe everything in my life to them, but I will try to keep it short. To my siblings: Kim, Erik, Evangel, and Crystal, thank you for being my security blanket. Whenever things go wrong or I feel insecure about myself, I just think of you guys and I become happy. I know, no matter what, I'll always have you guys and this thought is enough to get me through hard times. To my siblings-in-law: Brian, Curtis, Sharon, Shahrazad, and Paul, I have known you all for over ten years, which surely encompasses my graduate work, to you all, I thank you for your love and support –I'm so glad marriage has entwined our lives. To my parents… First, my in-laws: Babba Reza, Flora and Mommon Azar, thank you for the love, support and food you have provided to me over the years. You have opened your hearts to me

from the first moment I met you and as a result a huge part of my heart is filled with you in return, thank you! To my mom and dad, plain and simple, thank you for everything! Your love, and support has been the sustenance of my life, I love you both very much. To my husband… Sean. While writing this acknowledgement, I actually had to take a moment in order to compose myself because the very thought of you and endeavoring on thanking you for all you do is a very emotional task for me. But here it goes… you are the sun of my universe and from the first day I met you my world has only become brighter. I want to thank you for the endless love, tireless support and unwavering devotion you have given me over these past ten years. Understatement of the year: I could not have done it without you! I love you so much, thank you!

Chapter One

Introduction

I. Bacteria: *Francisella tularensis*

Francisella tularensis is the etiological agent of tularemia. It was first isolated by McCoy and Chapin from ground squirrels displaying plague-like symptoms in 1911 in Tulare County, California (Tarnvik and Berglund, 2003). In 1921, Edward Francis characterized the organism as a Gram-negative, facultative intracellular, nonmotile cocco-bacillus, and in 1928 the bacteria was renamed in his honor (Tarnvik and Berglund, 2003). *F. tularensis* is the only genus within the family *Francisellaceae*. Whole genome analysis and 16S gene sequencing has identified endosymbionts, such as *Wolbacchia persica,* to be the closest relatives of *F. tularensis* (Keim et al. 2007). Three species within the genus *F. tularensis* exist: *F. tularensis*, *F. philomiragia* (McLendon et al., 2006) and *F. piscicida* (Ottem, K. 2007). There are five additional subspecies of *F. tularensis: tularensis*, *holarctica*, *novicida, mediasiatica* and *japonica.* However, only three of these subspecies cause disease in humans (Svensson et al., 2005). *F. tularensis* subspecies *tularensis,* also known as the type A strain, causes a severe and potentially fatal infection in humans. *F. tularensis* subspecies *holarctica,* also known as the type B strain, causes a milder form of tularemia and very rarely results in a fatal infection. The live vaccine strain (LVS), discussed in more detail below, is derived from subspecies

holarctica. *F. tularensis* subspecies *novicida* is known to cause disease only in immunocompromised persons (Dennis et al., 2001).

Tularemia outbreaks occur worldwide but they are limited to the northern hemisphere. Both type A and type B strains are found in North America, but type A strains are more prevalent. In Europe and Asia, both type A and type B strains are found, but type B strains are more commonly isolated (Ellis et al., 2002). The disease is found in many mammalian species; important carriers of the disease are hares, rabbits, and rodents (Ellis et al., 2002). Another potential reservoir for *F. tularensis* is free-living amoebae (Abd et al., 2003). This finding is particularly interesting because a feature common to certain tularemia hotspots is large amounts of fresh water. The manifestation of the disease in humans is variable, and dependent upon the route of transmission, species biotype, infectious dose and status of host immune system (Ellis et al., 2002; McLendon et al., 2006).

The most common form of tularemia is ulceroglandular. Usually this form of tularemia occurs when humans manipulate contaminated animal carcasses, or receive bites from infected arthropods (Ohara et al., 1991). A lesion develops at the site of infection. The lesion becomes ulcerated and inflamed, and heals within a week. Although the ulcer heals, the local draining lymph node becomes painfully engorged. This is the glandular manifestation of the disease. Within a few days the victim develops many flu-like symptoms including fever, chills, headache and sore throat (Ohara et al., 1991). Oropharyngeal or gastrointestinal tularemia occurs in humans when contaminated meat or water is ingested (Stewart, 1996). Ulcers, pharyngitis, and swollen cervical lymph nodes develop. Other sysmptoms include mild to severe diarrhea depending upon the

initial infectious dose. Oculoglandular tularemia is a conjunctival mucous infection resultant of direct contamination of the eye (Steinemann et al., 1999). Typically, the eye becomes swollen and oozes pus, and if untreated the disease can spread to the local draining lymph node.

The most severe form of the disease is pneumonic tularemia caused by inhalation of aerosolized type A bacteria, with inhalation of as few as 10 colony-forming units (CFU) sufficient to cause disease. Mortality rates range anywhere from 30% to 60% in untreated infections (Dennis et al., 2001). Pneumonia can also arise from the haematogenous spread of other forms of tularemia, but this is less common. The clinical presentation of pneumonic tularemia is similar to the flu; symptoms include high fever, chills, nausea, cough, and delirium. Farming activities such as hay making and landscaping work including bush cutting and mowing are considered high risk activities for the spread of pneumonic tularemia, most likely because these activities create dust particles in the air, which can then be inhaled (Stewart, 1996). *F. tularensis* is classified as a Category A agent of bioterrorism by the U.S. Centers for Disease Control and Prevention (http://www.selectagents.gov/agenttoxinlist.htm) due to its low infectious dose, ease of aerosol dissemination and capacity to cause high morbidity and mortality (Dennis et al., 2001). The *F. tularensis, holarctica,* LVS and *novicida,* U112 strains maintain virulence in the murine model of infection, causing a disease closely resembling human tularemia. Therefore, these bacteria are frequently used as models for infection (Ellis et al., 2002; Green et al., 2005).

II. *Francisella tularensis* Vaccine Development

Currently, there is no vaccine against *F. tularensis* approved by the Food and Drug Administration (FDA) in the United States or the European Medicines Agency in the European Union. The live vaccine strain (LVS) is derived from subspecies *holarctica*. The LVS was developed by the U.S. Department of Defense from a stock of Russian tularemia live vaccine received in 1956 (Tigertt, 1962). However, different stocks yielded different immunogenic and adverse effects in vivo, and studies indicate that the strain is incapable of providing protection against a large dose of the highly virulent type A strain by the respiratory route. The original Russian tularemia vaccine was produced from a fully virulent type B strain by selecting individual bacterial colonies and subjecting them to repeated subculturing (Tigertt, 1962). Most likely, these repeated passages led to mutations in the LVS genome that rendered the strain avirulent. Because the genetic basis of the attenuation is unknown, the LVS is considered an experimental vaccine and its use is limited in the United States (Oyston et al., 2004).

Protective immunity against *Francisella* can be achieved in humans and some murine strains by vaccination with live, but not killed, vaccines (Foshay et al., 1942; Tarnvik, 1989). The safety standards set by the FDA for live vaccine candidates are high, which makes the development of a new live *F. tularensis* vaccine difficult. Development of a subunit vaccine appears to be much more promising, but thus far no immunodominant antigen for *F. tularensis* has been identified. Attempts in the past have included lipopolysaccharide (LPS) alone and the O-side chain of the LPS conjugated to bovine serum albumin (BSA) (Conlan et al., 2002; Fulop et al., 2001). Both *F. tularensis* LPS vaccine candidates failed in providing protection against type A strains. The LPS subunit vaccines did provide protection against intraperitoneal and intradermal infections with type B strains, but neither conferred protection against an intranasally acquired

tularemia (Conlan et al., 2002; Fulop et al., 2001). Ultimately, these vaccines failed because the LPS of *F. tularensis* is unable to prime T-cell mediated immune responses (Tarnvik, 1989), and T-lymphocytes are essential for resolution of *F. tularensis* infection (Conlan et al., 1994).

III. The Virulence Factors of *Francisella tularensis*

The molecular mechanisms behind the pathogenicity of *F. tularensis* are largely unknown. Both virulence factors and secretion capabilities remain unclear due to the fact that until recently few genetic tools compatible with the genome of *F. tularensis* existed. However, it is now possible to introduce DNA into all subspecies of *F. tularensis* using efficient and stable shuttle plasmids (LoVullo et al., 2006; Pavlov et al., 1996). It is also possible to make targeted mutations within the genome of *F. tularensis* through the use of suicide vectors and transposon insertions (Gallagher et al., 2007; LoVullo et al., 2006)

In vivo, *F. tularensis* is a stealth pathogen, evading host cell defenses and dampening host proinflammatory responses. LPS is a major component of outer membranes of Gram-negative bacteria. Typically LPS associates with pattern recognition receptors (PRRs) found within the plasma membrane of innate immune cells. One such PRR is the Toll-like receptor 4 (TLR4). This receptor commonly binds LPS, which initiates a proinflammatory signal transduction pathway and the release of proinflammatory cytokines (Gioannini et al., 2004). The LPS of *F. tularensis* is modified in such a way that it does not interact with TLR4 and is 1000-fold less efficient in stimulating proinflammatory cytokines compared to the LPS of other enteric bacteria

(Barker et al., 2006; Sandstrom et al., 1992). Ultimately, the LPS sensing molecules of the innate immune system such as LPS-binding protein (LBP) and TLRs are unable to recognize the LPS of *F. tularensis*, which may explain the poor proinflammatory response initiated by the innate immune system and the resistance of *F. tularensis* to oxygen-independent polymorphonuclear leukocyte killing (Barker et al., 2006). It has been shown that innate immune responses to *F. tularensis* are mediated by interactions of the bacteria with Toll-like receptor 2 (TLR2) (Malik et al., 2006). The LPS of *F. tularensis* does not bind to TLR2, but two lipoproteins, TUL4 and FTT1103, are known to interact with TLR2 and these interactions may be responsible for the release of proinflammatory cytokines observed during an in vivo infection (Thakran et al., 2008).

The capsule of *F. tularensis* is a known virulence factor made up of exopolysaccharide material. The capsule is neither toxic nor immunogenic, but has been shown to provide protection to the bacterium against serum-mediated lysis (Larsson et al., 2005; Sandstrom et al., 1988). Unencapsulated mutants of *F. tularensis* are attenuated for virulence in vivo (Sandstrom et al., 1988). It is unclear if the capsule is regulated in vivo or in vitro, but it has been shown that continuous growth of unencapsulated mutants in synthetic media restores the capsule and virulence (Cherwonogrodzky et al., 1994). In addition, recent data suggests that the capsule is downregulated once the bacteria are internalized (Golovliov et al., 2003a).

The study of *F. tularensis* has been aided greatly by the availability of sequenced genomes, including those of the highly virulent type A SchuS4 strain, the type B LVS and the subspecies *novicida* U112 strain (www.francisella.org). The genome of *F. tularensis* subspecies *tularensis* is small, approximately 1.9 Mb, and contains 1804

coding sequences, of which 302 are unique to *F. tularensis* (Larsson et al., 2005). Analysis of the genome has revealed many genotypic characteristics unique to the species, including a 33.9 kb region of DNA termed the *Francisella* Pathogenicity Island (FPI) (Larsson et al., 2005; Nano et al., 2004). Subspecies *novicida* has one copy of the FPI, whereas both type B and type A strains have two copies of the FPI. This could explain why type A and B strains are virulent in humans, whereas the *F. novicida* subspecies is normally avirulent (Larsson et al., 2005). The FPI contains twenty-five genes with no known bacterial homologs. Many of the genes encoded by the FPI are essential for intracellular survival and virulence, suggesting that *F. tularensis* utilizes uncharacterized novel virulence factors to achieve its high pathogenicity (Larsson et al., 2005).

Proteome analysis of *F. tularensis* revealed that a novel 23-kDa protein is upregulated by bacteria growing inside macrophages when compared to bacteria growing in broth (Golovliov et al., 1997). The *iglC* gene encodes this 23-kDa protein, which is part of the intracellular growth locus (*igl*) operon. The genes *iglABCD* form a large gene cluster within the FPI. *IglC* is required for phagosomal escape, intracellular survival and virulence (Nano et al., 2004). In addition, FPI genes *iglD*, *iglA*, *pdpA*, *pdpB*, and *pdpD* have been demonstrated to be required for virulence in at least one subspecies (de Bruin et al., 2007; Golovliov et al., 1997; Lai et al., 2004; Ludu et al., 2008; Nano et al., 2004; Weiss et al., 2007a).

Known regulators of virulence in *F. tularensis* include MglA, SspA, and PmrA, all of which control expression of FPI genes (Brotcke et al., 2006; Charity et al., 2007; Lauriano et al., 2004; Mohapatra et al., 2007). Each of these proteins also regulates

expression of genes outside the FPI; MglA and SspA regulate the same set of genes outside the FPI and PmrA controls a separate group of genes (Brotcke et al., 2006; Charity et al., 2007; Mohapatra et al., 2007). A protein called FevR was recently identified. This protein controls the same genes as MglA and SspA, and seems to act in parallel with MglA as a regulator of FPI gene expression (Brotcke and Monack, 2008). In addition, the RNA-binding protein Hfq was identified as a global regulator in *F. tularensis*; it controls expression of a subset of genes located in the FPI (Meibom et al., 2009).

F. tularensis contains genes encoding a type IV pilus biogenesis system that also functions in the secretion of soluble proteins by a type II-like mechanism (Chakraborty et al., 2008; Hager et al., 2006; Zogaj et al., 2008). In other bacterial species, type IV pili function in a number of different ways, including adherence to host cells, DNA uptake, twitching motility and biofilm formation (Gil et al., 2004). In *F. tularensis,* the type IV pili are involved in adherence and are virulence factors as a type IV pili mutant is attenuated in the murine model of infection (Chakraborty et al., 2008; Hager et al., 2006; Zogaj et al., 2008). Additionally, the FPI may encode a type VI secretion system (Pukatzki et al., 2009), but whether the FPI truly functions as a secretion system still needs to be confirmed (Ludu et al., 2008; Nano and Schmerk, 2007). Bacterial secretion systems are discussed in more detail below.

IV. Intracellular Survival of *Francisella tularensis*

A critical aspect of the pathogenesis of *F. tularensis* is its ability to escape the phagosome and replicate within the cytosol of a variety of host cells, including both murine and human macrophages and dendritic cells (Anthony et al., 1991; Bar-Haim et al., 2008; Clemens et al., 2004; Fortier et al., 1994; Tarnvik, 1989). Although *F. tularensis* does have an extracellular phase (Forestal et al., 2007), it is thought that cytosolic replication allows the bacteria to grow to large numbers while avoiding detection by the host immune system. Phagocytosis of *F. tularensis* by macrophages is mediated by complement receptor 3 (CR3), Fcγ receptors, and scavenger receptors such as the mannose receptor (Balagopal et al., 2006; Clemens et al., 2005). Once the bacterium is inside the macrophage, the *F. tularensis*-containing phagosome becomes acidified (Fortier et al., 1994). It was thought that acidification of the phagosome was required for the intracellular survival of *F. tularensis* as it provides the bacteria with a means of acquiring iron. Iron is essential for bacterial growth, and host cells defend against invading pathogens by limiting the amount of available iron. Recently, the gene cluster *fslABCD,* responsible for the synthesis of a siderophore, was identified (Sullivan et al., 2006). Siderophores are small molecules that have a high affinity for iron, and bacteria use siderophores to capture iron from their hosts. It is still unknown if acidification of the phagosome induces *Francisella* virulence factors that would enable escape of the bacteria into the cytoplasm. Three to 4 hours post infection the bacteria co-localize with the late endosomal-lysosomal markers LAMP-1 and CD63. However, soon after these markers are diminished, and by 5 hours post infection the bacteria are no

longer enclosed within phagosomes but are free within the cytoplasm. Once escaped from the phagosome, the bacteria begin to replicate (Chong et al., 2008).

The intracellular life cycle of *F. tularensis* is complex, and only a few genes required for phagosome escape, cytosolic replication and downmodulation of host innate immune responses have been identified. To date, the acid phophatase AcpA has been shown to be required for intracellular survival. AcpA inhibits the respiratory burst and is necessary for optimal phagosomal escape (Mohapatra et al., 2007; Reilly et al., 1996). As discussed above, the operons *iglABCD* and *pdpABCD,* which are both located within the FPI, are required for phagosomal escape, intracellular survival and virulence (de Bruin et al., 2007; Golovliov et al., 1997; Lai et al., 2004; Ludu et al., 2008; Nano et al., 2004).

V. Host Cell Defense Responses to *Francisella tularensis*

One way host cells defend themselves against intracellular pathogens is to initiate proinflammatory signal transduction pathways. Infected host cells mount proinflammatory responses to signal neighboring cells of the impending bacterial threat as well as attract professional phagocytes to the area of infection (Cole et al., 2006). The cytokines interferon (IFN)-γ, tumor necrosis factor-α (TNF-α) and interleukin (IL)-12 are all important to the murine host in clearance of both the LVS and subspecies *novicida* (Anthony et al., 1989; Elkins et al., 1996; Fortier et al., 1992). However, *F. tularensis* has been shown to actively suppress innate host responses. In one study, LVS infection of J774 murine macrophage-like cells initially activates the nuclear factor kappa-B (NFk-B) pathway, but by 4 to 5 hours post infection the activation of NFk-B disappears (Telepnev

et al., 2005). The NFk-B pathway is responsible for the expression of many proinflammatory cytokines and chemokines. It has been shown that the LVS disrupts Toll-like receptor signaling and blocks expression of the proinflammatory cytokines TNF-α and IL-1ß by murine and human macrophages (Telepnev et al., 2003; Telepnev et al., 2005). Similarly, the LVS inhibits secretion of the expression of proinflammatory cytokines TNF-α and IL-6 by murine pulmonary dendritic cells, while eliciting the production of TGF-β, a potent immunosuppressive cytokine (Bosio and Dow, 2005). Murine macrophages infected with the LVS produce prostaglandin E2, a highly immunosuppressive mediator (Woolard et al., 2008). Additionally, infection of mice with the fully virulent Schu4 strain (subsp. *tularensis*) causes an overall state of immunosuppression in the lungs. Multiple cell types fail to produce proinflammatory cytokines or stimulate resident dendritic cells (DC), but an upregulation in the production of TGF-β is observed (Bosio et al., 2007; Bosio and Dow, 2005).

In addition to mounting proinflammatory responses, host cells defend themselves against intracellular pathogens by inducing cell death pathways. Pathogen-induced cell death is a phenomenon that has been well studied. In some instances bacterial induction of apoptosis benefits the invading pathogen (Grassme et al., 2001). Bacterial species including *Yersinia pestis, Escherichia coli* and *Pseudomonas aeruginosa* are all known to target and trigger apoptosis in innate immune cells, thus allowing the pathogens to avoid phagocytosis and destruction, and enabling the systemic spread to distal sites of the body (Grassme et al., 2001). *F. tularensis* induces host cell death by both the apoptotic and pyroptotic pathways (Henry et al., 2007; Lai and Sjostedt, 2003). Characteristics of apoptosis include chromatin condensation, DNA fragmentation and cell death in the

absence of a large proinflammatory response (Budihardjo et al., 1999). Currently, two well defined caspase-activating pathways that mediate apoptosis exist: the intrinsic pathway is triggered by changes in mitochondrial integrity, and the extrinsic pathway is initiated by cell surface death receptors (Budihardjo et al., 1999). The extrinsic apoptotic pathway is initiated when proapoptotic signals bind and activate a pro-apoptotic death receptor, which in turn activates initiator caspase-8 and subsequently executioner caspase-3 (Figure 1.1) (Budihardjo et al., 1999). The intrinsic apoptotic pathway involves release of cytochrome C from mitochondria into the cytosol. Cytochrome C then binds to Apaf-1 of the apoptosome complex and activates caspase-9, and ultimately effector caspases such as caspase-3 and caspase-7 are activated resulting in apoptosis (Figures 1.1 and 1.2) (Budihardjo et al., 1999). Pyroptosis is not a form of apoptosis and is generally proinflammatory. Pyroptosis is triggered when conserved pathogen-associated molecular patterns (PAMPs) are recognized by cytosolic pattern recognition receptors (PRRs) such as Ipaf-1 or Nalp-3, which form part of the inflammasome. Ultimately, activation of caspase-1 triggers cell death and release of proinflammatory cytokines such as IL-1ß (Bergsbaken et al., 2009; Henry et al., 2007). Infection of murine J774 macrophage-like cells with the LVS activates the intrinsic apoptotic pathway as early as 12 h post infection. Activated caspase-3, but not caspase-1, is detected in the infected cells (Lai and Sjostedt, 2003). In contrast, infection of pre-activated murine peritoneal macrophages by either the LVS or strain U112 (subsp. *novicida*) triggers cell death via the inflammasome complex and caspase-1 activation (Mariathasan et al., 2005).

Although induction of cell death may benefit the pathogen, recent studies indicate that inhibition of apoptosis can also be beneficial to the invading pathogen. Many

pathogens are now known to inhibit host cell apoptosis, including the Gram-negative bacterial endosymbiont *Wolbachia,* which is the organism most closely related to *F. tularensis* (Forsman et al., 1994). Inhibition of apoptosis in polymorphonuclear cells such as neutrophils by *Wolbachia* enables the organism to maintain an endosymbiotic lifestyle (Bazzocchi et al., 2007). In a recent study, mutants of *F. novicida* strain U112 attenuated for virulence were isolated. These same attenuated mutants also cause increased inflammasome activation and cell death when compared to the wild-type U112 strain (Henry et al., 2007; Weiss et al., 2007b). This suggests that although host cells respond to *F. tularensis* infection by initiating death pathways, *F. tularensis* actively dampens these cell death responses and the reduced cell death is important for virulence.

VI. Secretion Systems of *Francisella tularensis*

Gram-negative bacterial species have complex cell envelopes comprising an inner membrane (IM), an outer membrane (OM), and a periplasm, which is the space in between the IM and OM. Therefore, Gram-negative bacteria have developed sophisticated systems to secrete proteins across this envelope (Thanassi and Hultgren, 2000). These systems are critical for the secretion of virulence factors and required for bacterial pathogenesis. During pathogenesis, bacteria secrete toxins and enzymes that affect host cells by altering cellular function. Additionally, proteins secreted by bacteria can assemble into extracellular structures such as pili and adhesins that promote adherence to host cell surfaces, which contribute to the overall pathogenesis of the organism (Chakraborty et al., 2008; Gerlach and Hensel, 2007). Gram-negative bacterial

species are known to use six protein secretion systems. The various secretions systems are referred to as type I–VI, or T1SS–T6SS (Gerlach and Hensel, 2007). These secretion systems are classified by the structural proteins that are used in their assembly, and by the characteristics of their substrates and the pathway the substrates take during secretion (Gerlach and Hensel, 2007; Thanassi and Hultgren, 2000).

Genome analysis of *F. tularensis* revealed that the pathogen lacks typical secretion systems found in other pathogenic bacteria. There is no genomic evidence to suggest the presence of type III, IV, or V secretion systems (Larsson et al., 2005). This is very surprising considering that this organism is highly pathogenic. There is evidence within the genome of *F. tularensis* for type I, II and possibly type VI secretion systems, although this evidence is not absolute (Larsson et al., 2005). The genome of *F. tularensis* contains genes encoding a type IV pilus biogenesis system that also functions in the secretion of soluble proteins by a type II-like mechanism and is important for virulence (Chakraborty et al., 2008; Hager et al., 2006; Zogaj et al., 2008). There is evidence suggesting that the FPI in *F. tularensis* may encode a type VI secretion system (Pukatzki et al., 2009), but it has yet to be determined if these genes within the FPI function in secretion or are important to virulence (Ludu et al., 2008; Nano and Schmerk, 2007). Additionally, the genome of *F. tularensis* contains at least 15 ATP-binding Cassette (ABC) systems, as well as three orthologs of the *E. coli* TolC protein, termed *tolC, ftlC* and *silC* (Atkins et al., 2006; Gil et al., 2006; Huntley et al., 2007). The *F. tularensis tolC* and *ftlC* genes have significant homology to the *E. coli* TolC protein and may participate in protein secretion, while the *silC* gene most closely resembles *E. coli* proteins involved in drug efflux. All three of the above mentioned secretion systems are discussed below.

This dissertation presents evidence for a functioning type I secretion system and multidrug efflux pump within *F. tularensis* that is important for virulence, and the type I system will be discussed in more detail.

The type II secretion system (T2SS) is a Sec-dependent system, as many proteins that pass through the T2SS must first reach the periplasm via the Sec pathway before they are secreted into the extracellular milieu (Thanassi and Hultgren, 2000). Therefore, the T2SS is considered a two-step secretion pathway. The system consists of an outer membrane translocation pore and inner membrane proteins and pseudopilin subunits that span the periplasm (Figure 1.3) (Thanassi and Hultgren, 2000). In addition the T2SS contains an intracellular ATPase that may provide the energy required to open and close the translocation pore (Cianciotto, 2005). The T2SS proteins that span the periplasm are believed to connect the outer membrane pore to the inner membrane (Figure 1.3). The structure of the inner membrane complex and the pseudopilins closely resembles the type IV piliation system, suggesting a common evolutionary origin (Cianciotto, 2005).

The type VI secretion system (T6SS) has only recently been identified, and less is known about the protein transport mechanism (Pukatzki et al., 2009). T6SS gene clusters are highly conserved and are found in many pathogenic Gram-negative bacterial species, including *Vibrio cholerae*, *Yersinia pestis*, *Salmonella enterica*, *Pseudomonas aeruginosa*, *Escherichia coli*, *Burkholderia mallei,* and *Francisella tularensis* (Bingle et al., 2008; Shrivastava and Mande, 2008). One of the proteins of the type VI secretion system resembles the tail spike of T4 phage, and much like the T3SS it has the ability to inject effector proteins directly into the cytoplasm of host cells (Bingle et al., 2008; Filloux, 2009). The proposed model of a T6SS includes a cytoplasmic chaperone with

ATPase activity, a channel bridging from the inner to the outer membrane, and a needle tipped with a pore-forming protein (Figure 1.4) (Shrivastava and Mande, 2008).

The type I secretion system (T1SS) secretes proteins directly from the cytoplasm to the extracellular milieu in a single energized step, without any periplasmic intermediates, and is considered a one-step secretion pathway (Holland et al., 2005). This system consists of an outer membrane protein (OMP), a membrane fusion protein (MFP), and an inner-membrane ATP-binding cassette protein (IM ABC) (Figure 1.5) (Holland et al., 2005). The OMP provides a channel through the outer membrane, and the periplasmic MFP mediates recruitment of the OMP and links the OMP exit duct to the energy-providing inner membrane translocase (Thanabalu et al., 1998). The most well characterized T1SS comes from *Escherichia coli* and is required for hemolysin (HlyA) secretion. Hemolysin is a secreted toxin that targets neighboring host cells, binds them and disrupts the integrity of the cell membrane. This causes the cells to lyse and release nutrients into the surrounding environment (Koronakis and Hughes, 1993). The OMP for hemolysin secretion is TolC, the MFP is HlyD, and the IM ABC is HlyB (Figure 1.5). TolC is a trimeric OMP, which forms a tapered hollow cylinder 140 Å in length. TolC contains three domains: the outer membrane domain, composed of a β-barrel, the periplasmic extension, comprising α-helices, and a third domain, a mixed α/β structure, which forms a belt around the periplasmic tunnel (Koronakis et al., 2000). The α-helical periplasmic extension is thought to gate the TolC channel via an iris-like motion (Koronakis et al., 2000). The TolC family of proteins is highly conserved throughout Gram-negative bacteria, and the type of secretion system a particular TolC homolog will partake in can be predicted from its primary nucleotide sequence (Andersen et al., 2000).

In addition to being involved in protein secretion (Figure 1.5, panel A), TolC can also participate in multidrug efflux by associating with other transporter families, such as the major facilitator superfamily (MFS) and resistance-nodulation-division (RND) superfamily (Figure 1.3, panel B). Usually, protein translocation utilizing the type 1 system is dependent upon ATP hydrolysis, while a proton antiporter is more commonly used in multidrug efflux (Koronakis et al., 1993; Thanassi and Hultgren, 2000). Type I secretion systems secrete a whole variety of virulence factors, including toxins, metalloproteases, adhesins and glycanases (Delepelaire, 2004). T1SS can also secrete exo-polysaccharides in addition to protein for the formation of biofilms (Delepelaire, 2004).

In this dissertation, I constructed *tolC* and *ftlC* deletion mutations in the LVS and investigated the role these genes play in survival and virulence. Antibiotic sensitivity assays revealed that both TolC and FtlC function in drug efflux. However, only TolC was determined to be an essential virulence determinant, as the *tolC* mutant was avirulent in the mouse model and defective in colonizing organs. In vitro analysis revealed that *F. tularensis* actively inhibits host cell death and secretion of proinflammatory cytokines in a TolC-dependent manner. Based on these results, we propose that in the absence of TolC *F. tularensis* induces rapid host cell death and a large proinflammatory response. This causes the bacteria to lose its intracellular replicative niche and with insufficient bacterial numbers the pathogen is cleared by the increased innate immune response of the host.

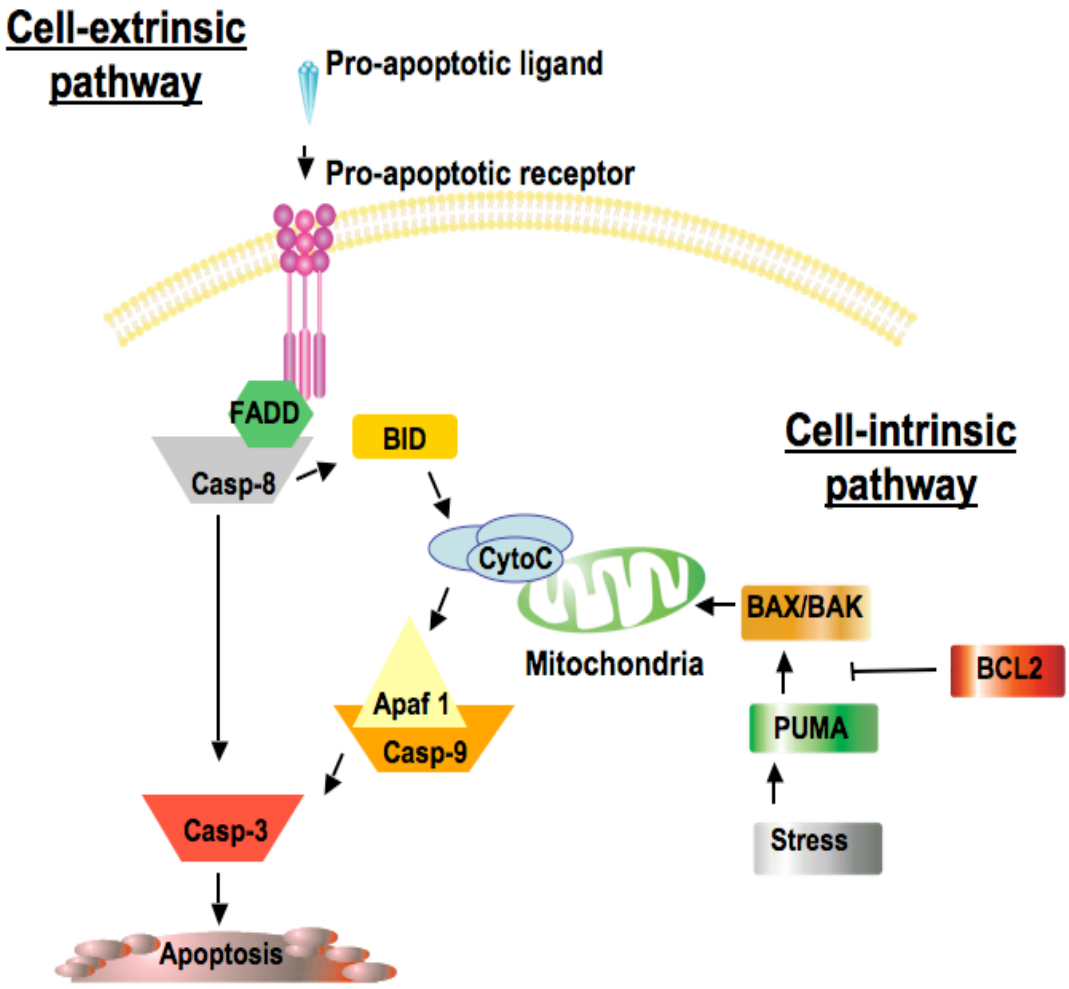

Figure 1.1 The apoptosis pathways. Intrinsic and extrinsic pathways activate apoptosis. In the intrinsic pathway, apoptotic stimuli such as bacterial PAMPs cause a loss in mitochondrial membrane integrity, and this causes the release of cytochrome *c*. Newly released cytochrome *c* binds Apaf1 of the apoptosome, activating caspase-9, which subsequently activates the executioner caspase-3. In the extrinsic pathway, a proapoptotic ligand such as TNF-α binds death receptors in the membrane of the host. Trimerization of the death receptors and assembly of the death inducing signaling complex (DISC), which includes Fas-associated death domain (FADD) and caspase-8, follows. Caspase-8 is activated, which subsequently activates executioner caspase-3.

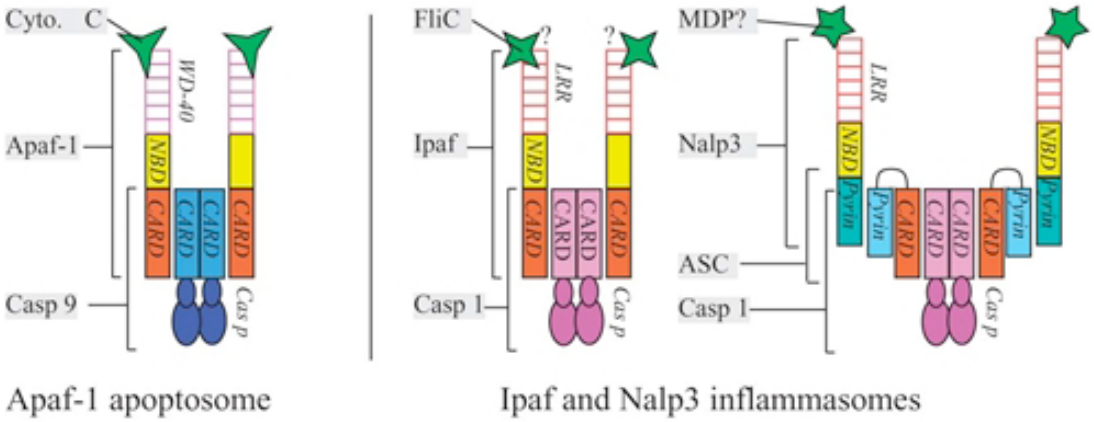

Figure 1.2 The apoptosome and inflammasome. The Apaf-1 apoptosome is formed by the release of cytochrome *c* from the mitochondrial membrane and leads to the activation of caspase-9. The Ipaf inflammasome is assembled upon recognition of bacterial flagellin. Assembly of the Nalp3 inflammasome is dependent upon ASC and the binding of muramyyl-dipeptide (MDP) and leads to the activation of caspase-1. *WD-40* repeats, leucine-rich repeats (LRR), nucleotide biding domain (NBD), caspase recruitment domain (CARD), catalytic caspase domain (*Casp*), and *Pyrin* domains are shown. This image was taken from Henry, *et al.,* 2007.

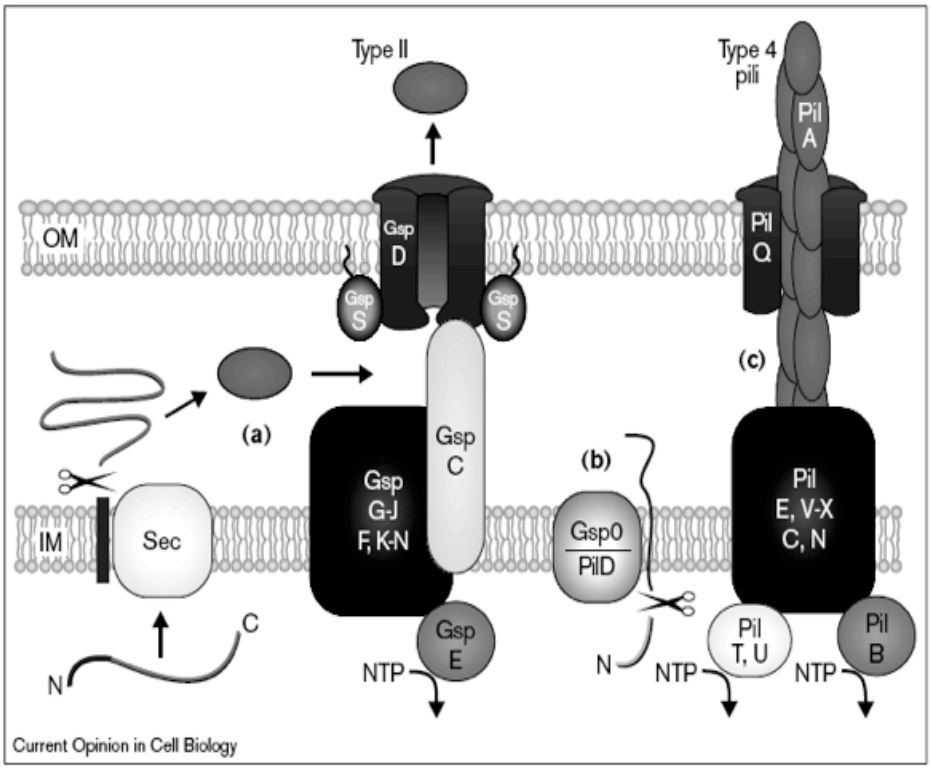

Figure 1.3 The type II secretion and type 4 pilus biogenesis systems. The T2SS is used by Gram-negative bacteria to secrete soluble proteins and for pilus biogenesis. Components of the T2SS are indicated using the Gsp nomenclature, and type 4 pilus proteins are labeled according to the *Pseudomonas aeruginosa* Pil system (Thanassi and Hultgren, 2000). This image was provided by D. G. Thanassi.

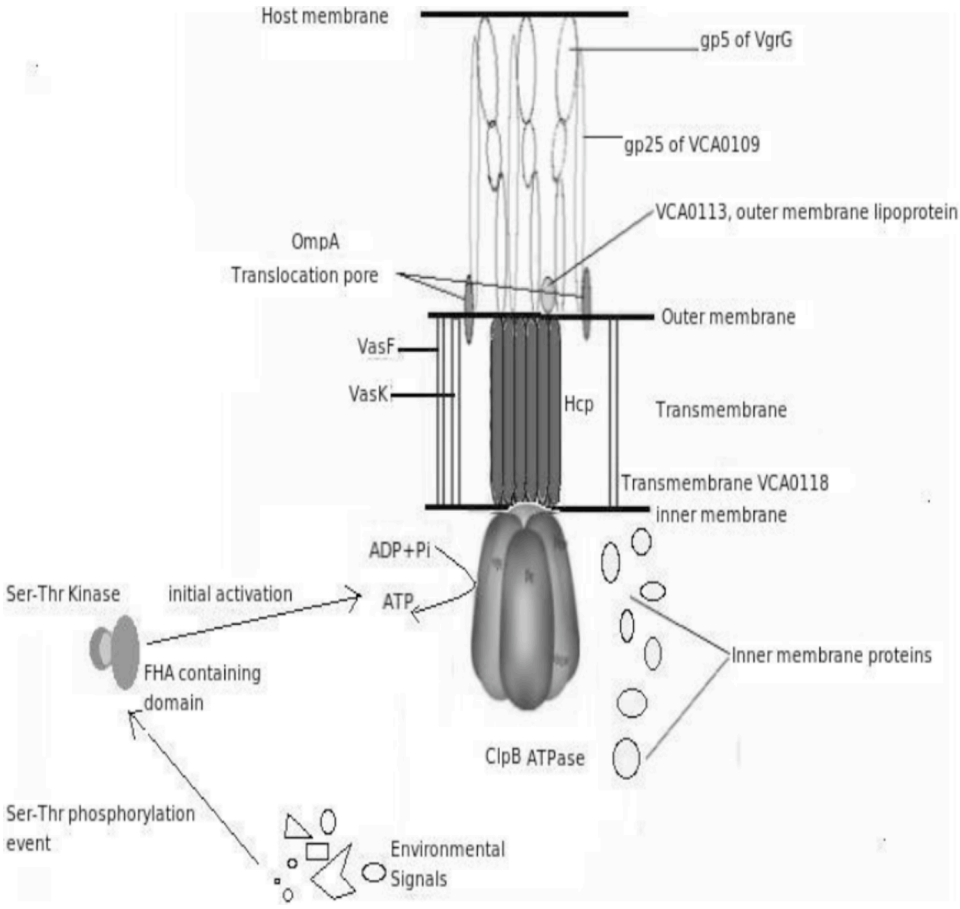

Figure 1.4 The proposed model of a T6SS includes a cytoplasmic chaperone with ATPase activity, a channel bridging from the inner to the outer membrane, and a needle tipped with a pore-forming protein. This image was taken from Shrivastava, *et al.,* 2008, with permission.

A

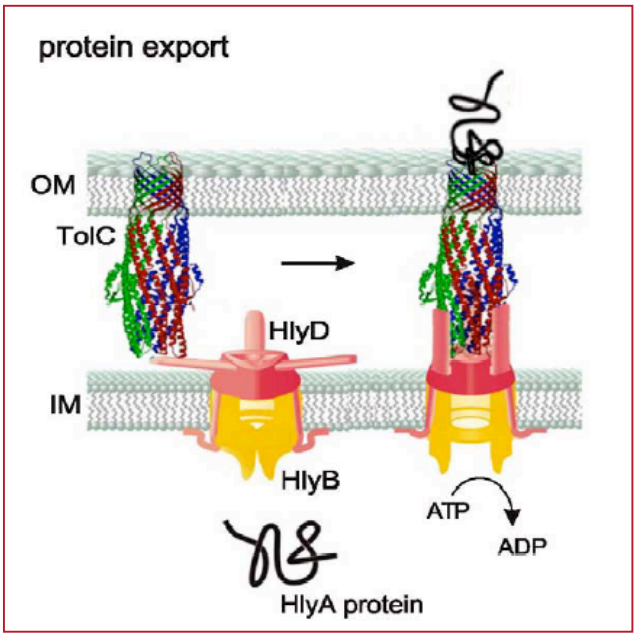

B

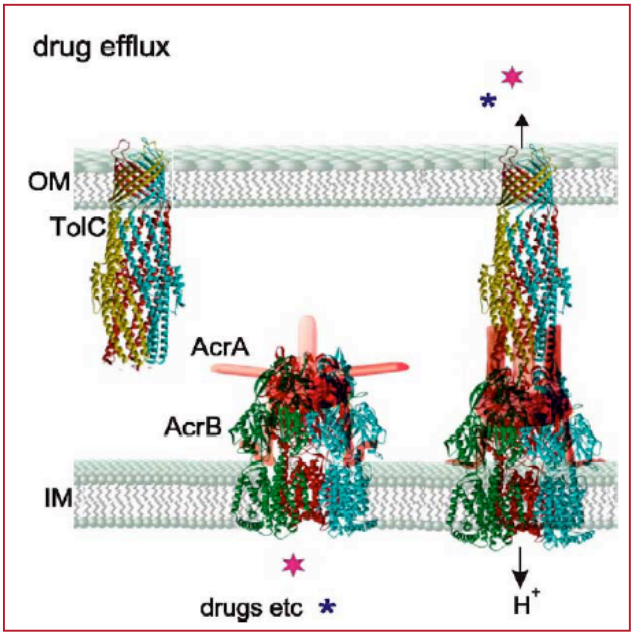

Figure 1.5 Crystal structure and functional model of *Escherichia coli* TolC. *E. coli* TolC functions as part of type 1 secretion and multidrug efflux pumps. Panel A depicts type 1 secretion of the hemolysin protein HlyA. Panel B depicts secretion of harmful molecules using a multidrug efflux pump. This image was taken from Koronakis *et al.,* 2005.

Chapter Two
Materials and Methods

Strains and plasmids

The strains and plasmids used in this study are described in Table 1. *F. tularensis* strains were incubated at 37°C with 5% CO_2 in different media as follows. The LVS was grown on Mueller-Hinton II Chocolate agar plates (MHC) or in Mueller-Hinton broth (MHB) as described previously (Chakraborty et al., 2008; Gil et al., 2006). *F. tularensis* subspecies *novicida* U112 was grown in tryptic soy medium supplemented with 0.1% cysteine (Chakraborty et al., 2008). *E. coli* strains were grown on Luria agar plates (LA) or in Luria broth (LB) supplemented with 10 μg/ml chloramphenicol, 100 μg/ml ampicillin or 50 μg/ml of kanamycin as appropriate.

Identification and analysis of *Francisella* TolC orthologs

F. tularensis tolC orthologs were identified by BLAST (Altschul et al., 1990) using the *E. coli* TolC protein sequence (NP_755652) (Figure 2.1). BLAST analysis was performed against the genomes of *F. tularensis* SchuS4 (Larsson et al., 2005) and *F. tularensis* LVS (http://bbrp.llnl.gov/bbrp/bin/f.tularensis_blast). The *tolC* and *ftlC* genes in subspecies *novicida* (strain U112) were amplified by PCR using the primers listed in Table 2. The amplicons were purified using the QIAGEN Gel Purification kit (Qiagen

Inc., Valencia, CA) and sequenced using the BigDye terminator V3.1 cycle sequencing kit (Applied Biosystems, Foster City, CA). The sequences of TolC and FtlC from the three *F. tularensis* subspecies were aligned with *E. coli* TolC using ClustalW (Atkins et al., 2006) and the MacVector software program (Oxford Molecular Ltd., Madison, WI). The presence of conserved domains in the TolC homologs was investigated using NCBI Structure (http://www.ncbi.nlm.nih.gov/Structure/) (Thompson et al., 1994), the presence of a leader sequence was determined using SignalP3 (http://www.cbs.dtu.dk/services/SignalP/) (Marchler-Bauer and Bryant, 2004), and the cellular localization of the proteins was predicted using PsortB (http://www.psort.org/psortb/) (Bendtsen et al., 2004). The locations of promoters and operons were investigated using the FGENESB and BPROM programs available from Softberry (http://www.softberry.com/berry.phtml). Subspecies *novicida tolC, hlyD* and *HlyB* orthologs were identified by BLAST (Altschul et al., 1990) using the *E. coli* TolC protein sequence, HlyD protein sequence and HlyB protein sequence, respectively. BLAST analysis was performed against the genomes of subspecies *novicida* U112 (www.francisella.org).

Construction and verification of suicide plasmids for the allelic replacement of *tolC* and *ftlC*

We used an allelic exchange protocol (Tatusov et al., 2000) to generate the LVS deletion mutants. The allelic replacement technique employs a pPV suicide vector. The pPV suicide vector, created by Golovliov *et al.*, was made by ligating a *sacB* gene

(*Bacillus subtilis*) from pDM4, an origin of transfer (*oriT*) from pRP4, and a chloramphenicol (Clm^r) resistance gene *crg* (*Shigella flexneri*) from pSa into the high copy plasmid pUC19 (Figure 2.2) (Golovliov et al., 2003b; Milton et al., 1996; Priefer et al., 1985; Watanabe et al., 1968; Yanisch-Perron et al., 1985). The resulting plasmid harbors unique XbaI and SalI restriction sites for cloning (Figure 2.2). The oriT confers efficient conjugal transfer from donor strain to recipient strain, and the *sacB* gene encodes the enzyme levansucrase, which produces a toxic product in the presence of sucrose (Priefer et al., 1985; Reyrat et al., 1998). We first amplified approximately 1500 bp of the upstream and downstream regions of *tolC* and *ftlC* using the following primer pairs: UTA3580F and UTAXBAI, DTA7791R and DTAXBAI, UTB3755F and UTBPSTI, and DTB7802R and DTBPSTI (Table 2). PCR was performed using the High Fidelity Plus PCR system (Roche, Mannheim, Germany), and the amplicons were cloned into the pGEM Easy vector system (Promega, Madison, Wisconsin) following the instructions of the manufacturer (Figure 2.3). Plasmids were purified using the Wizard Plus SV Minipreps DNA Purification System (Promega) and sequenced using the primers listed in Table 2 to confirm the absence of unwanted mutations. Plasmids were then digested with *Sal*I and *Xba*I for the *tolC* regions and *Sal*I and *Pst*I for the *ftlC* regions. The upstream and downstream regions for each gene were ligated together into the *Sal*I site of the pGEM easy vector. These new plasmids were digested sequentially with *Bgl*I, which cuts the pGEM easy vector backbone, and *Sal*I to release the approximately 3000 bp insert. This insert was finally subcloned into the *Sal*I site of plasmid pPV (Figure 2.3), which was kindly provided by Anders Sjöstedt. As mentioned above, plasmid pPV is a suicide vector for *F. tularensis* containing a chloramphenicol resistant cassette (*cat*)

and *sacB,* which confers sensitivity to sucrose. We generated two suicide plasmids: pPVTAH1 for knocking out *tolC* and pPVTBH3 for knocking out *ftlC* (Table 1). These plasmids were transformed into *E. coli* S17-1 by electroporation. Strain S17-1 contains the machinery needed for conjugation (Golovliov et al., 2003b).

Prior to conjugating with *F. tularensis*, the *E. coli* strains containing the suicide vectors were tested for proper performance. We confirmed sensitivity to sucrose and resistance to chloramphenicol, growing the bacteria on LA with 5% sucrose and 10 μg/ml chloramphenicol, respectively. We also checked the efficiency of conjugation between *E. coli* strains, using SF110 (Kan^R) as the recipient strain. The conjugation was performed as described below for *F. tularensis*, except transformants were selected on LA containing 10 μg/ml chloramphenicol plus 50 μg/ml kanamycin, and the number of colonies was compared with selection on LA plates containing only kanamycin. A ratio of 1 transformant per 10 recipient cells was considered adequate to proceed with the *F. tularensis* conjugations. Frozen aliquots of the donor strains were kept at -80ºC, and a new aliquot was used for each experiment.

Conjugation and selection of *F. tularensis* deletion strains

An aliquot of *E. coli* S17-1/pPVTAH1 or S17-1/pPVTBH3 was spotted onto LA containing 10 μg/ml chloramphenicol and incubated overnight at 25ºC. The next morning, 10 ml of MHB was inoculated with LVS from an MHC plate, and the culture was incubated for 6 h at 37ºC with 200 rpm shaking. The LVS culture was centrifuged (10,000 *g*, 10 min) and washed once with PBS. The *E. coli* strain was collected with a

loop and washed with PBS as above. The bacterial pellets were resuspended in LB to obtain a concentration of 200 mg/ml bacteria for the LVS and 100 mg/ml bacteria for *E. coli*. From these bacterial suspensions, we mixed in a tube 160 µl of LVS and 40 µl of *E. coli*. Four 25 µl aliquots of the bacterial mixture were spotted onto LA, allowed to dry, and then four additional 25 µl aliquots of the remiaining bacterial suspension was spotted on top of the previous spots. The plate was incubated at 25°C overnight. The next morning, two spots were inoculated together into 1 ml of MHB containing 100 µg/ml polymyxin B, and the other two spots were inoculated together into 2 ml of the same medium (*E. coli* is sensitive to polymyxin B, whereas *F. tularensis* is resistant). The cultures were incubated at 37ºC for 3 h with shaking at 200 rpm. Then, five 200 µl aliquots per culture were plated for single colonies onto Modified Medium for *Francisella* (MMF; Vitaly Pavlov, personal communication), which contains 1.5% peptone, 0.1% NaCl, 23 mM K_2HPO_4, 7 mM KH_2PO_4, 1% glucose, 1% Isovitalex (Becton Dickinson, Sparks, MD), 0.1% cysteine, 1% hemoglobin, 1.2% agar supplemented with 100 µg/ml polymyxin B and 2 µg/ml chloramphenicol. The plates were incubated at 37ºC with 5% CO_2, with colonies appearing within 5-6 days. To check for the proper phenotype, colonies were resuspended in 15 µl MHB, and 4 µl aliquots were spotted in parallel onto MMF containing 100 µg/ml polymyxin B plus 1 µg/ml chloramphenicol, or MMF containing 100 µg/ml polymyxin B and 5% sucrose. Colonies that grew well in MMF plus chloramphenicol and poorly in MMF plus sucrose were analyzed by PCR to confirm the first recombination event using primers external to the deleted region. The primers used to check the *tolC* knockout were UTA4131F and DTA7334R, and the primers used to check the *ftlC* knockout were UTB4268F and

DTB7264R (Table 2). Colonies positive for the integration of the suicide plasmid were streaked from the MMF plus chloramphenicol plates to MMF supplemented with 100 μg/ml polymyxin B and 5% sucrose. Colonies obtained from these plates were checked for the second recombination event by PCR using four sets of primers (Table 2). One set was the external primer set mentioned above. The second set of primers was located within the deleted gene (TA3580F and TA7895R for *tolC*, TB5593F and TB6588R for *ftlC*). The third set of primers amplified *sacB* (SacB787F and SacB1243R), and the fourth set of primers (PilT168F and PilT682R) amplified the *F. tularensis pilT* gene to confirm that the isolated colonies were *F. tularensis* and not a contaminating bacterium. Colonies passing these controls were grown for 11 hours in MHB (to mid-log phase), and aliquots of the cultures containing 20% glycerol were frozen at -80ºC. The final LVS Δ*tolC* and Δ*ftlC* strains were named DTH1 and DTB3, respectively, but will be referred to in this dissertation as LVS Δ*tolC* and Δ*ftlC*.

Complementation of the Δ*tolC* and Δ*ftlC* mutants

Plasmids pGPTA and pGPTB (Table 1), expressing *tolC* or *ftlC*, respectively, were constructed as follows. The LVS *tolC* or *ftlC* genes were amplified using High Fidelity Plus PCR system (Roche) with primers TANHEIF and TABAMHIR for *tolC* and TBHNEIF and TBBAMHR for *ftlC* (Table 2). The amplicons were cloned into the pGEM Easy vector system (Promega, Madison, Wisconsin) following the instructions of the manufacturer and transformed into *E. coli* DH5α. The plasmids were purified using the Wizard Plus SV Minipreps DNA Purification System (Promega), and the cloned genes

were sequenced using primers listed in Table 2, to confirm the absence of mutations. The genes were then subcloned into plasmid pFNLTP6-gro-gfp (Table 1) (Figure 2.4) (Maier et al., 2004), which was kindly provided by Thomas Zahrt, as follows. Plasmid pFNLTP6-gro-gfp was digested with *Nhe*I and *Bam*HI, releasing *gfp* (Figure 2.4). These same restriction sites were then used for subcloning our genes, placing them under control of the *groE* promoter of *F. tularensis* (Maier et al., 2004).

Transformation of the plasmids into *F. tularensis* was done by electroporation as follows. Strains Δ*tolC* and Δ*ftlC* were grown overnight in 50 ml of MHB. The cultures were centrifuged (3,000 *g*, 10 min) and washed twice with sterile 500 mM sucrose. The pellets were resuspended in 2 ml of 500 mM sucrose, split into two tubes and centrifuged again (9,000 *g*, 3 min). The final pellets were resuspended in 40 µl of 500 mM sucrose and transferred to a 0.1-cm-gap electroporation cuvette. Plasmids pGPTA and pGPTB were introduced into Δ*tolC* and Δ*ftlC*, respectively, using a Bio-Rad Gene Pulser II (Bio-Rad, Hercules, CA) set at 1.5 kV, 25 µF capacitance and a resistance of 400 Ω. After the pulse, the cells were resuspended in 1 ml of MHB and incubated at 37ºC with 200 rpm shaking for 4 h. For selection of the transformants, 100 µl aliquots were plated on MHC supplemented with 1 µg/ml of kanamycin. Frozen aliquots of the complemented strains were prepared as described above. These complementation strains will be referred to in this dissertation as Δ*tolC/tolC*$^{+}$ and Δ*ftlC/ftlC*$^{+}$.

Multidrug sensitivity assay

F. tularensis LVS strains were grown on MHC and then suspended into MHB. *F. tularensis novicida* strains were grown on TSP and then suspended into TSB. The bacteria were spread with a cotton swab onto MHC (supplemented with 1 μg/ml kanamycin for complemented strains) to obtain a bacterial lawn. Sterile discs (Becton Dickinson, San Jose, CA) soaked with different drugs, as indicated in Table 3, were placed on the plates. After 3 days, the growth inhibition halos around the discs were measured as the diameter of the zone of inhibition including the diameter of the disc (6 mm). The experiments were repeated at least three times for each drug and strain.

Mouse infection experiments

Groups of five 6-to-8-week-old C3H/HeN mice were intradermally infected with LVS, Δ*tolC*, Δ*ftlC*, or Δ*tolC/tolC*$^{+}$. The bacteria were grown in MHB overnight to an OD_{600} of 0.2 and diluted in MHB to inoculate 10^7, 10^6 or 10^5 microorganisms per mouse. The animals were monitored for 15 days.

For intranasal infections of mice, bacterial stocks were prepared as follows (Huntley et al., 2008). Bacteria were grown as a lawn on six cystine heart agar (CHaB; Difco) plates at 37°C, 5% CO_2 for 48 h. Bacteria were then scraped from the plates, washed with sterile phosphate buffered saline (PBS), and resuspended in 15 ml of MHB supplemented with 10% sucrose. Serial dilutions were then made and aliquots of the dilutions frozen at -80°C. A CFU assay was performed on each dilution to obtain the true bacterial counts for each dilution. For lethal infections, groups of five C3H/HeN mice (6-

8 weeks old; Jackson Laboratories) were inoculated intranasally with 20 µl (10 µl per nare) of a thawed bacterial aliquot that was chosen to provide a dose of 10^5 CFU. The actual infectious doses were determined by CFU counts. The animals were observed twice daily and monitored for survival for 20 days.

For intraperitoneal infections, groups of five 6-to-8-week-old C3H/HeN mice were infected with the LVS, Δ*tolC* or Δ*ftlC*. The bacteria were grown in MHB overnight to an OD_{600} of 0.2 and diluted in MHB to inoculate 10^3 microorganisms. Bacterial aliquots (100 µl total) were injected directly into the peritoneum of each mouse. The animals were monitored for 15 days.

For intradermal infections, groups of five 6-to-8-week-old Balb/C mice were infected with subspecies *novicida* U112, transposon mutant U112 FTN_1703::Tn18, or transposon mutant U112 FTN_0079::Tn18. The bacteria were grown in TSB overnight to an OD_{600} of 0.6 and diluted in TSB to inoculate 10^6 microorganisms per mouse. The animals were monitored for 15 days.

For protective immunity assays, groups of five 6-to-8-week-old C3H/HeN mice were infected intradermally with LVS, Δ*tolC*, Δ*ftlC*, or a PBS control. One day prior to infection, 1 ml of blood was collected from the tail vein of each animal to serve as naïve serum. For the infection, the bacteria were grown in MHB overnight to an OD_{600} of 0.2 and diluted in MHB to inoculate 2×10^5 microorganisms per mouse; 100 µl in total was injected. The animals were monitored for survival. Six weeks after the initial sub-lethal infection, serum was collected and the mice were challenged with a lethal dose of the LVS administered intradermally. For the lethal challenge, the LVS was grown in MHB

overnight to an OD_{600} of 0.2 and diluted in MHB to inoculate 1 x 10^8 microorganisms per mouse. The animals were monitored for survival.

For the intradermal and intranasal organ burden assays, groups of 15 C3H/HeN mice were either intradermally or intranasally inoculated with a sub-lethal dose of the LVS or Δ*tolC,* and for both experiments an additional mouse was administered PBS to serve as a control. For the intradermal infections, the bacteria were grown in MHB overnight to an OD_{600} of 0.2 and diluted in PBS to inoculate 10^5 microorganisms per mouse in a 100 μl injection. For the intranasal infections, stocks prepared and administered as described were chosen to inoculate 5 x10^3 CFU per mouse. Actual infectious doses were determined for all infections by CFU counts. Five mice from each group were sacrificed on days 2, 4 and 7 PI for the intradermal infections and days 3, 5 and 9 PI for the intranasal infections, and necropsy of the lung, liver and spleen performed. The organs were placed in pre-weighed 1.5 ml tubes containing 1 ml of sterile PBS and re-weighed after the addition of the organs to determine individual organ weights. The organs were homogenized using Stomacher bags (Seward), and then neat and serial dilutions were plated to determine CFU.

The Institutional Animal Care and Use Committee of Stony Brook University approved all studies with mice.

Histology and immunohistology

For histopathology, organs were fixed in 10% neutral buffered formalin, embedded in paraffin, sectioned at 1-4 μm, stained with hematoxylin and eosin,

dehydrated in graded alcohols, cleared with Histoclear (National Diagnostics) and mounted on glass slides. McClain Laboratories (Smithtown, NY) performed all sectioning and staining. The tissue sections were examined by light microscopy.

Bacterial colonization within the organs was visualized by immunohistochemistry. Organs were harvested from the intradermal infections described above, fixed overnight in formalin and frozen using liquid nitrogen. The frozen tissue samples were sectioned into 1-4 μm thick slices, fixed in acetone for 30 seconds and incubated with an anti-*Francisella tularensis* LPS rabbit polyclonal antibody (Rasmussen et al., 2006) at a 1:200 dilution in 1% bovine serum albumin (BSA) for 3 hours. The stained tissue sections were washed 3X with PBS and stained with goat anti-rabbit IgG alkaline phosphotase conjugated antibody at a 1:200 dilution in PBS + 1% BSA for 3 hours. All organ sections were stained with Vulcan Red (BIOCARTA) to visualize the secondary antibody, and stained bacteria were viewed using light microscopy. For immunohistochemistry to visualize mature caspase-3, organs were harvested from the intradermal infections described above, fixed, and frozen as described above. The sections were stained as described in Rasmussen et al., 2007. Briefly, the frozen organs were embedded in paraffin, dewaxed, and rehydrated with xylene and graded alcohols. To quench endogenous peroxidase, sections were bathed in methanol and hydrogen peroxide. The tissue sections were then blocked with BSA and stained overnight at 4°C with anti-cleaved caspase-3 rabbit polyclonal antibody (Trevigen) at a 1:500 dilution in PBS + 1% BSA. The following day all organ sections were stained with goat anti-rabbit IgG Alexa Fluor 590-conjugated secondary antibody (Invitrogen) at a 1:500 dilution in

PBS + 1% BSA for 3 hours in the dark. Tissue samples stained positive for mature caspase-3 were visualized using fluorescence microscopy.

Preparation of cells for tissue culture and bacterial infections

Murine bone marrow-derived macrophages (muBMDM) were obtained as described (Celada et al., 1984) from the femurs of female wild-type C3H/HeN or C57BL/6 mice (Jackson Laboratories), or from caspase-$1^{-/-}$ C57BL/6 mice (Lilo et al., 2008) (kindly provided by J. B. Bliska, Stony Brook University). The muBMDM were resuspended in bone marrow medium [BMM; DMEM (Invitrogen, Carlsbad, CA) containing 2 mM L-glutamine, 1 mM sodium pyruvate, 20% heat-inactivated fetal bovine serum (FBS; HyClone, Logan, UT), and 30% medium previously conditioned by L929 cells], and seeded in 24-well plates (Corning) at a concentration of 1.5 x 10^5 cells per well. The conditioned medium was obtained by plating 2 x 10^5 L929 cells in 75-cm^2 culture flasks in Minimum Essential Medium (Invitrogen) containing 2 mM L-glutamine, 1 mM sodium pyruvate, 1 mM nonessential amino acids (Invitrogen), and 10% FBS and collecting the medium after 10 days. The muBMDM were used for experiments the following day. For each *F. tularensis*, *holarctica* experiment, strains were streaked from frozen stocks to MHC and incubated at 37°C, 5% CO_2 for 48 h. A single colony was picked and grown in MHB to late-log phase (16 to 18 h) at 37°C with shaking at 100 rpm in a 5% CO_2 atmosphere. Aliquots (~1 ml) of the bacterial cultures were centrifuged, resuspended in Infection-BMM (supplemented with 5% FBS vs. 20% FBS), and added at a multiplicity of infection (MOI) of 50 to the muBMDM. Bacterial concentrations were

initially estimated by the OD_{600} of the suspension culture, and actual numbers of viable bacteria were determined by CFU counts. For each *F. tularensis*, *novicida* experiment, strains were streaked from frozen stocks to TS plates and incubated at 37°C, 5% CO_2 for 24 h. A single colony was picked and grown in TSB to late-log phase (16 to 18 h) at 37°C with shaking at 100 rpm in a 5% CO_2 atmosphere. Aliquots (~1 mL) of the bacterial cultures were centrifuged, resuspended in BMM, and added at a MOI of 50 to the muBMDM. Bacterial concentrations were initially estimated by the OD_{600} of the suspension culture, and actual numbers of viable bacteria were determined by CFU counts. All infected plates were subsequently centrifuged for 5 min at 800 *g* to facilitate contact between the macrophages and bacteria. After 2 h of co-culture at 37°C, 5% CO_2, the infected muBMDMs were washed three times with sterile PBS and incubated with 5 μg/ml gentamicin for 1 h to kill any remaining extracellular bacteria. After gentamicin treatment, cells were washed three times with PBS, and 1 ml of fresh BMM without antibiotics was added back. The plates were incubated at 37°C, 5% CO_2, until designated time points were reached.

For human monocyte derived macrophage (huMDM) infections, cells were isolated as previously described (Bolger et al., 2005) from healthy human donors. The huMDMs were plated at 2 x 10^5 cells/ml in 24-well plates (Corning), 1 ml/well, in RPMI medium (Invitrogen) supplemented with 10% (FBS) and 50 ng/ml macrophage colony stimulating factor (Sigma). The cells were cultured for 5 days, and infectedafter 6 days. For cytotoxicity lactate dehydrogenase release (LDH) experiments, infection of huMDM with *F. tularensis* strains was carried out as described above for the muBMDM infections. For cytokine detection experiments in huMDM, bacterial inoculums were

prepared as described above, but the huMDM were infected at an MOI of 10, plates were subsequently centrifuged for 5 min at 800 *g* to facilitate contact between the macrophages and bacteria, and the plates were then incubated at 37°C, 5% CO_2 until designated time points were reached.

For human umbilical vein endothelial cell (HUVEC) infections, cells were isolated by collagenase perfusion as previously described (Huang et al., 1988). HUVEC were grown to confluence on 60-mm dishes (Corning) in medium 199 supplemented with 20% heat-inactivated FBS, and 100 u/ml penicillin, 100 µg/ml streptomyocin and 2 µg/ml amphotericin B. Upon reaching confluence, 1.2 x 10^5 cells in 0.5 ml were seeded in a 48-well plate (BD Biosciences). Bacterial inoculums were prepared as described above for the muBMDM infections. HUVEC were infected at an MOI of 75 and plates were incubated (no centrifugation) for 24 h at 37°C, 5% CO_2.

For FL83B murine hepatocyte cell infections, cells were purchased from the Stony Brook University Tissue Culture Facility and cultured in F12K medium (ATCC) supplemented with 10% FBS for 5 to 6 days. Confluent monolayers were trypsinized and seeded in 24-well plates at 1 x 10^5 cells/well (Corning). The FL83B cells were used for experiments the following day. Infection was carried as described above for muBMDM, except bacteria were resuspended in F12K medium with 5% FBS and added at an MOI of 1000 to the hepatocytes.

For A549 human lung epithelial cell infections, cells were purchased from the Stony Brook Universitiy Tissue Culture Facility and cultured in DMEM (Invitrogen) supplemented with 10% FBS for 5 to 6 days. Confluent monolayers were trypsinized and seeded in 24-well plates at 1 x 10^5 cells/well (Corning). The A549 cells were used for

experiments the following day. Infection was carried as described above for muBMDM, except bacteria were resuspended in DMEM with 5% FBS and added at an MOI of 400 to the epithelial cells.

In vitro replication assays

For quantification of viable bacteria, infected muBMDMs, A549 lung epithelial cells, or FL83B murine hepatocytes were washed extensively at 2 hours post infection (HPI) and 24 HPI. Samples were lysed with water at room temperature for 10 minutes, and serial dilutions were plated to determine CFU. The amount of viable intracellular bacteria present at 2 HPI was compared to the amount of viable intracellular bacteria present at 24 HPI.

To visualize intracellular replication, the infected muBMDMs, A549 lung epithelial cells, or FL83B murine hepatocytes were washed extensively at 2 hours post infection (HPI) and 24 HPI. Cells were fixed with 2.5% *p*-formaldehyde for 30 min, washed with PBS, and permeabilized with 0.5% Triton X-100 in PBS. Cells were blocked with 3% bovine serum albumin in PBS and stained with a 1:100 dilution of rabbit antiserum to *F. tularensis* followed by a fluorescent-conjugated goat anti-rabbit IgG antibody (both from BD Biosciences, Lincoln Park, NJ). The intracellular bacteria were observed using fluorescent microcopy.

LDH assay

Macrophage infection assays were conducted as described above. At designated time points, the supernatant fractions were collected and analyzed for LDH release using the CytoTox 96 NonRadioactive Cytotoxicity Assay (Promega) according to the manufacturer's protocols. Background LDH release was measured in medium conditioned by uninfected cells, while total LDH content (= 100%) was measured using uninfected cells that were lysed by freezing and thawing.

TUNEL staining

Macrophages infected as described above were analyzed for apoptosis by terminal deoxynucleotidyl transferase-mediated dUTP nick end labeling TUNEL staining using the *In Situ* Cell Death Detection Kit, TMR red (Roche), according to the manufacturer's protocols. The cells were visualized by fluorescence microscopy using a Zeiss Axiovert S100 microscope. Images were captured using a Spot camera (Diagnostic Instruments) and processed with Adobe Photoshop. To calculate the percent TUNEL-positive cells, the total number of cells from ten different fields was divided by the number of TUNEL positive cells in those fields.

Caspase-3 detection

Murine macrophages were isolated as described above and seeded in a 96-well, white-walled plate (Corning) at a concentration of 20,000 cells/well. Three wells each

were plated for the LVS, Δ*tolC*, Δ*tolC/tolC*$^{+}$ and an uninfected negative control. Macrophage infections were conducted as described above. At 17 HPI, activated caspase-3 and caspase-7 were detected using the Caspase-Glo 3/7 Assay (Promega), according to the manufacturer's instructions. Caspase-3/7 activation was measured using a FLUOstar OPTIMA luminometer (BMG Labtech).

To detect cleaved caspase-3, infected muBMDM cells were stained with a rabbit polyclonal antibody targeted specifically against cleaved caspase-3 (Trevigen). The isolation and infection of muBMDM was conducted as described above. At 17 and 24 HPI, the cells were washed one time with PBS, fixed with p-formaldehyde for one hour at room temperature, permeabilized with 0.1% Triton X-100 for 10 minutes at room temperature, washed with PBS and incubated overnight at 4°C with the anti-cleaved caspase-3 diluted 1:500 in PBS + 1% BSA. The following day, the cells were washed 3 times with PBS and stained with a Tetramethyl Rhodamine Iso-Thiocyanate (TRITC)-conjugated, goat anti-rabbit IgG secondary antibody (Invitrogen) diluted 1:1000 in PBS + 1% BSA. The caspase-3 positive cells were quantified using fluorescence microscopy as described above for the TUNEL staining.

Detection of CXCL8, CCL2 and IL-1β secretion

MuBMDM, huMDM and HUVEC infections were conducted as described above. At 24 h PI, the conditioned media were collected, centrifuged for 10 min at 12,000 *g,* and frozen at -80°C until assayed. ELISA kits (Antigenix) were used according to the manufacturer's instructions to detect CXCL8 (IL-8), IL-1β and CCL2 (MCP-1) secretion

from the human cells. Quantikine ELISA kits (R&D Systems) were used to detect IL-1β secretion from the murine macrophages.

Statistical analysis

The CFU/g results obtained from the organ burden assays were compared using the Mann-Whitney test for non-parametric data with one-tailed probability (*P*) value. The mouse survival curves were compared using the log rank test. All other results were analyzed for significance using data obtained from three independent experiments with multiple replicates unless otherwise stated. *P* values were calculated by one-way analysis of variance and Tukey's multiple-comparison posttest. Statistical calculations were performed using Prism 4.0 (GraphPad Software). *P* values < 0.05 were considered significant.

Antibody Production

To develop antibodies directed against TolC and FtlC, purified proteins were injected into rabbits and immune serum collected some three month later. To purify the proteins, His-tags were added to the 3' end of the *tolC* and *ftlC* genes. Primers TA4782F and TA6362R-His and TB5224F and TB6588R-His were used, respectively, to amplify the *tolC* and *ftlC* genes with a C-terminal His-tag (Table 2). The primers were also designed with restriction enzyme sites, to enable ligation into the pBAD18 vector. Utilizing the restriction enzyme sites, the amplified genes were cloned into the arabinose inducible vector pBAD18, and then transformed into the *E. coli* TUNER strain (Table 1). The resultant vectors were named pBAD18-TA and pBAD18-TB (Table 1). The wild-

type LVS *ftlC* gene contains an unusual TTG start codon, which reduced expression of the protein. Primers TB(ATG)F and TB(ATG)R were used to amplify the *ftlC* gene. Then using a Stratagene Quick Change Kit®, the TTG start codon of the *ftlC* was point mutated to an ATG start codon following manufacturer's instructions. The resultant vector was named pBAD18-TB(ATG)(His); this vector was used for all subsequent experiments requiring a His-tagged *ftlC* (Table 1). As described in Saulino *et al*., 500 ml cultures of the TUNER strains harboring the *tolC*(His) and *ftlC*(His) pBAD18 vectors were grown, and the outer and inner membranes of the bacteria were separated using a French press. Fast protein liquid chromatography (FPLC) was used to purify the his-tagged proteins. Additional His-tagged TolC and FtlC protein was purified at the Wadsworth Center, NYS Department of Health in Albany, New York. This protein purification was achieved by isolating the protein from inclusion bodies. To retain the proteins within inclusion bodies and not have them targeted to the outer membrane, the signal sequence, located on the N-termini of the genes, was removed. Primers Nhe-4782F and SalI-6364R, and Nde-5298F and EcoRI-6588R, were used to amplify the genes just downstream of their respective signal sequences (Table 2). The primers were also designed with new restriction enzyme sites, to enable ligation into the pET-28a vector. The resultant vectors were named pET-28a-TA and pET-28a-TB (Table 1). These vectors were transformed into *E. coli* BL21(DE3) strain. The BL21(DE3) strains harboring the pET-28a-TA and pET-28a-TB were shipped to the Wadsworth Center, and the proteins were purified using FPLC.

Once the TolC and FtlC proteins were purified, they were injected into rabbits to generate polyclonal antibodies. Two rabbits were pre-bled and then subcutaneously (SC)

injected with Freund's Complete Adjuvant (CA) (Pierce) and purified TolC or FtlC. Total protein concentration was 100 μg in 400 μl. Two weeks later, the rabbits were boosted with a SC injection of Freund's incomplete adjuvant (IA) (Sigma) and purified TolC or FtlC. Ten days later, the rabbits were boosted with a SC injection of IA and purified TolC or FtlC. Five days later, the rabbits were bled to check titers. Three weeks later, a final boost of protein in PBS was administered by SC injection, and five days later, approximately 90 ml of serum from the rabbit injected with purified TolC protein and 75 ml of serum from the rabbit injected with purified FtlC protein was prepared.

Complementation of *E. coli* Δ*tolC* with *F. tularensis tolC*

E. coli RAM strains containing TolC transposon mutations, listed in Table 1, were complemented with *tolC (*pGPTA) or *ftlC* (pGPTB) rescue vectors. Three assays were performed on the RAM strains: MacConkey plating assays, colicin sensitivity assays, and hemolysin secretion assays. For MacConkey plating assays, MacConkey agar plates were made as described in McCleery and Rowe, 1995 (McCleery and Rowe, 1995). The *E. coli* RAM strains were grown as single colonies on LB plates (supplemented with appropriate antibiotics), incubated overnight at 37°C. The following day a single colony was picked and streaked onto the MacConkey plates and grown overnight at 37°C, and the plates were monitored for bacterial growth. For colicin sensitivity assays, the *E. coli* RAM strains were grown overnight on LB plates (supplemented with appropriate antibiotics) at 37°C and then suspended into 5 ml of MHB. The bacteria were spread with a cotton swab onto MHC (supplemented with appropriate antibiotics) to obtain a bacterial lawn. Sterile discs (Becton Dickinson, San Jose, CA) soaked with different concentrations of colicin E1

(Sigma) were placed on the plates. After 24 hours of growth at 37°C, halos around the discs were measured as the diameter of the zone of inhibition including the diameter of the disc (6 mm). For hemolysin secretion assays, the *E. coli* RAM strains were grown overnight on LB plates (supplemented with appropriate antibiotics) at 37°C, and then a single colony was streaked onto LB (supplemented with appropriate antibiotics), which contained 5% sheep's blood (Colorado Serum Company). After 24 hours of growth at 37°C, lysis of the red blood cells around the bacterial growth was measured. The experiments were repeated at least three times for each strain.

Siderophore Assays

For siderophore secretion assays, the LVS, Δ*tolC* and Δ*ftlC* were plated on MHC plates and incubated for 48 hours at 37°C, 5% CO_2. After growth, a single colony was inoculated into Chamberlain's defined media (CDM) containing 0 μg/ml, 0.1 μg/ml, or 2 μg/ml of ferric oxide (FeIII). CDM was prepared as described in Chamberlain, 1965 (Chamberlain, 1965), with the K_2HPO_4 and K_2HPO_3 withheld. This medium was then stirred overnight at 4°C with 1% w/v Chelex-100, (Sigma Aldrich) to remove trace amounts of iron from the medium. The following day, the CDM was divided into three aliquots, and various concentrations of FeIII listed above were added back to the respective CDM preparations. One 50 ml culture of each CDM preparation was inoculated with a single colony of the LVS, Δ*tolC* or Δ*ftlC*, and these cultures were grown at 37°C with shaking (200 rpm). After growth, a Chrome Azurol S (CAS) assay was performed. The CAS assay is described in Schwyn and Neilands, 1987. The assay measures the amount of free siderophore. CAS is mixed with iron to form a dye-Fe complex. When a strong chelator

such as siderophore is present, it removes the iron from the dye, changing the solution color from blue to orange (Schwyn and Neilands, 1987). After 55 hours of growth, 1 ml of each culture was centrifuged at 6500 *g* for 5 minutes to remove whole bacteria. Supernatants were then added to CAS reagent (60.5 g of CAS in 50 ml of water, plus 10 ml of FeIII solution [1 mM FeIII and 2 mM HCl] and 40 ml of HDTMA [72.9 mg in 40 ml H_2O]) and 1% shuttle solution [CAS reagent and 4 mM 5-sulfosalicylic acid] at a 1:1 ratio in 96-well flat bottom plate (Corning). A SPECTRAmax plate reader was used to measure absorbance (λ 630) once reagents were mixed together and 30 minutes after reagents were mixed together.

Secretion Profiles

LVS and Δ*tolC* strains were grown on MHC plates as a 100 μl spot; these plates were grown for 48 hours at 37°C, 5% CO_2. The entire spot was scraped into 10 ml of CDM. This culture was then used to inoculate 400 ml of CDM, and then the culture was grown at 37°C, 5% CO_2, with shaking for 5 and 17 hours. At designated time points, 200 ml of culture was centrifuged at 6,500 g for 5 minutes to pellet out bacteria. The supernatants were then filtered twice through a 0.2 micron filter to remove any trace bacteria. The proteins in the filtered supernatants were concentrated using an Amicon Ultra15 centrifugal filter device as per manufacturer's instructions (Millipore). A Better Bradford Protein Assay (Pierce) was performed to quantify the amount of protein present in the samples. Equal amounts of protein were resuspended in 4X SDS buffer and heated at 96°C for 10 minutes. The protein samples (20 μg/well) were loaded onto two 15% acrylamide gels, electrophoresed, and stained with Coomassie stain or silver stain. The resulting gels were dried and compared for differences in protein banding patterns.

Hemolysin Secretion Assay with subspecies *novicida*

Subspecies *novicida* strain U112 and transposon mutants U112 FTN_1703::Tn18, U112 FTN_0079::Tn18, and U112 FTN_1277::Tn18 were grown overnight on TS plates at 37°C. The following day, a single colony was used to inoculate 50 ml of TS broth. These cultures were grown overnight at 37°C, 5% CO_2, with shaking. The following day the cultures were centrifuged at 6500 g for 5 minutes, and resuspended in PBS, and OD_{600} measurements were taken. Diluting bacteria in PBS normalized the bacterial concentrations. The bacteria were then added in a 1:1 ratio of culture to horse red blood cells (Colorado Serum Company) to a 24-well plate (Corning) and incubated at 37°C, 5% CO_2 for 48, 72, 84 and 120 hours. At each designated time point, the plate was removed from the incubator, and 100 μl of PBS was added to each well. The plate was then centrifuged at 300 *g* for 10 minutes. The top-most 100 μl was then carefully transferred to a new plate and A_{540} measurements taken (Lai et al., 2003). Red blood cells that were destroyed due to hemolytic activity of the wild-type *novicida* U112 and transposon mutants caused the supernatant to turn red in color.

Table 2.1 Strains & Plasmids

Bacteria or plasmid	Characteristics	Source or Ref.
E. coli		
DH5α	F- (ϕ80dlacZΔM15) recA1 endA1 gyrA96 thi-1 hsdR17 (r-k m+k) supE44 relA1 deoR Δ(lacZYA –argF) U169	Hayes, E. B.
TUNER	Tuner strains are lacZY deletion mutants of BL21, IPTG inducible	Novagene
BL21(DE3)	BL21 lacks lon (3), ompT proteases, and lacZY	Stratagene
S17-1	thi thr leu tonA lacY supE recA::RP4-2-Tc::Mu, Kn::Tn7	Hughes, J.M.
SF110	F- (ΔlacX74 galE galK thi rpsL, ΔphoA degP41, ΔompT)	Sjostedt, A.
RAM 958	Tn10:48, tetR	Misra, R.
RAM 960	Tn10:48, tetR, pTrC-*tolC*+, AmpR	Misra, R.
RAM 970	Tn10:48, tetR, pHly (SF4000 HlyA operon), ClmR	Misra, R.
RAM 972	Tn10:48, tetR, pTrC-tolC+, AmpR, pHly, ClmR	Misra, R.
RAM 958-gfp	Tn10:48, tetR, pFNLTP6-gro-gfp	This study
RAM 958-TA	Tn10:48, tetR, pFNLTP6 gro-gfp with gfp replaced by *tolC*	This study
RAM 958-TB	Tn10:48, tetR, pFNLTP6 gro-gfp with gfp replaced by *ftlC*	This study
RAM 970-gfp	Tn10:48, tetR, pHly, ClmR, pFNLTP6-gro-gfp	This study
RAM 970-TA	Tn10:48, tetR, pHly, ClmR, pFNLTP6-gro-gfp, gfp replaced by tolC	This study
RAM 970-TB	Tn10:48, tetR, pHly, ClmR, pFNLTP6-gro-gfp, gfp replaced by ftlC	This study
RAM 958-BADA	Tn10:48, tetR, pBAD18-tolC(His)	This study
RAM 958-BADB	Tn10:48, tetR, pBAD18-ftlC(His)	This study
RAM 970-BADA	Tn10:48, tetR, pHly, ClmR, pBAD18-tolC(His)	This study
RAM 970-BADB	Tn10:48, tetR, pHly, ClmR, pBAD18-ftlC(His)	This study
F. tularensis		
LVS	Pmr; Vaccine Strain; *Francisella tularensis* subspecies *holarctica*	ATCC 29684, Elkins, K.
DTH1	LVS ΔtolC	This study
DTB3	LVS ΔftlC	This study

U112	*Francisella tularensis* subspecies *novicida*	ATCC 15482, Klose, K
U112 Tn:1703	U112 with transposon insert gene position 1703, KanR	U. Washington
U112 Tn:0779	U112 with transposon insert gene position 0779, KanR	U. Washington
U112 Tn:1277	U112 with transposon insert gene position 1277, KanR	U. Washington
U112 Tn:0720	U112 with transposon insert gene position 0720, KanR	U. Washington
U112 Tn:0793	U112 with transposon insert gene position 0793, KanR	U. Washington
U112 Tn:0757	U112 with transposon insert gene position 0757, KanR	U. Washington
U112 Tn:1692	U112 with transposon insert gene position 1692, KanR	U. Washington
U112 Tn:1609	U112 with transposon insert gene position 1609, KanR	U. Washington
U112 Tn:0029	U112 with transposon insert gene position 0029, KanR	U. Washington
U112 Tn:1276	U112 with transposon insert gene position 1276, KanR	U. Washington
U112 Tn:0718	U112 with transposon insert gene position 0718, KanR	U. Washington
U112 Tn:0454	U112 with transposon insert gene position 0454, KanR	U. Washington
U112 Tn:1275	U112 with transposon insert gene position 1275, KanR	U. Washington
U112 Tn:1693	U112 with transposon insert gene position 1693, KanR	U. Washington
U112 Tn:1610	U112 with transposon insert gene position 1610, KanR	U. Washington
Plasmids		
pGEM Easy	AmpR; PCR cloning vector	Promega
pPV	AmpR, ClmR, sacB, mob; vector for allelic replacement in F.t.	Pavlov, V.
pFNLTP6 gro-gfp	AmpR, KanR; contains gfp under control of F.t. groE promoter	Zahrt, T.C.
pPVTAH1	pPV with upstream and downstream regions of tolC	This study
pPVTBH3	pPV with upstream and downstream regions of ftlC	This study
pGPTA	pFNLTP6 gro-gfp with gfp replaced by tolC	This study
pGPTB	pFNLTP6 gro-gfp with gfp replaced by ftlC	This study
pBAD18	Arabinose inducible AraC promoter	Beckwith Lab
pBAD-TA(His)	pBAD18-tolC+(His-tag)	This study
pBAD-	pBAD18-ftlC+(His-tag)	This study

TB(His)		
pBAD-TB(ATG-His)	pBAD18-ftlC+(His-tag), plus ATG start codon	This study
pET28a	pPET28A, high copy number plasmid	Novagen
pET28a-TA	pPET28A-tolC+(His)(N-terminal signal sequence removed)	This study
pET28a-TB	pPET28A-ftlC+(His)(N-terminal signal sequence removed), ATG start	This study
pMP590	KanR, sacB, groE promoter; vector for allelic replacement in SchuS4	Pavelka, M.
pMP620	HygR, gro-E promoter; vector for complementation in Schus4	Pavelka, M.

AmpR, ampicllin resistance; ClmR, chloramphenicol resistance;
Kanr, kanamycin resistance, Pmr, polymyxin B resistant.

Table 2.2 Primers

Primer	Sequence*	Features
TA3522F	5'- CAG TCT CAT AAT TTA CAG C	Sequencing upstream of *tolC*
TA3580F	5'- CCT CCA AAG CAA ACA TAC G	Sequencing *tolC*
TA5309F	5'- CTC AGG TTC TTT TTG ATT GG	Sequencing *tolC* (I1)†
TA5891R	5'- TTT CGG CTA TTT GTG CTG G	Sequencing *tolC* (I2)†
TA6065F	5'- TAC GCT GGT ACA GTA GAG GC	Sequencing *tolC*
TA7895R	5'- GCA AAT GTT GGC ATA TTA CC	Sequencing downstream of *tolC*
TABAMHR	5'- ATC A**GG ATC C**TT ACT CCG TTG CAA TCT GC*	Cloning *tolC* with *Bam*HI site
TANHEIF	5'- ATA A**GC TAG C**CT CCA AAG CAA ACA TAC G	Cloning *tolC* with *NheI* site
TB3598F	5'- GGA GCT TGT AAG CCA GAT GG	Sequencing upstream of *ftl*C
TB5124F	5'- TGA TAT GGC TCA AGG TGG TGG	Sequencing upstream of *ftlC*
TB5593F	5'- CAG CAC AGT TTG CCC AAC AGG	Sequencing *ftlC* (I2)†
TB6588R	5'- TTA TAG CTC CAC GTC TTG ACC	Sequencing *ftlC* (I1)†
TB7913R	5'- CCA CCT TTA GGT TTA CCT GG	Sequencing upstream of *ftl*C
TBBAMHR	5'- ATA T**GG ATC C**TT ATA GCT CCA CGT CTT GAC C	Cloning *ftlC* with *Bam*HI site
TBNHEIF	5'- GG**G CTA GC**T GAT ATG GCT CAA GGT GGT GG	Cloning *ftlC* with *Nhe*I site
UTA3580F	5'- ACT G**GT CGA C**AA CAA GCA TTA TCA TCC CTG G	Cloning upstream *tolC* region with *Sal*I site
UTAXBAI	5'- GCA A**TC TAG A**TA CCA ATA GGT CTT CCT GC	Cloning upstream *tolC* region with *Xba*I site
UTA4131F	5'- GTA GTA AGG TTT CTT TTG CTG TGG	Sequencing upstream of *tolC* (E1)†
UTB3755F	5'- GCA A**GT CGA C**AC AAT ATC TGG GGA AGT AGC	Cloning upstream *ftl*C region with *Sal*I site
UTBPSTI	5'- TGA T**CT GCA G**TA CTA GTA TAG TCA GCT ACA GG	Cloning upstream *ftlC* region with *Pst*I site
UTB4268F	5'- ACA GCT GCT AAT CAT AGT GC	Sequencing upstream of *ftlC* (E1)†
DTA7791R	5'- ACC C**GT CGA C**GC GAT ATT GGT AAT CTA AAG TCC C	Cloning downstream *tolC* region, *SalI* site
DTAXBAI	5'- TCT G**TC TAG A**CA GGT ATA GCT TCT GTA AAA GCG	Cloning downstream *tolC* region, *XbaI* site
DTA7334R	5'- GCT GAA GAG TTC CAT AGG TTT GC	Sequencing downstream of *tolC* (E2)†
DTB7802R	5'- AAT A**GT CGA C**CC TTC ACA GCT GCT GCA AAT GG	Cloning downstream *ftlC* region, *Sal*I site
DTBPSTI	5'- GGA G**CT GCA G**TC AGA ATG ATG CGA TG TAT GC	Cloning downstream *ftlC* region, *Pst*I site
DTB7264R	5'- CTT TAC CGA CTA TTG ATA CC	Sequencing downstream of *ftlC*

		(E2)†
PILT186F	5’- GCT GAT AGA AAC CTA CGA ATG TG	Detecting *pilT* (T1)
PILT682R	5’- TCC CTA AAA CCA AAT GCC C	Detecting *pilT* (T2)
SAC1243R	5’- TTC CTT TCG CTT GAG GTA CAG C	Detecting *sacB* (S1)
SAC787F	5’- GCA AAC ACT GGA ACT GAA GAT GG	Detecting *sacB* (S2)
SP6	5’- CGA TTT AGG TGA CAC TAT AG	Sequencing insert in pGEM easy vector
T7	5’- TAA TAC GAC TCA CTA TAG GG	Sequencing insert in pGEM easy vector
TA6364R-His	5' - ATC AGT CGA CTT AGT GAT GGT GAT GGT GAT GCT -	C-Terminal His-Tag *tolC*
	CCG TTG CAA TCT GCG ATA TTA TAT CTG	
TB6588R-His	5'- ATC GGA ATT CTT AAT GGT GAT GGT GAT GGT GTA -	C-Terminal His-Tag *ftlC*
	GCT CCA CGT CTT GAC CTA ATA GTA ACC	
TB(ATG)F	5'- GAG TAG TGG TGG CAT GAA AGT AGT GCG	Point mutation TTG to ATG for *ftlC*
TB(ATG)R	5'- CGC ACT ACT TTC ATG CCA CCA CTA CTC	Point mutation TTG to ATG for *ftlC*
Nhe-4782F	5'- GCT **GCT AGC** AAT GAA GAT ACG CCT GTT	Nhe-1 site, remove Signal Seq. from *tolC*
SalI-6364R	5'- ATC A**CT CGA C**TT ACT CCG TTG CAA TCT GC	Sal-1 site, remove Signal Seq. from *tolC*
Nde-5298F	5'- GCT CGT ACT **CAT ATG** AAT CCT GTA GCT GAC TAT ACT	Nde-1 site, remove Signal Seq. from ftl*C*
EcoRI-6588R	5’- ATCG**GAATTC**TTA TAG CTC CAC GTC TTG ACC	EcoRI site, remove Signal Seq. from ftl*C*

*Bold letters indicate restriction sites.

†These primers were also used to verify the *tolC* and *ftlC* deletions.

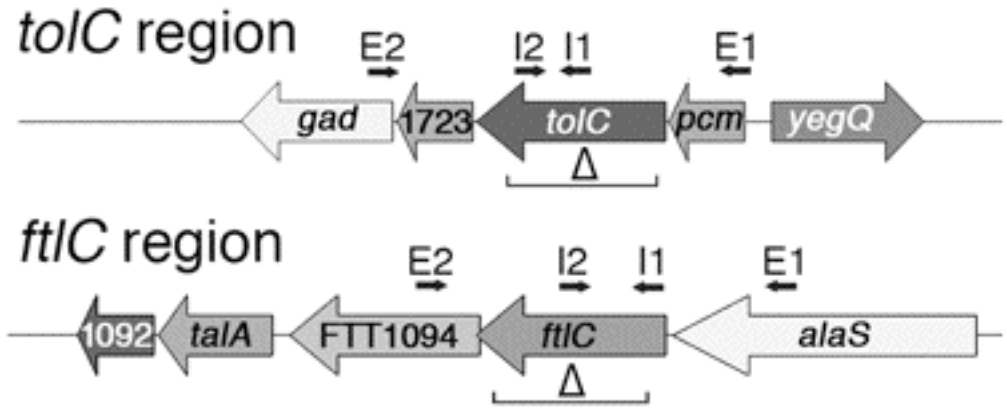

Figure 2.1 Chromosome regions encoding *tolC* and *ftlC*. The genes and predicted functions in the *tolC* region are: *gad*, glutamate decarboxylase; FTT1723, 4'-phosphopantetheinyl transferase; *pcm*, protein L-isoaspartate O-methyltransferase; *yegQ*, protease. *tolC* may be in an operon together with *pcm* and FTT1723, with a possible promoter located upstream of *pcm*. The genes and predicted functions in the *ftlC* region are: FTT1092, hypothetical protein; *talA*, transaldolase; FTT1094, cytosol aminopeptidase; *alaS*, alanyl tRNA synthetase. *ftlC* likely forms an operon together with FTT1094 and possibly *alaS*. The regions deleted in *tolC* and *ftlC* are indicated, as are the locations of the internal (I1 and I2) and external (E1 and E2) primers used for PCR.

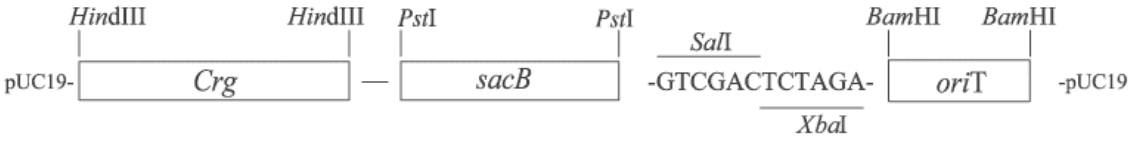

Figure 2.2 Description of the genes inserted in the multicloning site of pUC19 to yield the pPV suicide vector. *Crg,* Clm resistance gene (*Shigella flexneri*); *sacB* gene (*Bacillus subtilis*); origin of transfer (*oriT*). This image was taken from Golovliov *et al.,* 2003.

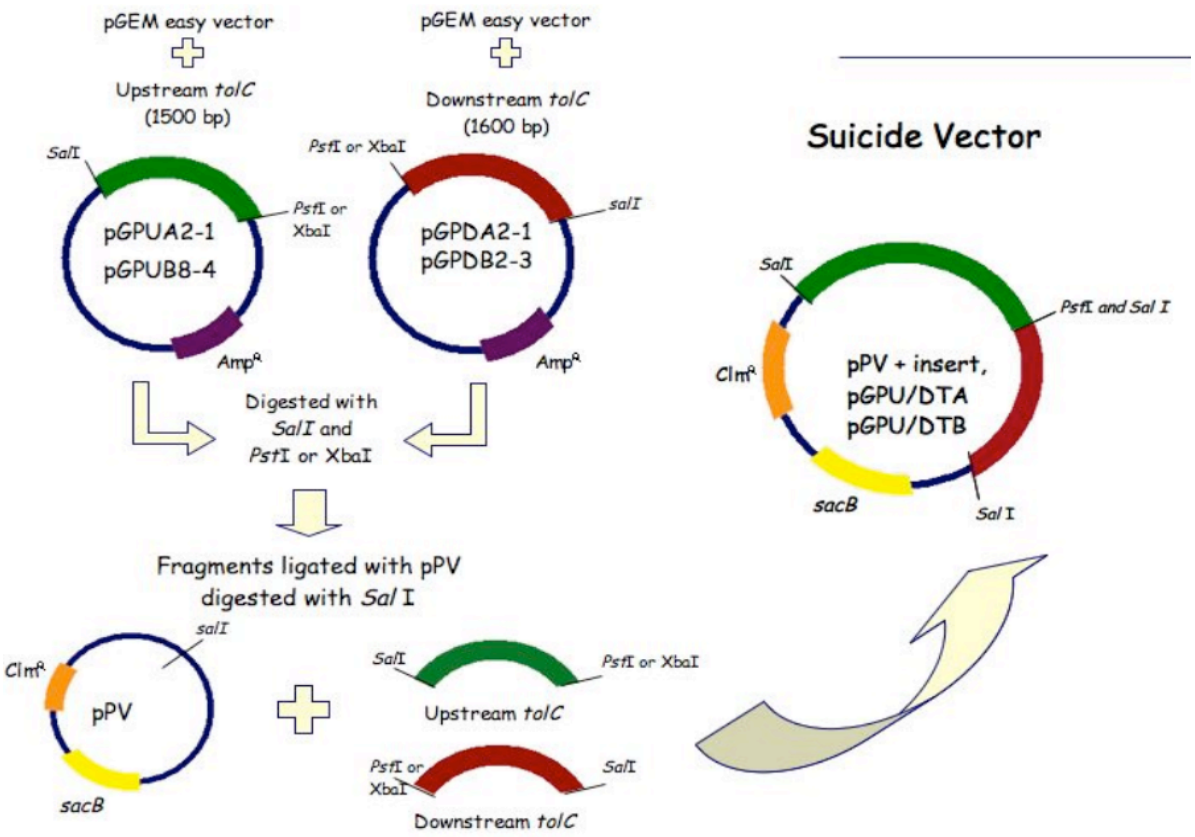

Figure 2.3 Construction of the suicide vectors. Genomic regions flanking the respective TolC homologs were amplified by PCR and cloned into the pGEM Easy Vector System. The fragments were then ligated into the pPV suicide vector.

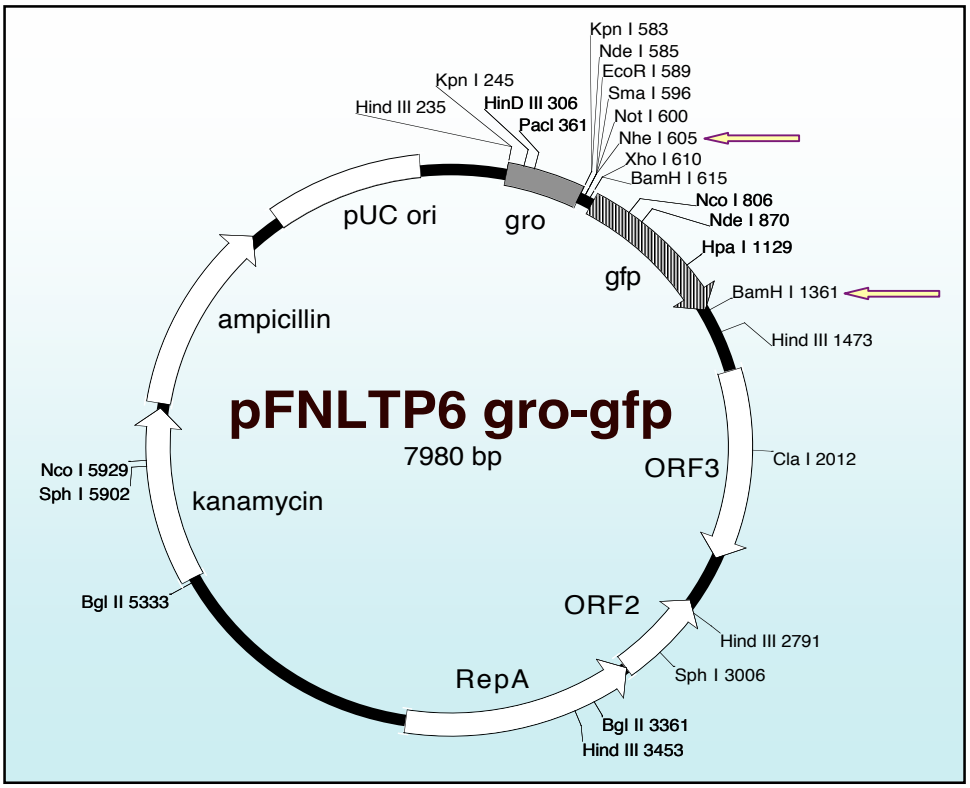

Figure 2.4 The *F. tularensis* expression vector pFNLTP6-gro-gfp. The *tolC* and *ftlC* genes were cloned into the multiple cloning site using the NheI and BamHI restriction sites. The constitutively active *F. tularensis groESL* promoter drives expression. Figure provided by T. C. Zahrt.

Chapter Three

Deletion of TolC orthologs in *Francisella tularensis* identifies roles in multidrug resistance and virulence

I. Introduction

We report here that the *F. tularensis* genome encodes two orthologs of the *E. coli* TolC protein, termed *tolC* and *ftlC*. TolC is the prototypical OM channel component utilized by multidrug efflux pumps and the type I secretion system. The type I system consists of three separate components: an outer membrane channel-forming protein, a periplasmic adaptor or membrane fusion protein, and an inner-membrane pump that typically belongs to the ATP-binding cassette (ABC) family (Holland et al., 2005; Koronakis et al., 2000). Type I secretion systems are important for the virulence of a variety of Gram-negative bacteria and are required for the secretion of different toxins, proteases and lipases (Delepelaire, 2004; Koronakis et al., 2004). The prototypical *E. coli* type I secretion system is required for hemolysin secretion (Koronakis and Hughes, 1993). TolC is also involved in multidrug efflux systems that are responsible for resistance to a broad range of detergents, dyes and antibiotics (Zgurskaya and Nikaido, 1999).

In this study, we constructed *tolC* and *ftlC* deletion mutants in the LVS using an allelic replacement technique. We found that both *tolC* and *ftlC* function in multidrug efflux. Deletion of either *tolC* or *ftlC* caused increased sensitivity to various antibiotics, detergents and dyes, indicating both genes are involved in the multidrug resistance machinery of *F. tularensis*. When the deletion strains were complemented with a wild-type copy of either *tolC* or *ftlC* in *trans,* the observed increase in sensitivity to various antibiotics was restored to levels observed with the LVS. Intradermal murine infections showed that the Δ*tolC* strain, but not the Δ*ftlC* strain, was attenuated for virulence. This suggests that TolC is a critical virulence factor of *F. tularensis* in addition to its role in multidrug resistance, which suggests the presence of a functioning type I secretion system. Neither the *tolC* nor *ftlC* gene is required for intracellular replication of the LVS in murine bone marrow-derived macrophages (muBMDM), murine hepatocytes or human lung epithelial cells; this is in contrast to other deletion mutants of *F. tularensis* reported in the literature, which are attenuated in vivo but are unable to replicate intracellularly.

II. Results

F. tularensis has two genes with high homology to TolC

Using BLAST analysis of the *F. tularensis* SchuS4 genome (Altschul et al., 1990; Larsson et al., 2005), we identified two open reading frames sharing significant homology with the *E. coli* TolC protein (NP_755652) (Figure 2.1). TolC is the prototypical OM channel component of both type I protein secretion and multidrug efflux systems (Delepelaire, 2004; Koronakis et al., 2004). One *F. tularensis* ortholog was already annotated as *tolC* (FTT1724) in the SchuS4 genome. For the second ortholog, which is annotated as a hypothetical gene (FTT1095), we propose the name *ftlC*, for *Francisella tolC*. BLAST analysis of the LVS genome (http://bbrp.llnl.gov/bbrp/html/microbe.html) revealed that it also contains both *tolC* and *ftlC* and that both genes are intact. In addition, we amplified both genes from *F. tularensis* subspecies *novicida* strain U112 by PCR. Sequencing of the PCR products revealed that both genes are intact in U112 as well (GenBank accession number DQ394299 for *tolC* and DQ394298 for *ftlC*).

F. tularensis tolC and *ftlC* code for proteins of 509 and 460 amino acids, respectively, compared to 506 amino acids for *E. coli* TolC. *F. tularensis* TolC has 20% identity and 32% similarity (identical plus similar residues) with *E. coli* TolC. FtlC has 18% identity and 30% similarity with *E. coli* TolC. *F. tularensis* TolC and FtlC share 23% identity and 38% similarity with each other and both proteins are highly conserved among the three *Francisella* subspecies. Both *F. tularensis* proteins contain predicted leader sequences, with the cleavage site for TolC located between residues 19-20 (ALA↓NE) and for FtlC between residues 23-24 (SIA↓NP). TolC and FtlC are predicted

to localize to the OM and both contain duplicate domains belonging to the OM efflux protein family (pfam02321) (Delepelaire, 2004). These domains are hallmarks of TolC proteins and form part of the TolC domain (COG1538) (Tatusov et al., 2000). The *ftlC* gene has an unusual initial codon (TTG), which suggests that the expression of this protein is low. The *tolC* gene is surrounded by two open reading frames that encode transferases and could be part of an operon together with these two genes (Figure. 2.1). A predicted promoter is located upstream of the *pcm* gene. The *ftlC* gene is surrounded by *alaS* and open reading frame FTT1094, which encodes an aminopeptidase. The initial codon for FTT1094 is within *ftlC* and is likely part of an operon together with *ftlC* and possibly *alaS*.

Construction of LVS mutants deleted for *tolC* or *ftlC*

Tools for the genetic manipulation of *F. tularensis* have only recently become available (Golovliov et al., 2003b; Lauriano et al., 2003; Maier et al., 2004). We used the allelic replacement method of Goloviov et al. to construct deletion mutations of *tolC* and *ftlC* in the LVS (Golovliov et al., 2003b). The allelic replacement technique used to delete *tolC* or *ftlC* requires double homologous recombination events (Figure 3.1). The pPV-derived suicide vector (Figure 2.4), introduced into the LVS by conjugation, integrates into the LVS chromosome by a single homologous recombination event between the cloned upstream or downstream regions of the target gene in the suicide vector and the chromosome (Figure 3.1, upper part of figure). This first recombination generates an intermediate strain containing the plasmid genes incorporated into the

chromosome. As a result, the intermediate strain is chloramphenicol-resistant and sucrose-sensitive (Figure 3.1, middle part of figure). Plating this intermediate strain on sucrose-containing medium allows selection for a second recombination event. In this step, the bacteria eliminate *sacB* and the other vector-encoded genes from the chromosome. If the desired recombination occurs, the wild-type copy of the target gene is also eliminated, leaving only the deleted gene (Figure 3.1, lower part of figure). Proper construction of strains DTH1 (Δ*tolC*) and DTB3 (Δ*ftlC*) was validated both phenotypically and genotypically. Intermediate strains obtained after the first recombination event, which contain the *crg* and *sacB* genes from the suicide vector integrated into the chromosome (Figure 3.2), were resistant to chloramphenicol and sensitive to sucrose compared with the parental LVS. In contrast, the final deletion strains, obtained after the second recombination event, were sensitive to chloramphenicol and resistant to sucrose (Figure 3.2). PCR products could be amplified from the intermediate strains using primer pairs both internal and external to *tolC* or *ftlC* (Figure 3.3). The expected simultaneous presence of the intact and truncated target gene was detected in the *tolC* intermediate strain (Figure 3.3, lane 1). However, only the amplicon corresponding to the truncated gene was detected in the *ftlC* intermediate strain (Figure 3.3, lane 1). We believe this was due to preferential amplification of the smaller PCR product from the truncated gene. Note that in both intermediate strains, integration of the suicide plasmid was verified by amplification of the *sacB* gene (Figure 3.3, lanes 1 and 3, bottom row). In contrast to the intermediate strains, only the external primers generated products with the final deletion strains (Figure 3.3, lane 2). The amplicons were smaller in size compared to the parental LVS (Figure 3.3, lane 4), as expected for deletion of the

genes. In addition, *sacB* was no longer detected in the final deletion strains (Figure 3.3, lane 2, bottom row), confirming loss of the vector genes during the second recombination event. We also verified that all intermediate and final strains were *F. tularensis* and not contaminants by using PCR to detect the *F. tularensis pilT* gene (Gil et al., 2004) (data not shown). Growth curve analysis was performed to determine if the Δ*tolC* or Δ*ftlC* mutants were defective for growth in liquid media. Our data shows that neither deletion strain is defective for growth (Figure 3.4).

Complementation of the *tolC* and *ftlC* deletion strains

Vectors for stable gene expression in *F. tularensis* have only recently become available (Maier et al., 2004). We cloned the *tolC* and *ftlC* genes from the LVS by PCR and placed them under control of the constitutive *groE* promoter in the *F. tularensis* expression vector pFNLTP6-gro-gfp (Figure 2.4) (Maier et al., 2004). The resulting plasmids, pGPTA (*tolC*) and pGPTB (*ftlC*), were used to complement the Δ*tolC* and Δ*ftlC* mutant strains, respectively (Table 1).

TolC and FtlC are part of the multidrug resistance machinery of *F. tularensis*

TolC serves as the OM channel component for multidrug efflux pumps that provide resistance to a variety of antibiotics, detergents, dyes and other harmful compounds (Koronakis et al., 2004). In fact, TolC mutants of *E. coli* exhibit increased

sensitivity to these substances (Delepelaire, 2004). We tested Δ*tolC* and Δ*ftlC* for sensitivity to a variety of agents using a disk diffusion assay. As shown in Table 3.1, both deletion mutants had increased sensitivity to a number of different antibiotics, detergents and dyes compared to the parental LVS. Thus, both *tolC* and *ftlC* participate in multidrug resistance in *F. tularensis*. The drug sensitivity profiles for Δ*tolC* and Δ*ftlC* strains were similar, suggesting either that TolC and FtlC participate in the same multidrug efflux pathway or that independent efflux systems are present that recognize similar substrates. Deletion of *tolC* or *ftlC* did not increase sensitivity to all the drugs tested; therefore, the drug resistance phenotype was not due to a non-specific effect on the bacteria or a defect in OM integrity due to loss of TolC or FtlC. This conclusion is supported by the fact that no increased sensitivity to vancomycin, which is unable to penetrate the intact OM of Gram-negative bacteria (Vaara and Nurminen, 1999), was detected in the mutant strains (Table 3). Furthermore, the OM protein profiles of Δ*tolC* and Δ*ftlC* strains were similar to the profile of the parental LVS, and no differences in the lipopolysaccharide profiles of the strains were observed (data not shown). As shown in Figure 3.5, expression of *tolC* or *ftlC* in trans restored drug sensitivity of the mutants back to levels matching the parental LVS. This observation confirms that the multidrug sensitivity of the deletion strains was due to loss of *tolC* or *ftlC* and not caused by a secondary effect.

Deletion of *tolC* attenuates virulence of the LVS in mice

We next examined the roles of *tolC* and *ftlC* in virulence using a mouse model of tularemia. Groups of five mice were inoculated intradermally with the LVS, Δ*tolC* or

Δ*ftlC*, and the mice were monitored for survival for fifteen days. In the experiment shown in Figure 3.6, mice inoculated with 10^7 colony-forming units (CFU) of the LVS or strain Δ*ftlC* began succumbing to the infection days two and three post-inoculation and all mice died by day five. In comparison, strain Δ*tolC* was highly attenuated, with only one mouse dying on day five (Figure 3.6, panel A). Similarly, none of the mice inoculated with 10^6 CFU of strain Δ*tolC* succumbed to infection (Figure 3.6, panel B), whereas 4 or 3 mice inoculated with the LVS or Δ*ftlC*, respectively, died by day six. In total, 91% of mice inoculated with 10^7 or 10^6 CFU of the LVS died compared to only 17% of mice inoculated with strain Δ*tolC* (DTH1). Thus, *tolC* is critical for virulence of the LVS in mice by the intradermal route. In contrast, *ftlC* does not appear to play an important role in virulence, as strain Δ*ftlC* behaved similarly to the LVS (Figure 3.6).

To confirm the role of *tolC* in virulence, we conducted mouse experiments as described above, comparing the LVS, Δ*tolC*, and Δ*tolC*/*tolC*$^+$ strains. As shown in Figure 3.6, panel C, expression of *tolC* in trans restored the virulence of Δ*tolC* strain when mice were inoculated with 10^7 CFU. This confirms that the virulence defect of strain Δ*tolC* was specifically due to loss of *tolC*. However, complementation of the *tolC* deletion was partial, as not all mice inoculated with 10^7 CFU of Δ*tolC*/*tolC*$^+$ succumbed to infection (Figure 3.6, panel C). This was likely due to use of the heterologous *groE* promoter to drive expression of *tolC* from plasmid pGPTA. Nonetheless, our results clearly demonstrate that *tolC* is an important virulence determinant of the LVS.

The LVS Δ*tolC* is attenuated for infection of mice by the intranasal route

The analysis of intradermally infected mice suggested that the TolC of *F. tularensis* is a virulence factor as the *tolC* deletion mutant was attenuated for virulence. To assess ithe role of TolC during an intranasal infection we compared the virulence of the Δ*tolC* mutant and wild-type LVS in mice infected via the intranasal route. Groups of five mice were intranasally inoculated with the LVS, Δ*tolC* or Δ*tolC*/*tolC*$^{+}$, and the mice were monitored for survival for eighteen days. In the experiment shown in Figure 3.7, mice inoculated with 10^5 CFU of the LVS began succumbing to the infection days nine post-inoculation, and all mice died by day fifteen. In comparison, strain Δ*tolC* was highly attenuated; none of the mice inoculated with 10^5 CFU of strain Δ*tolC* succumbed to infection (Figure 3.7). Expression of *tolC* in trans restored the virulence of the Δ*tolC* strain, confirming that the virulence defect of strain Δ*tolC* was specifically due to loss of *tolC*. Again, complementation of the *tolC* deletion was partial, as not all mice inoculated with 10^5 CFU of Δ*tolC*/*tolC*$^{+}$ succumbed to infection (Figure 3.7).

tolC and *ftlC* are not required for intracellular replication of the LVS

F. tularensis is capable of surviving and replicating inside macrophages (Bolger et al., 2005; Golovliov et al., 2003a). This ability is critical for virulence, as mutants of *F. tularensis* defective for replication in macrophages are attenuated in the mouse infection model (Golovliov et al., 2003b; Lauriano et al., 2004; Nano et al., 2004). To determine if

the attenuation of the Δ*tolC* strain was due to an inability to replicate in macrophages, we examined growth of Δ*tolC*, Δ*ftlC* and the LVS in murine bone marrow-derived macrophages (muBMDM). Macrophages were infected with the bacteria at a multiplicity of infection (MOI) of 50 and inspected at 2 and 24 hours post infection for bacterial replication by indirect immunofluorescence microscopy and determination of viable intracellular bacteria. At 2 h post infection, association of the parental LVS and mutant strains with the muBMDM was similar, with infection rates of approximately 40% and viable bacterial counts of 10^3 CFU/ml (Figure 3.8). At 24 h post infection, significant increases in intracellular bacteria were observed for macrophages infected with all strains, giving viable bacterial counts of 10^6 to 10^7 CFU/ml (Figure 3.8). Thus, *tolC* and *ftlC* are not required for replication of the LVS in macrophages. However, the Δ*tolC* strain consistently showed a slight replication defect compared to the parental LVS or Δ*ftlC* strain, yielding 5-fold lower CFU at 24 h post infection (Figure 3.8). This observation suggests that *tolC*, but not *ftlC*, is required for optimal growth in macrophages. The slight replication defect of strain Δ*tolC* strain in muBMDM could be complemented by addition of plasmid pGPTA (*tolC*) (data not shown). Since the Δ*tolC* and Δ*ftlC* strains exhibited increased sensitivity to gentamicin compared to the wild-type LVS (Table 3), we conducted the macrophage infection experiments without adding gentamicin to kill extracellular bacteria. However, experiments performed with addition of gentamicin gave identical results (data not shown).

Additionally, we tested the ability of the deletion strains to grow within murine hepatocytes, cell line FL83B, and human lung epithelial cells, cell line A549. The different cell lines were infected for two hours at varying MOI. Intracellular replication

was analyzed at 2 and 24 HPI by indirect immunofluorescence microscopy and CFU quantification. Murine FL83B hepatocytes, were infected with the bacteria at a MOI of 1000. At 2 HPI uptake of the parental LVS and mutant strains was similar (Figure 3.9). By 24 HPI all strains had replicated inside the murine hepatocytes with no significant differences in the intracellular replication rates (Figure 3.9). Human A549 lung epithelial cells, were infected at a MOI of 400. At 2 HPI the bacterial uptake and replication rates of the deletion strains were similar to those of the LVS (Figure 3.10). By 24 HPI a significant increase in intracellular replication was observed from lung epithelial cells infected with the LVS, Δ*tolC* strain or Δ*ftlC* strain, indicating that neither *tolC* or *ftlC* is required for replication of the LVS in macrophages (Figure 3.10). Similar to the replication rate of the Δ*tolC* strain in muBMDMs, replication of the Δ*tolC* strain in A549 cells was decreased by 1 to 2 logs when compared to the LVS (Figure 3.10). This data suggests that *tolC* is required for optimal growth in human lung epithelial cells.

III. Discussion

We show here that *F. tularensis* contains two genes, *tolC* and *ftlC*, encoding proteins homologous to *E. coli* TolC, which is the prototypical OM channel component involved in multidrug resistance and type I secretion. Both *tolC* and *ftlC* are highly conserved among the three subspecies of *F. tularensis* studied and free of disabling mutations, indicating the genes play important roles in the biology of this pathogen. We found that both *F. tularensis* orthologs, similar to *E. coli* TolC, participate in multidrug resistance. Furthermore, mouse infection experiments demonstrated that *tolC* is a significant virulence determinant of *F. tularensis.*

In recent years more tools for the genetic manipulation of *F. tularensis* have become available, including a number of techniques for the generation and complementation of mutants in the LVS (Golovliov et al., 2003b; Lauriano et al., 2003; Maier et al., 2004; LoVullo et al., 2006; Rodriguez et al., 2009). We deleted the *tolC* and *ftlC* genes in the LVS using an allelic exchange protocol (Golovliov et al., 2003b). The Δ*tolC* and Δ*ftlC* LVS strains were sensitive to a variety of antibiotics, detergents and dyes, indicating that TolC and FtlC form part of the multidrug resistance machinery of *F. tularensis*. The absence of the OM channel component prevents the bacteria from pumping such drugs to the external environment, leading to the accumulation of the drugs and producing greater sensitivity. The drug sensitivity of the Δ*tolC* and Δ*ftlC* LVS mutants was restored back to wild-type levels upon complementation with the deleted genes in trans. (Maier et al., 2004; Nano et al., 2004).

In addition to increased drug sensitivity, we found that the Δ*tolC* LVS mutant was highly attenuated for virulence in mice when inoculated by the intradermal route.

Moreover, this attenuation was reversed when the gene was reintroduced in trans, indicating the virulence defect was due specifically to the deletion of *tolC*. Complementation of the Δ*tolC* mutation was partial, as virulence was restored for the 10^7 but not the 10^6 inoculum (Table 2). This partial complementation may be explained by constitutive and likely excessive expression of *tolC* from the heterologous *groE* promoter (26), as compared to its natural promoter. Previously characterized *F. tularensis* mutants attenuated for virulence in mice were also severely defective for replication in macrophages (Golovliov et al., 2003b; Lauriano et al., 2004; Nano et al., 2004). In contrast, our Δ*tolC* mutant exhibited only a slight growth defect in murine macrophages. Although it is possible that this defect is amplified within the host and could account for the virulence attenuation of the Δ*tolC* strain, this result argues for a function of TolC in *F. tularensis* pathogenesis separate from growth in macrophages.

Only the Δ*tolC* mutant had a virulence defect in mice, despite the fact that both Δ*tolC* and Δ*ftlC* showed equivalent increases in drug susceptibility. TolC and FtlC may participate in distinct multidrug efflux systems, with overlapping but different substrate profiles. Thus, the Δ*tolC* mutant may not be able to pump out a harmful agent encountered in vivo, whereas the Δ*ftlC* mutant retains this ability (Koronakis et al., 2004). A second and more exciting possibility is that *tolC* participates in a type I secretion system in addition to its role in multidrug efflux, whereas *ftlC* participates only in drug efflux. If this is the case, TolC may be involved in the secretion of a toxin or other factor important for the pathogenesis of *F. tularensis*. Until now, no toxins have been described in *F. tularensis* (Larsson et al., 2005), other than the presence of a potential hemolysin in *F. tularensis* subspecies *novicida* and *F. philomiragia* (Lai et al.,

2003). This potential hemolysin appears to be absent in *F. tularensis* subspecies *tularensis* and *holarctica*. A *F. tularensis* virulence factor could also be secreted via a TolC-containing multidrug efflux system, as evidence from *Pseudomonas aeruginosa* suggests that multidrug efflux systems can secrete virulence determinants in addition to pumping out harmful compounds (Lai et al., 2003).

The presence of more than one TolC homolog and multiple multidrug efflux systems is common in Gram-negative bacteria. In addition to the TolC OM efflux protein, multidrug efflux and type I secretion systems require a periplasmic adaptor protein and an IM energy-providing protein (Koronakis et al., 2004). The *F. tularensis* genome contains a number of genes that could provide these additional components for multidrug efflux or protein secretion in conjunction with TolC and/or FtlC (Larsson et al., 2005). The IM component of type I secretion and some multidrug efflux pathways is an ATP-binding cassette (ABC) transporter. The genome of SchuS4 encodes fifteen potential ABC transporters, five to seven of which may be involved in efflux or secretion (Atkins et al., 2006). For multidrug efflux systems, the IM component is more commonly a proton antiporter belonging to either the resistance-nodulation-division (RND) or major facilitator superfamily (MFS) (Koronakis et al., 2004). Open reading frame FTT0105 of the SchuS4 genome is homologous to the RND exporter AcrB and open reading frame FTT1257 is homologous to the MFS exporter EmrB. The Acr and Emr systems work together with TolC in other bacteria to pump out a broad range of antibiotics and harmful compounds (Koronakis et al., 2004).

In summary, we have described the presence of two genes, *tolC* and *ftlC*, that belong to the multidrug resistance machinery of *F. tularensis*. Significantly, we identified

tolC as a new virulence factor of *F. tularensis*, which could participate in a type I secretion system for the export of a toxin or other virulence determinant critical for the pathogenesis of *F. tularensis*. These findings open new avenues for understanding the molecular basis underlying the high virulence of *F. tularensis* and provide new targets for the development of therapeutic agents. In addition, the virulence attenuation of the *F. tularensis* Δ*tolC* mutant holds promise for the construction of a defined, attenuated vaccine strain.

Table 3.1 Drug Sensitivity of the LVS

Drug Class	Name	µg/disc	LVS	Δ*tolC*	Δ*filC*	Δ*tolC* / Δ*tolC*$^{+}$	Δ*filC* / Δ*filC*$^{+}$
Penicillins	Ampicillin	10	6 ± 0*	6 ± 0	6 ± 0	ND†	ND
Aminoglycosides	Streptomycin	10	20 ± 1	25 ± 1	23 ± 1	23 ± 1	21 ± 1
	Gentamicin	10	27 ± 1	32 ± 1	31 ± 1	29 ± 1	29 ± 1
	Kanamycin	5	18 ± 1	22 ± 1	20 ± 0	ND	ND
Tetracyclines	Tetracycline	5	29 ± 1	33 ± 2	34 ± 1	29 ± 2	29 ± 2
Macrolides	Erythromycin	15	6 ± 0	6 ± 0	6 ± 0	ND	ND
Quinolones	Nalidixic acid	30	25 ± 1	30 ± 3	27 ± 1	26 ± 3	27 ± 1
Others	Polymyxin B	100	6 ± 0	6 ± 0	6 ± 0	ND	ND
	Chloramphenicol	5	20 ± 1	24 ± 1	26 ± 1	21 ± 1	22 ± 1
	Vancomycin	20	6 ± 0	6 ± 0	6 ± 0	6 ± 0	6 ± 0
	Novobiocin	30	18 ± 1	21 ± 1	22 ± 1	16 ± 1	17 ± 1
Detergents	SDS	750	9 ± 1	13 ± 1	13 ± 1	10 ± 1	9 ± 1
	DOC	100	6 ± 0	10 ± 1	10 ± 0	6 ± 0	6 ± 0
Dyes	Acriflavin	25	18 ± 1	19 ± 1	19 ± 1	19 ± 0	19 ± 0
	Ethidium Bromide	5	6 ± 0	18 ± 1	17 ± 1	6 ± 0	6 ± 0

*Average diameter of the zone of inhibition (including filter disc) in mm ± standard deviation. The diameter of the filter disk is 6 mm.
†ND, not determined. The plasmids used in the complemented strains confer resistance to ampicillin and kanamycin.

IV. Figures

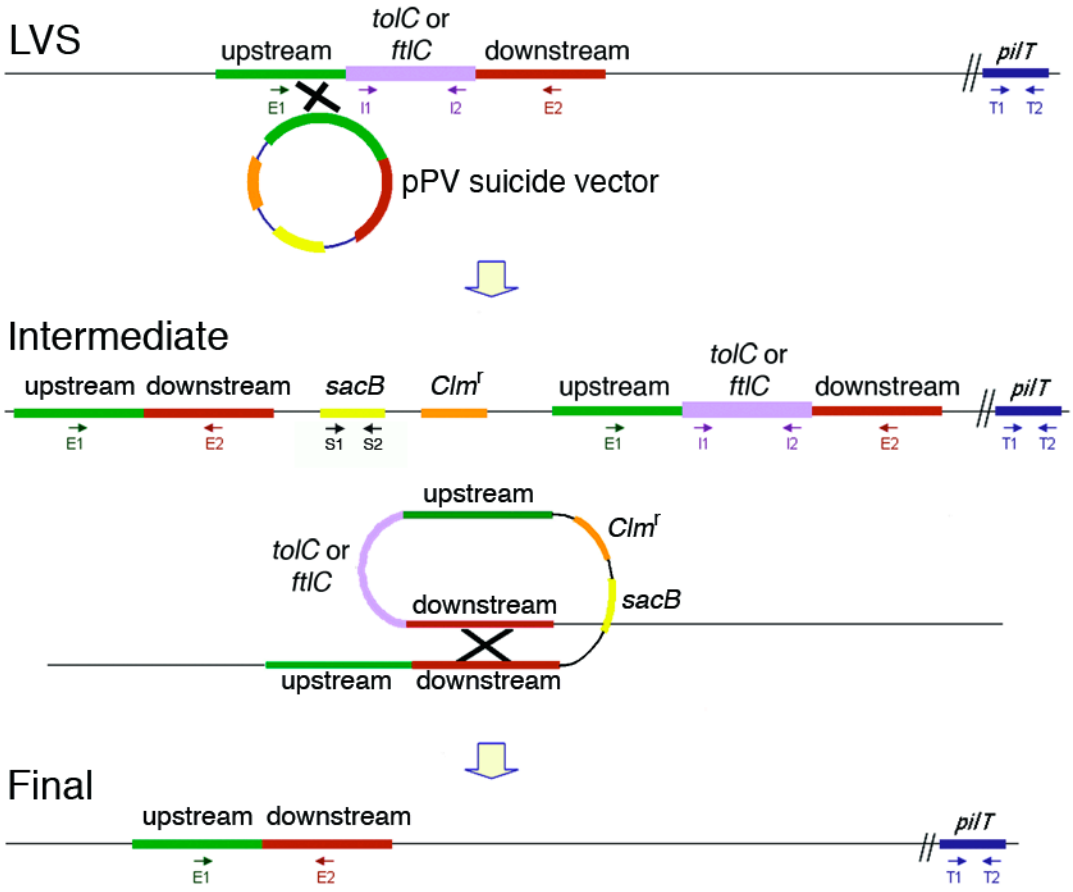

Figure 3.1 Overview of the allelic replacement technique used to delete *tolC* or *ftlC*. The pPV-derived suicide vector, introduced into the LVS by conjugation, integrates into the LVS chromosome by a single homologous recombination event between the cloned upstream or downstream regions of the target gene in the suicide vector and the chromosome (upper part of figure). This first recombination generates an intermediate strain containing the plasmid genes incorporated into the chromosome. In the second recombination event, the bacteria eliminate *sacB* and the wild-type copy of the target gene encoded in the suicide vector (lower part of figure). The four sets of PCR primers used to validate the gene deletions are shown as follows: external primers (E1 and E2) located outside the targeted gene; internal primers (I1 and I2) located within the targeted gene; *sacB* primers (S1 and S2) for detection of the vector-encoded *sacB*; and primers for *pilT* (T1 and T2) to confirm the colonies selected are *F. tularensis*.

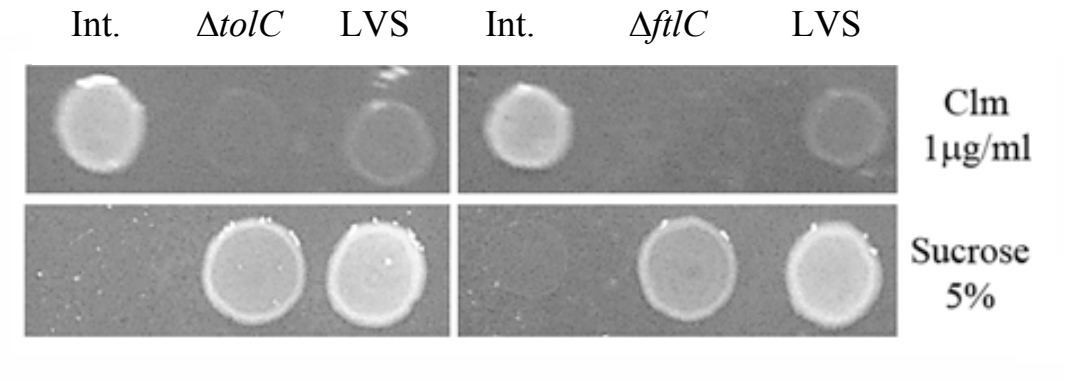

Figure 3.2 Phenotypic validation of the LVS deletion strains Δ*tolC* (DTH1) and Δ*ftlC* (DTB3). Growth of the parental LVS, intermediate (int.) and final deletion strains on MMF supplemented with 1 μg/ml chloramphenicol (clm) or 5% sucrose. The intermediate strains are resistant to chloramphenicol and sensitive to sucrose. The final deletion strains are sensitive to chloramphenicol and resistant to sucrose.

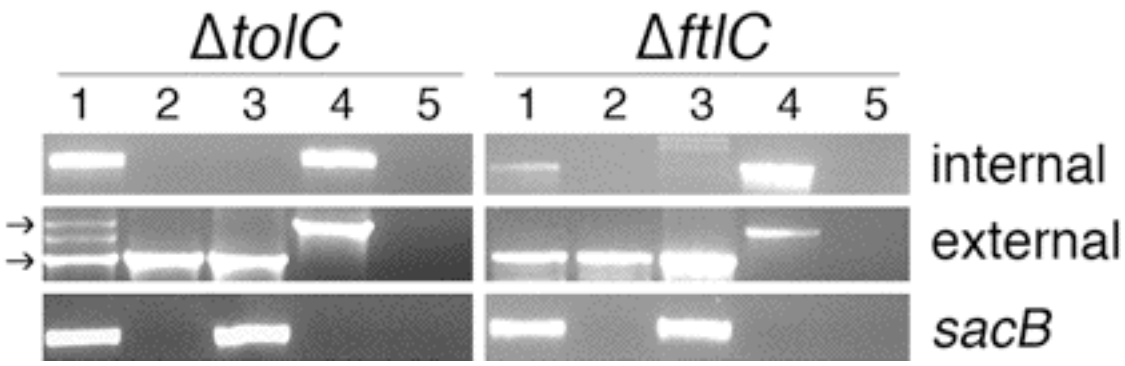

Figure 3.3 Genotypic validation of strains Δ*tolC* (DTH1) and Δ*ftlC* (DTB3). PCR was performed using primers internal or external to the targeted gene, or to *sacB*. Lanes: 1, intermediate strain; 2, final deletion strain (Δ*tolC* or Δ*ftlC*); 3, suicide vector (pPVTAH1 or pPVTBH3); 4, LVS; 5, water control. The arrows on the left indicate the expected positions of the intact and truncated versions of the targeted gene.

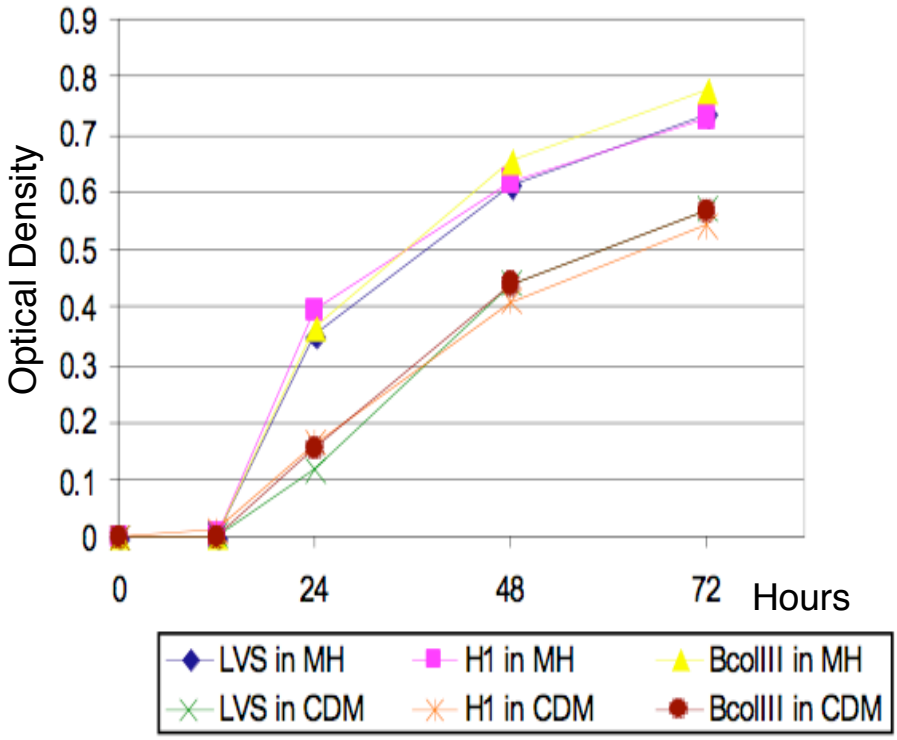

Figure 3.4 Growth curve analysis. The growth of LVS, H1 (Δ*tolC)*, and BcolIII (Δ*ftlC)* strains was comparable in both Mueller Hinton Broth (MHB) and Chamberlain's chemically defined medium (CDM).

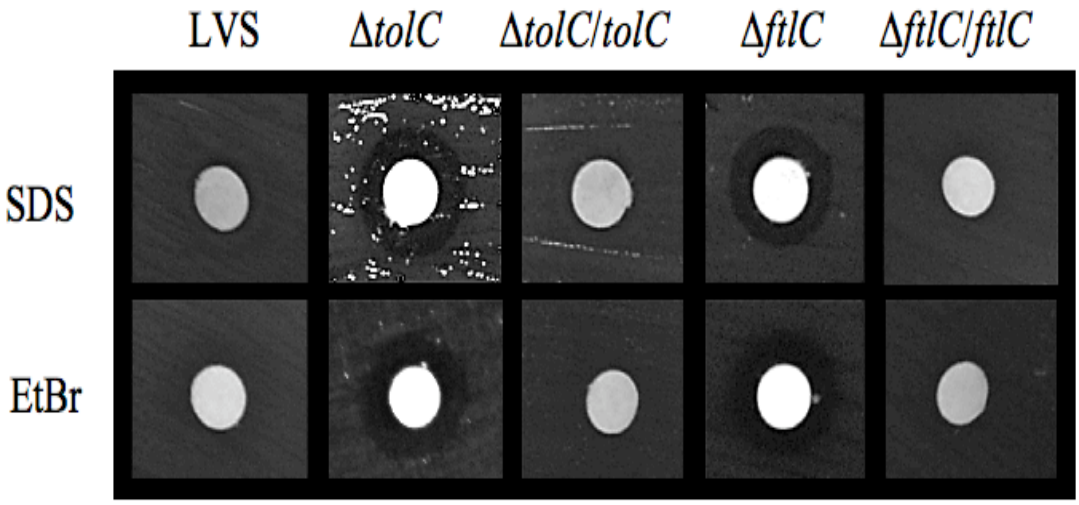

Figure 3.5 Drug sensitivity assay. The LVS, Δ*tolC* and Δ*ftlC* were spread as lawns on Mueller-Hinton Chocolate plates, and a small paper disc containing a drug was laid upon the plate. After 48 hours of growth the strains were determined sensitive if they displayed a clearing (no growth zone) around the disc containing the drug. The top panel (SDS), shows the sensitivity of the various strains to the detergent SDS (750 μg/disc). The bottom panel (EtBr), shows the sensitivity of the various strains to ethidium bromide (5 μg/disc).

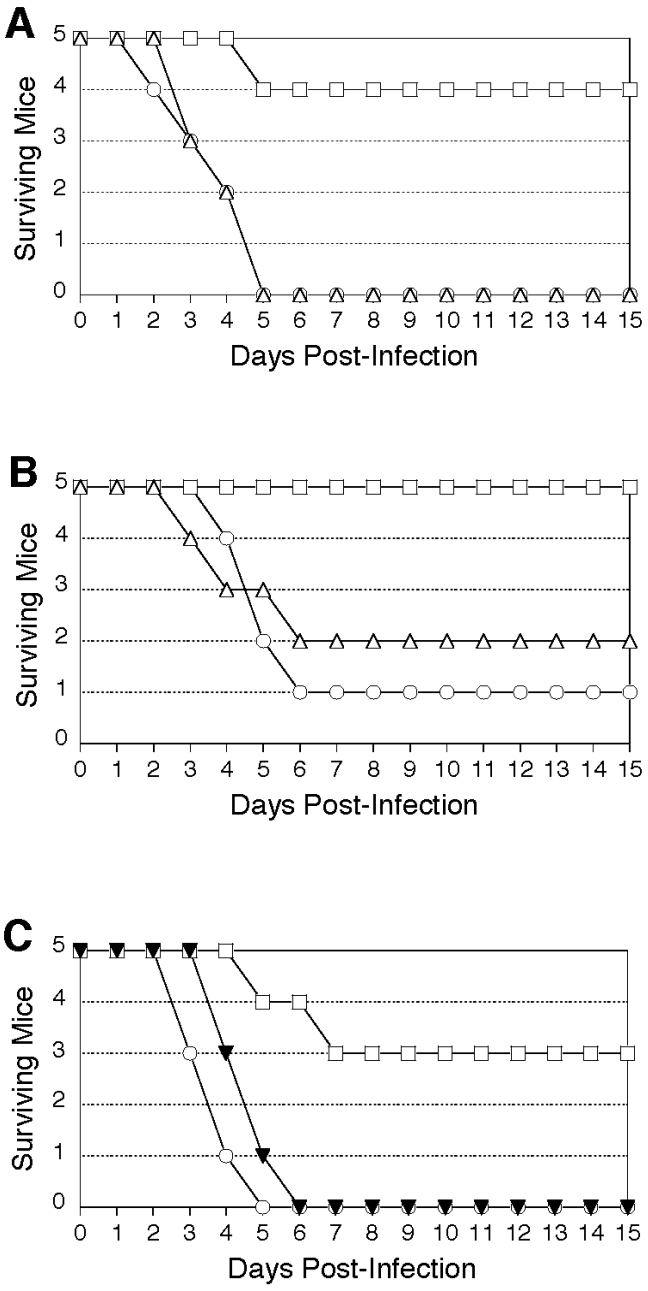

Figure 3.6 Intradermal murine infection. In all experiments, groups of five mice were inoculated intradermally and monitored for survival for fifteen days. (*A*) Infection with 10^7 CFU of the parental LVS, Δ*tolC* (DTH1) or Δ*ftlC* (DTB3). (*B*) Infection with 10^6 CFU of the LVS, Δ*tolC* or Δ*ftlC*. (*C*) Infection with 10^7 CFU of the LVS, Δ*tolC* or Δ*tolC/tolC*$^+$ (DTH1/pGPTA). Symbols: circles, LVS; triangles, Δ*ftlC*; squares, Δ*tolC*; black triangles, Δ*tolC/tolC*$^+$.

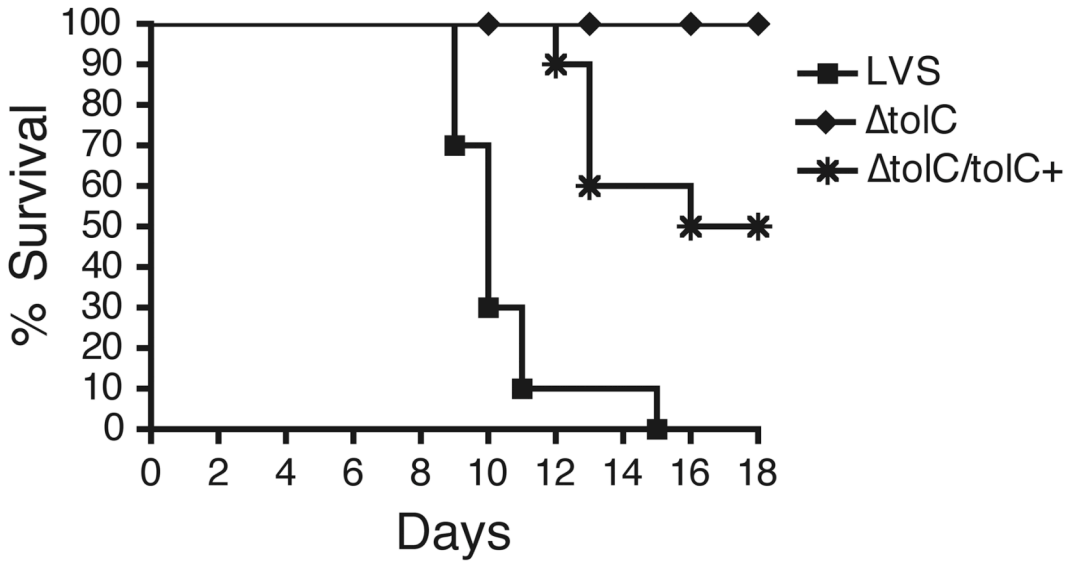

Figure 3.7 Intranasal murine infection. C3H/HeN mice were infected intranasally with a lethal dose ($1x10^5$ CFU) of the LVS, Δ*tolC* or complemented strain (Δ*tolC*/Δ*tolC*$^+$). The animals were monitored for survival for 18 days. Two independent experiments with 5 mice per bacterial strain were performed and the data combined together. The Δ*tolC* mutant was significantly attenuated compared to the parental LVS ($P < 0.0001$) and complementation significantly restored virulence to the Δ*tolC* mutant ($P < 0.01$).

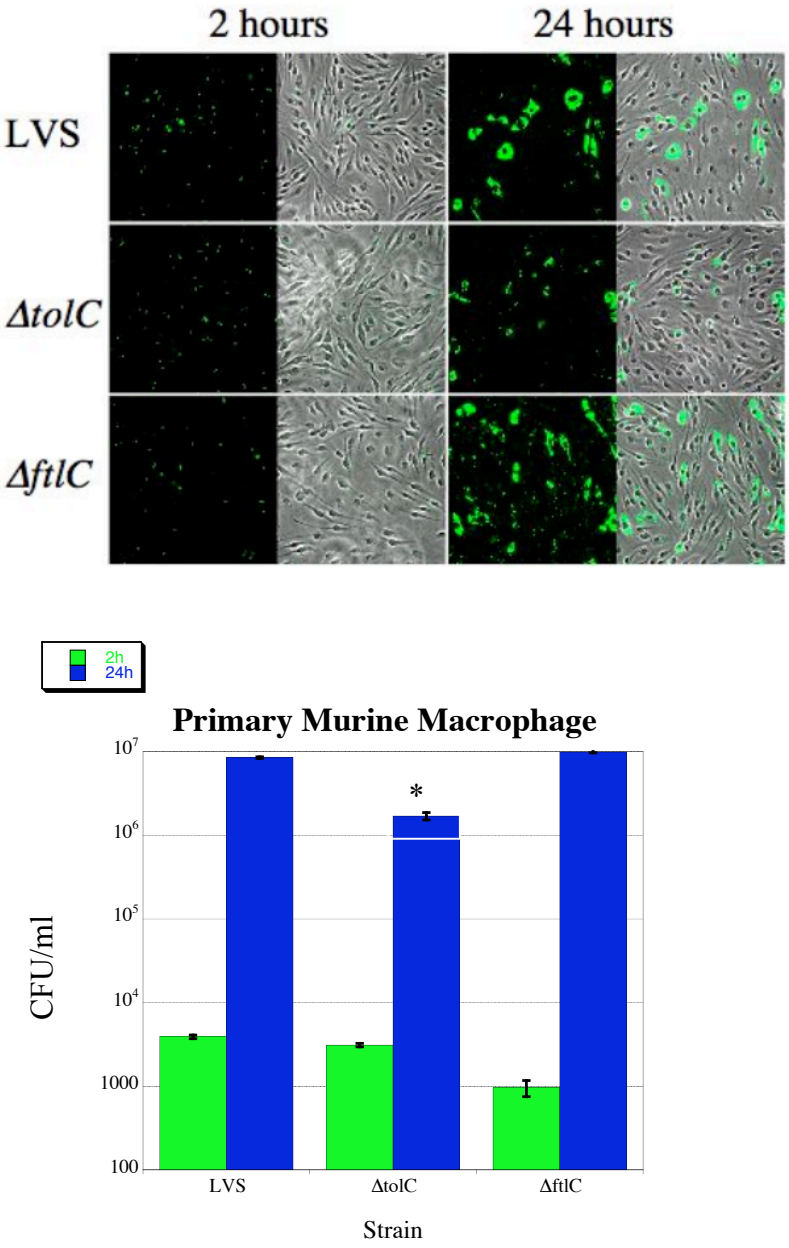

Figure 3.8 MuBMDM infections. Cells were infected with LVS, Δ*tolC* or Δ*ftlC,* and 2-hour and 24-hour time points were recorded. Immunofluorescence analysis was conducted using anti-LVS antibody and viable intracellular bacteria were quantified by CFU assay. MuBMDM were infected at a MOI of 50. ($*P < 0.01$; unpaired analysis of variance and Tukey–Kramer multiple comparison post test).

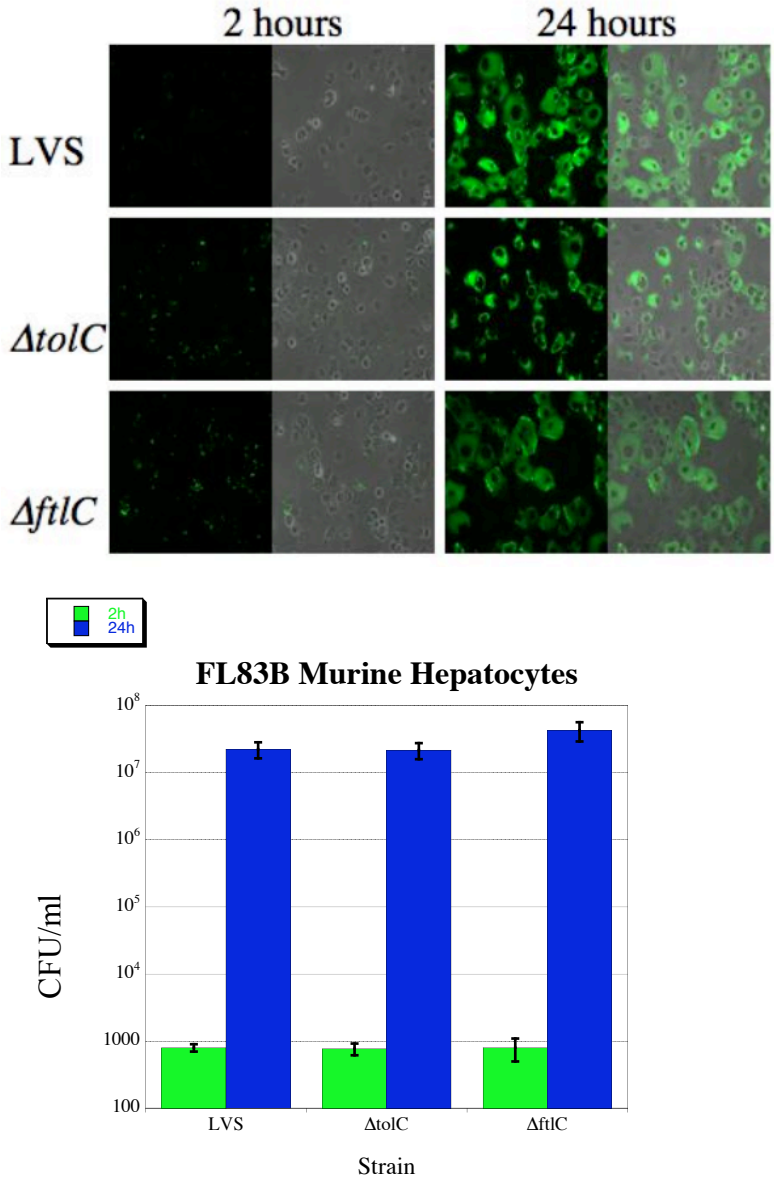

Figure 3.9 FL83B murine hepatocyte infections. Cells were infected with LVS, Δ*tolC* or Δ*ftlC,* and 2-hour and 24-hour time points were recorded. Immunofluorescence analysis was conducted using anti-LVS antibody and viable intracellular bacteria were quantified by CFU assay. FL83B cells were infected at a MOI of 1000.

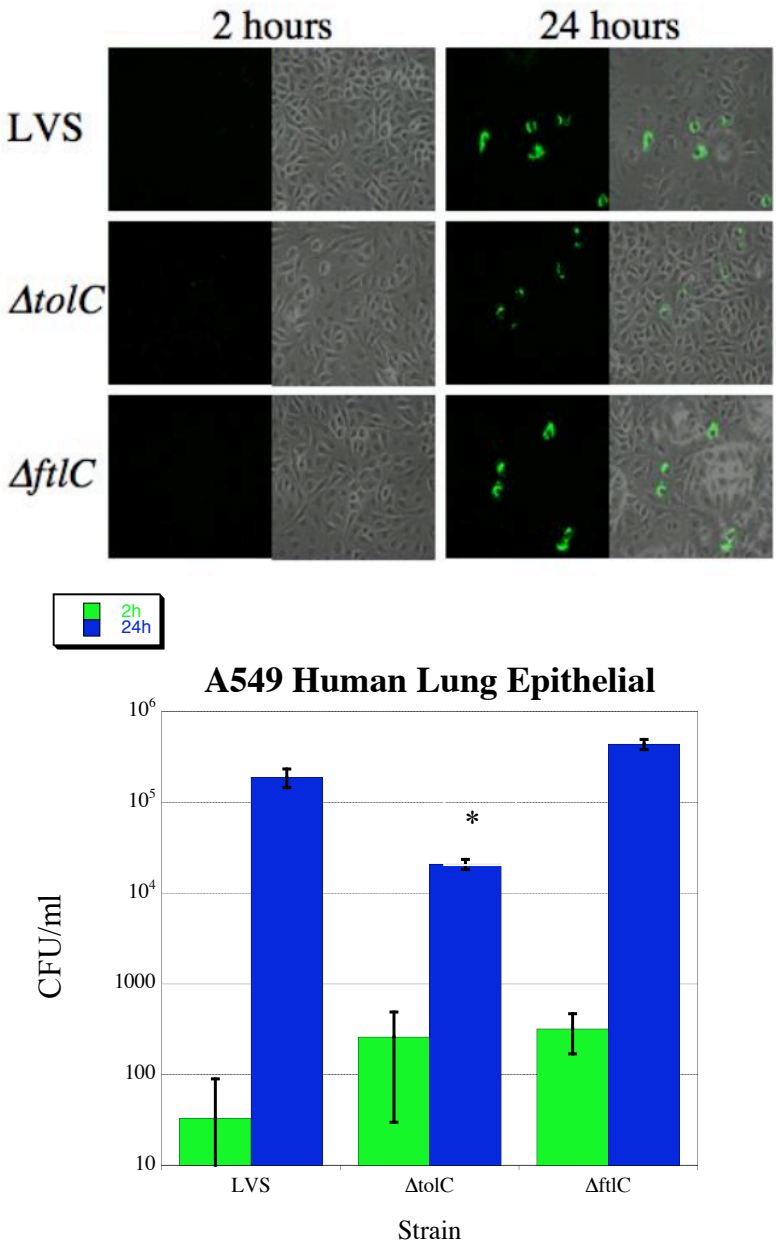

Figure 3.10 Human A549 lung epithelial cell infections. Human A549 lung epithelial cellswere infected with LVS, Δ*tolC and* Δ*ftlC,* and 2-hour and 24-hour time points were recorded. Immunofluorescence analysis was conducted using anti-LVS antibody and viable intracellular bacteria were quantified by CFU assay. A549 cells were infected at a MOI of 400. ($*P <$ 0.01; unpaired analysis of variance and Tukey–Kramer multiple comparison

Chapter Four

A *tolC* mutant of *Francisella tularensis* is hypercytotoxic and elicits increased proinflammatory responses from host cells

I. Introduction

In our previous study, summarized in chapter three, we identified two genes, *tolC* and *ftlC*, that belong to the multidrug resistance machinery of *F. tularensis*. We determined that *tolC* is a virulence factor of *F. tularensis* as it was attenuated for virulence in the murine model of infection for both the intradermal and intranasal routes. Additionally, our earlier results indicate a function for TolC in the pathogenesis of *F. tularensis* separate from growth in macrophages.

Here, we delineate the molecular mechanisms behind the attenuation of the LVS Δ*tolC* mutant in mice infected by both the intradermal and intranasal routes. In vivo organ burden assays revealed that the Δ*tolC* strain is decreased for bacterial colonization of liver, spleen and, most prominently, lungs. In vitro experiments revealed that the Δ*tolC* mutant is hypercytotoxic to murine macrophages, causing increased apoptosis via a mechanism involving caspase-3 but not caspase-1. In addition, the LVS Δ*tolC* mutant was hypercytotoxic toward human macrophages and elicited significantly increased secretion of the proinflammatory chemokines CXCL8 (also known as IL-8) and CCL2 (also known as MCP-1). Taken together, these data demonstrate a critical role for TolC –

likely via a TolC-secreted toxin(s) – in the successful intracellular lifestyle of *F. tularensis*, its ability to evade host innate immune responses, and its overall virulence.

II. Results

The LVS Δ*tolC* exhibits decreased colonization within the lung, liver and spleen of mice infected via the intradermal and intranasal routes

We previously found that *tolC* is critical for the virulence of the LVS in the mouse model of tularemia by the intradermal and intranasal routes (Chapter 3). To understand the basis for the attenuation of the Δ*tolC* mutant, we analyzed dissemination to and colonization of the liver, spleen and lungs of mice infected with sublethal doses of the mutant and parental strains. Mice intradermally inoculated with 10^5 bacterial CFU were sacrificed on days 2, 4, and 7 post infection (PI), and liver, spleen and lungs were removed for bacterial enumeration and histology. Both the LVS and LVS Δ*tolC* were detected in all three organs by day 2 PI, indicating normal dissemination of the mutant strain. For both strains, bacterial loads were highest in the spleen and peaked around day 4, after which bacterial colonization decreased (Figure 4.1, panel B). Notably, compared to mice infected with the LVS, the Δ*tolC* strain exhibited decreased CFU within the liver, spleen and lung (Figure 4.1, Panels A and B). In both the liver and spleen, CFU for the Δ*tolC* mutant were consistently 1 to 2 logs lower than obtained with the parental LVS. The largest differences in colonization were seen on day 7 PI, indicating that the *tolC* mutant was being cleared more rapidly from the mice. The CFU of the Δ*tolC* mutant in the liver and spleen increased from day 2 to 4 PI, similar to the wild-type strain. Therefore, the mutant is capable of replicating within these tissues, but to lower numbers (Figure 4.1, panel B and C). In agreement with this, analysis of liver sections from day 4 PI showed that the Δ*tolC* mutant formed characteristic infection foci similar to the wild-

type LVS (Figure 4.2, panel A). Spleens from infected mice also exhibited comparable pathology for both the LVS and Δ*tolC* mutant, with disorganization of the red and white pulp and expansion of the white pulp (Figure 4.2, panel B).

The in vivo growth defect of the Δ*tolC* mutant was particularly prominent in the lungs. CFU were obtained from only 3 of 10 mice on day 2 PI, and whereas CFU for the wild-type LVS increased from days 2 to 7, CFU for the mutant decreased over the course of the experiment to undetectable levels (Figure 4.1, panel A). Thus, in contrast to the liver and spleen, the Δ*tolC* mutant showed no evidence for replication within the lung from days 2 to 4. Analysis of lung sections taken on day 4 PI did not reveal much pathology for either the wild-type or Δ*tolC* LVS compared to uninfected controls. This was not surprising given the low overall bacterial numbers in the lung (Figure 4.2, panel C) and the fact that *F. tularensis* infections cause only limited lung pathology (Conlan et al., 2003).

We next conducted organ burden assays to quantify bacterial loads within the lungs, liver and spleen of mice intranasally infected with the Δ*tolC* mutant or wild-type LVS. Mice inoculated with sublethal doses of 5 X 10^3 CFU were sacrificed on days 3, 5 and 9 PI, and the lungs, liver and spleen were harvested for bacterial enumeration and histology. The organ burden results from these intranasal infections were very similar to the results from the intradermal assay (Figure 4.1), with CFU for the Δ*tolC* mutant consistently one or more logs lower than for the parental LVS (Figure 4.3). Bacterial loads were highest in the lung, as expected for an intranasal infection, and both the LVS and Δ*tolC* mutant disseminated from the lung to the liver and spleen. Similar to the intradermal infections, CFU for both strains peaked in the liver and spleen on day five PI,

and then stayed flat or decreased from day 5 to 9 (Figure 4.3, panels B and C). Liver and spleen CFU for the Δ*tolC* mutant increased from days 3 to 5 PI, indicating ability of the mutant to replicate in these organs, but to lower numbers than the wild-type LVS. By day 9 PI, numbers for the Δ*tolC* mutant dropped significantly, particularly in the liver, indicating greater clearance of the mutant compared to the parental LVS. Also similar to the intradermal infections, the phenotype of the Δ*tolC* mutant was strongest in the lung. In this organ, the mutant did not increase in CFU from days 3 to 5 PI, but instead decreased steadily throughout the duration of the experiment (Figure 4.3, panel A). This is in contrast to the wild-type LVS, which increased in CFU from days 3 to 9. Note that the Δ*tolC* mutant apparently was able to replicate in the lung early after inoculation, since the CFU/g lung tissue obtained at day 3 PI were higher than could be obtained from the input dose alone (mouse lung weights ranged from approximately 0.10-0.15 g). In addition, histological analyses of lung sections taken from mice on day 5 PI revealed no obvious differences between the wild-type and Δ*tolC* LVS (Figure 4.4). Nevertheless, by both the intradermal and intranasal routes, the LVS Δ*tolC* mutant was defective for replication within the lungs by 4-5 days after inoculation.

The LVS Δ*tolC* is hypercytotoxic to host macrophages

Given that TolC typically functions in the export of bacterial toxins such as hemolysin, we reasoned that the attenuation of the LVS Δ*tolC* mutant in the mouse model of tularemia could be explained by loss of secretion of a similar *F. tularensis* toxin or other virulence factor. To compare toxicity of the Δ*tolC* and wild-type LVS toward host

cells, we infected murine bone marrow-derived macrophages (muBMDM) isolated from C3H/HeN mice and measured lactate dehydrogenase release (LDH) as a marker for cell death. Cells were infected at a multiplicity of infection (MOI) of 50 and LDH release was quantified at 7, 9, 17 and 24 hours PI. Surprisingly, rather than being less cytotoxic, the Δ*tolC* mutant caused significantly more LDH release compared to the wild-type strain at each time point (Figure 4.5, panels A and B; data not shown). Complementation of the Δ*tolC* mutant with a *tolC* expression plasmid reduced the toxicity of the mutant back to wild-type levels (Figure 4.5). The largest fold increase in LDH release caused by the mutant versus the wild-type LVS (~3 fold) was consistently observed at 17 h PI and 24 h PI; these time points were chosen for all subsequent experiments unless otherwise specified.

F. tularensis has been shown to cause cell death in infected host cells by inducing apoptotic or pyroptotic pathways (Henry et al., 2007; Lai and Sjostedt, 2003). To determine if the hypercytotoxicity of the Δ*tolC* mutant was a result of either apoptosis or pyroptosis, we infected muBMDM as described above and performed a TUNEL staining assay. TUNEL positive cells were quantified by fluorescence microscopy. As shown in Figure 4.6, muBMDM infected with the *ΔtolC* mutant exhibited an approximately 3-fold increase in the amount of TUNEL positive cells compared to macrophages infected with the wild-type LVS, and this was reversed with the complemented strain (Figure 4.6). The increase in cell death induced by the LVS Δ*tolC* mirrored the increased cell death measured by LDH release. Thus, the Δ*tolC* mutant is defective in suppressing host cell death responses.

The hypercytotoxicity of the LVS Δ*tolC* is caspase-1 independent and correlates with increased caspase-3 activation

Death of pre-activated murine peritoneal macrophages upon infection by *F. tularensis* subsp. *novicida* as well as the LVS was shown to involve the inflammasome complex and caspase-1 activation (Henry et al., 2007; Mariathasan et al., 2005). In contrast, death of unstimulated muBMDM infected with the LVS was found to involve the intrinsic apoptotic pathway and caspase-3 activation, but not caspase-1 (Lai and Sjostedt, 2003). To determine if caspase-1 was required for the LVS-induced cell death we observed, we compared LDH released from caspase-1 deficient versus wild-type muBMDMs. The caspase-1 deficient muBMDM cells were isolated from a caspase-$1^{-/-}$ C57BL/6 strain (Lilo et al., 2008). As observed above for muBMDM isolated from C3H/HeN mice (Figure 4.5), the LVS Δ*tolC* mutant exhibited hypercytotoxicity at 24 h PI toward macrophages isolated from wild-type C57BL/6 mice (Figures 4.7, panel A and B). Moreover, a similar increase in cell death was observed for muBMDM isolated from caspase-1 deficient C57BL/6 mice (Figures 4.7, panel A and B). This demonstrates that caspase-1 is not required for the hypercytotoxicity of the LVS Δ*tolC*. Caspase-1 activation leads to maturation and secretion of IL-1ß. We assayed conditioned media from C3H/HeN muBMDM infected with either the wild-type or mutant LVS for the presence of IL-1ß. In agreement with a lack of capase-1 involvement, neither the wild-type LVS nor Δ*tolC* mutant caused increased IL-1β release above levels obtained from uninfected control cells (Figure 4.8).

To examine the role of caspase-3 in the hypercytotoxicity of the LVS Δ*tolC* mutant, we assayed infected C3H/HeN muBMDM using a luminescence-based method

that measures caspase-3/7 activity. Macrophages infected with the Δ*tolC* mutant exhibited significantly higher caspase 3/7 activity at 17 h PI compared to cells infected with the wild-type LVS or complemented strain (Figure 4.9, panel A and B). As an additional assay for caspase-3 activation, we infected muBMDM with the LVS, Δ*tolC* or complemented strain and detected the mature form of caspase-3 at 24 h PI by immunofluorescence microscopy. As shown in Figure 4.10, muBMDM infected with the Δ*tolC* mutant displayed ~3-fold more mature caspase-3 positive cells than macrophages infected with the LVS (Figure 4.10). Collectively, the increased caspase-3 activation triggered by the LVS Δ*tolC* correlates well with the hypercytotoxicity of the mutant toward muBMDM, suggesting that the increased apoptosis is mediated by a caspase-3 dependent pathway.

The LVS Δ*tolC* is hypercytotoxic toward human macrophages and elicits increased secretion of proinflammatory chemokines

To analyze if *F. tularensis* TolC functions similarly in interactions with human host cells as found for murine cells, we infected human monocyte-derived macrophages (huMDM) with the LVS or Δ*tolC* mutant and quantified cell death by measuring LDH release at 17 and 24 h PI. As with the murine macrophage infections, huMDM infected with the *ΔtolC* mutant exhibited increased LDH release compared to cells infected with the wild-type LVS (Figure 4.11). Again, the hypercytotoxic phenotype of the *ΔtolC* mutant was reversed in macrophages infected with the *tolC*-complemented strain (Figure 4.11). Thus, a TolC-dependent function is required to suppress host cell death pathways

in both human and murine macrophages. The level of LDH released by the huMDM upon infection with both wild-type and mutant strains was higher than found for muBMDM. This is likely due to the higher infectivity of *F. tularensis* for huMDM (Bolger et al., 2005). To assess caspase-1 involvement in the death of infected human macrophages, we measured release of IL-1ß. At 24 h PI there was a significant increase in IL-1β release from huMDM infected by the *ΔtolC* mutant compared to cells infected by the wild-type strain (Figure 4.12), implying that caspase-1 is activated in human macrophages in response to infection by the Δ*tolC* mutant. This is in contrast to the murine macrophage results, where we found no increase in IL-1ß release and caspase-1 was not required for the hypercytotoxicity of the Δ*tolC* mutant (Figures 4.8). Thus, there appear to be differences in the specific pathways stimulated by infection of human and murine macrophages by the LVS Δ*tolC* mutant.

F. tularensis has been shown to play an active role in dampening innate immune responses initiated by host cells (Bosio et al., 2007; Telepnev et al., 2003; Telepnev et al., 2005). To determine if *tolC* participates in manipulation of host immune responses in addition to suppressing proapoptotic pathways, we examined secretion of the proinflammatory chemokines CXCL8 (also known as IL-8) and chemokine CCL2 (also known as MCP-1) by infected huMDM and human umbilical vein endothelial cells (HUVEC). We did not detect a significant increase in the amount of CCL2 secreted by HUVEC infected with the LVS Δ*tolC* compared to cells infected by the wild-type LVS (data not shown). However, huMDM infected with the Δ*tolC* mutant produced significantly higher amounts of CCL2 (Figure 4.13). Furthermore, infection of both huMDM and HUVEC with the Δ*tolC* mutant caused significantly higher secretion of

CXCL8 into conditioned media compared to cells infected with the wild-type LVS (Figures 4.14 and 4.15). This demonstrates that a TolC-related function is required for *F. tularensis* to suppress proinflammatory immune responses in human host cells.

III. Discussion

In the previous chapter, we demonstrated that TolC is critical for the virulence of *F. tularensis* LVS in mice by both the intranasal and intradermal routes of infection. Therefore, TolC is a general virulence factor of *F. tularensis* and represents a potential therapeutic target. To understand the role of TolC during pathogenesis, we analyzed bacterial colonization within the livers, spleens and lungs of both intradermally and intranasally infected mice. The Δ*tolC* mutant spread to all organs following inoculation at either site, demonstrating that TolC is not required for *F. tularensis* to spread systemically. Although the Δ*tolC* mutant spread to all organs, CFU counts for the mutant were consistently lower by one or more logs compared to the parental LVS. The lower organ burden levels are likely a key part of the attenuation of the Δ*tolC* mutant, since this may allow the host to gain an upper hand against the invading bacteria.

Despite the organ colonization defect, CFU for the Δ*tolC* mutant roughly paralleled the wild-type LVS in the liver and spleen for mice infected by both the intradermal and intranasal routes. Importantly, both the mutant and wild-type strains increased in numbers between the first and second time points, indicating that the mutant retains the ability to replicate in these organs. In agreement with these observations, the Δ*tolC* mutant caused pathology characteristic of *F. tularensis* infections in both the liver and spleen. This suggests that TolC is critical for a step in pathogenesis other than intracellular replication.

The greatest difference in organ colonization between the wild-type and Δ*tolC* LVS strains was observed in the lungs. For both the intradermal and intranasal routes of infection, the number of CFU for the wild-type LVS increased in the lung from the first

through the last time points. In contrast, the number of CFU for the Δ*tolC* mutant decreased over the three time points, with the mutant completely cleared from the lungs in the intradermal infections. These results suggest that TolC function is particularly important for colonization of *F. tularensis* within the lung. Moreover, given that the *tolC* mutant is highly attenuated for virulence in mice, this finding further suggests that successful colonization of the lungs may be critical for a lethal infection.

The organ colonization data we obtained correlates well with in vitro tissue culture studies showing that the LVS Δ*tolC* replicates within muBMDM, but to lower numbers compared to the wild-type LVS (Gil et al., 2006). Similarly, we found that the Δ*tolC* mutant retained the ability replicate in both the murine hepatocyte cell line FL83B and the human lung epithelial cell line A549. The Δ*tolC* mutant exhibited similar growth kinetics to the wild-type LVS in FL83B cells, but replication of the mutant was consistently one log lower in the A549 cells. The ability of the *ΔtolC* mutant to grow intracellularly makes this strain a plausible vaccine candidate, as it should provoke a strong cellular immune response. Indeed, preliminary vaccination studies showed that the LVS *ΔtolC* provided full protection against subsequent lethal challenge with the parental LVS (see Chapter 6).

In vitro studies showed that the Δ*tolC* mutant is hypercytotoxic to host macrophages. This could explain the growth defect of the mutant in tissue culture cells and mouse organs; the bacteria may kill its host cell too quickly and lose its intracellular replicative niche. Compared to infection with the parental LVS, muBMDM infected with the Δ*tolC* mutant exhibited approximately 3-fold higher rates of cell death. This increased cell death was correlated with caspase-3 activation and was independent of caspase-1. In

agreement with a lack of caspase-1 activation, we did not detect increased release of IL-1ß by the muBMDM. Our results match those of Lai and Sjostedt, 2003, who reported that infection of J774 murine macrophage-like cells with the LVS triggered apoptosis by the intrinsic pathway, with activation of caspase-3 but not caspase-1 (Lai and Sjostedt, 2003). In contrast, Mariathasan et al. reported that infection of pre-activated murine peritoneal macrophages by either the LVS or strain U112 triggered cell death via the inflammasome complex and caspase-1 activation (Henry et al., 2007; Mariathasan et al., 2005). The different cell death pathways detected by these studies may reflect the different infection conditions used; our infection conditions most closely resemble those used by Lai and Sjostedt (Lai and Sjostedt, 2003).

We found that the LVS Δ*tolC* mutant was hypercytotoxic toward huMDM, demonstrating conserved function of *F. tularensis* TolC in the human and murine hosts. Interestingly, in contrast to what was seen in murine macrophages, we observed increased secretion of IL-1ß from huMDM infected with the Δ*tolC* mutant, indicating activation of caspase-1. These results support the idea that *F. tularensis* induces different cell death pathways depending on the specific infection conditions and host cell type, and suggest that the TolC-related inhibitory function is active against different cell death pathways. Similar to our LVS Δ*tolC* mutant, two transposon mutants of strain U112 isolated by Weiss and coworkers displayed hypercytotoxicity toward murine macrophages (Weiss et al., 2007a). One of these mutations was in a gene of unknown function and the other was in a putative transcriptional regulator (Weiss et al., 2007a). Although these U112 mutants were shown to modulate inflammasome/caspase-1-mediated cell death, it is possible that

the same or similar effectors could be connected to the phenotypes we observed for the LVS Δ*tolC* mutant.

Inhibition of host cell death is increasingly recognized as a strategy used by intracellular pathogens to prolong the time they have to replicate (Faherty and Maurelli, 2008). Bacteria employ a variety of mechanisms to inhibit apoptosis, including activation of host cell survival pathways, prevention of cytochrome C release from mitochondria, and inhibition of caspases (Faherty and Maurelli, 2008). Many intracellular pathogens, including *Shigella* and *Legionella*, use secretion systems to deliver effector proteins into host cells to suppress apoptosis (Abu-Zant et al., 2007; Clark and Maurelli, 2007; Knodler et al., 2005). Others, such as *Neisseria* and *Wolbachia*, employ surface proteins to inhibit apoptosis (Bazzocchi et al., 2007; Massari et al., 2000). TolC is located in the bacterial outer membrane and could directly interact with host proteins to mediate suppression of apoptosis upon infection by *F. tularensis*. However, we favor the hypothesis that TolC is required for secretion of a toxin via the type I secretion pathway. In support of TolC functioning in type I secretion in *F. tularensis*, we found that a *tolC* transposon insertion mutant of strain U112 (Gallagher et al., 2007) was defective for hemolysin secretion (G. J. P. and D. G. T., unpublished data; see Chapter 5). Hemolysin is a prototypical type I secretion substrate, but the LVS and most other strains of *F. tularensis* lack hemolytic activity (Lai et al., 2003). Work is underway to identify the putative TolC-secreted toxin or toxins in the LVS and fully virulent strains of *F. tularensis*.

In addition to causing increased cell death, infection of huMDM by the LVS Δ*tolC* caused a significant increase in secretion of the proinflammatory chemokines

CXCL8 and CCL2 compared to infection by the wild-type LVS. CXCL8 secretion was also significantly increased in HUVEC exposed to the Δ*tolC* mutant. CXCL8 functions to attract and activate neutrophils (Modi et al., 1990), whereas CCL2 recruits monocytes, memory T cells, and dendritic cells to sites of tissue injury and infection (Carr et al., 1994). During pathogenesis, increased secretion of these proinflammatory chemokines would bring additional immune cells to the site of infection and contribute to the clearance of the pathogen. This data suggests that the attenuation in virulence of the Δ*tolC* mutant is due not only to hypercytotoxicity and premature loss of its intracellular niche, but also to increased activation of the host innate immune system. This increased proinflammatory response could explain the more rapid clearance of the Δ*tolC* mutant observed in the mouse organ burden assays.

F. tularensis is known to suppress or interfere with innate immune responses by macrophages, dendritic cells and endothelial cells (Bosio et al., 2007; Bosio and Dow, 2005; Telepnev et al., 2003; Telepnev et al., 2005). Furthermore, a recent study found that a component secreted by *F. tularensis* acted to suppress proinflammatory responses of uninfected bystander dendritic cells (Chase et al., 2009). Based on our findings, we propose that the ability of *F. tularensis* to actively suppress proinflammatory host responses is at least partially dependent upon TolC, and likely via a TolC-secreted factor or factors. Note that HUVEC are not professional phagocytes and do not readily take up *F. tularensis* (Forestal et al., 2003). This implies that the TolC-secreted factor(s) is able to dampen host immune responses from extracellular as well as intracellular locations.

Tularemia severity is dependent upon the size of the initial infectious dose; we observed that a single log difference in CFU dramatically alters survival of the host

(Figure 3.6). The Δ*tolC* mutant consistently displays a 1 to 2 log decrease of CFU in tissue culture and in vivo, in lung, liver and spleen. Additionally, the Δ*tolC* mutant is hypercytotoxic to macrophage cells. Replication inside macrophages is essential for the survival of *F. tularensis*. Thus, when TolC is deleted from the genome the bacteria lose their intracellular replicative niche and the organism is unable to replicate to sufficiently or cause lethal infection.

In conclusion, our data shows that *tolC* is required for the virulence of *F. tularensis* in mice by both the intradermal and intranasal routes of infection. When TolC functions in virulence by acting to suppress both the proapoptotic and proinflammatory innate responses of the host, and we propose that these functions are carried out by a *F. tularensis* toxin or toxins that require TolC for secretion by the type I pathway. Collectively, these TolC-related activities afford the bacteria a protected intracellular replicative niche, while blocking innate immune responses that would clear these bacteria. These host suppressive activities likely underlie the extreme virulence of *F. tularensis*.

IV. Figure

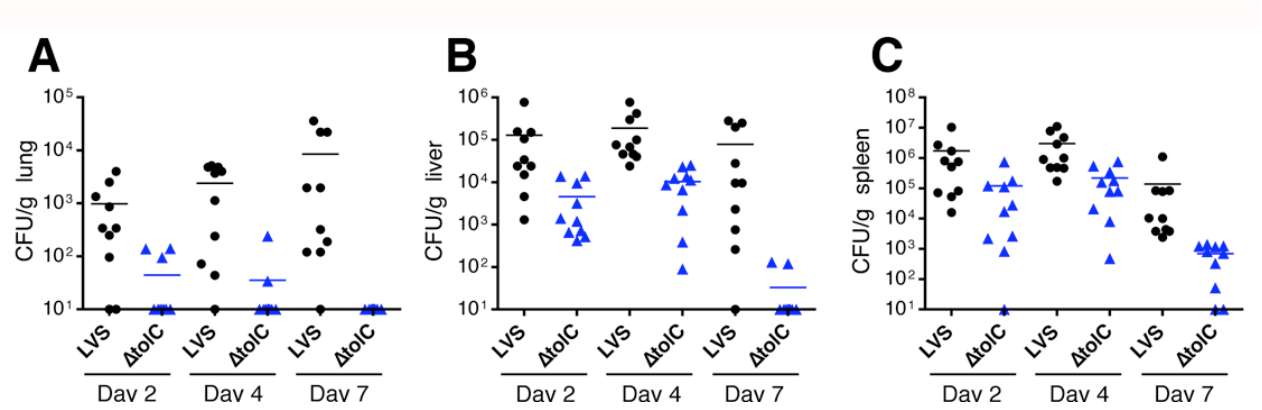

Figure 4.1 Intradermal organ burden assay. C3H/HeN mice were infected intradermally with a sub-lethal dose (10^5 CFU) of the LVS or Δ*tolC* mutant. Organs were harvested on days 2, 4 and 7 PI, and CFU/g of organ weight were determined for the (A) lung, (B) liver and (C) spleen. The limit of detection per organ was 10 CFU. Two independent experiments with 5 mice per time point per bacterial strain were performed, and these data were combined together. The bars indicate mean CFU values. Colonization by the Δ*tolC* mutant was significantly decreased compared to the wild-type LVS at each time point in each organ ($P < 0.01$).

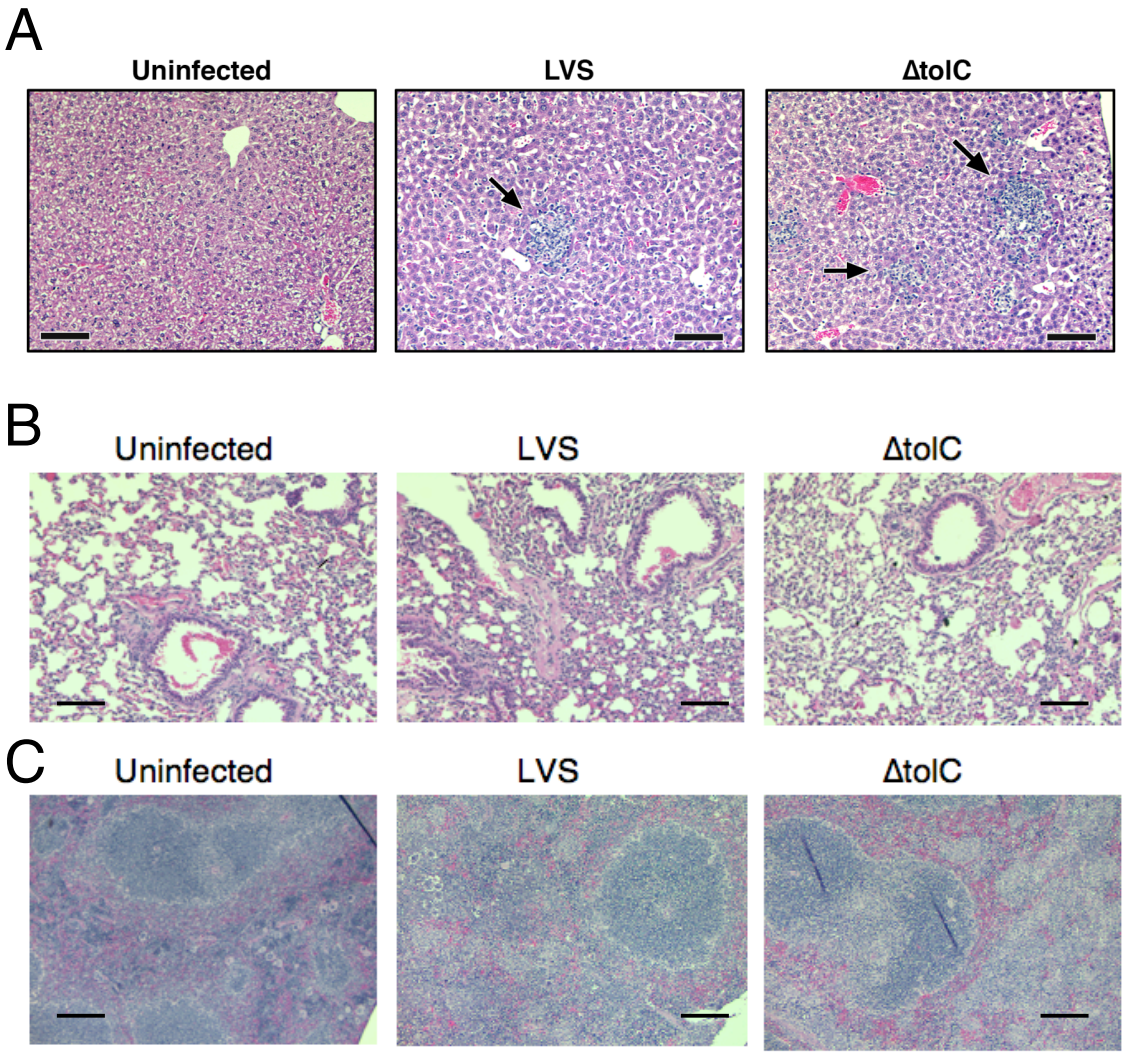

Figure 4.2 Intradermally infected lung, liver and spleen hematoxylin- and eosin-stained sections. C3H/HeN mice were infected intradermally with a sub-lethal dose (10^5 CFU) of the LVS or Δ*tolC* mutant. Organs were harvested on day 4 PI. Hematoxylin- and eosin-stained sections obtained from (A) infected livers harvested at day 4 PI show that the wild-type LVS and Δ*tolC* mutant cause similar pathology. Arrows indicate granuloma-like lesions. Scale bars = 100 µm. (B) Infected lungs harvested at day 4 PI show that the wild-type LVS and Δ*tolC* mutant cause very little pathology. Scale bars = 100 µm. (C) Infected spleens harvested at day 4 PI show that the wild-type LVS and Δ*tolC* mutant cause similar pathology. Scale bars = 200 µm.

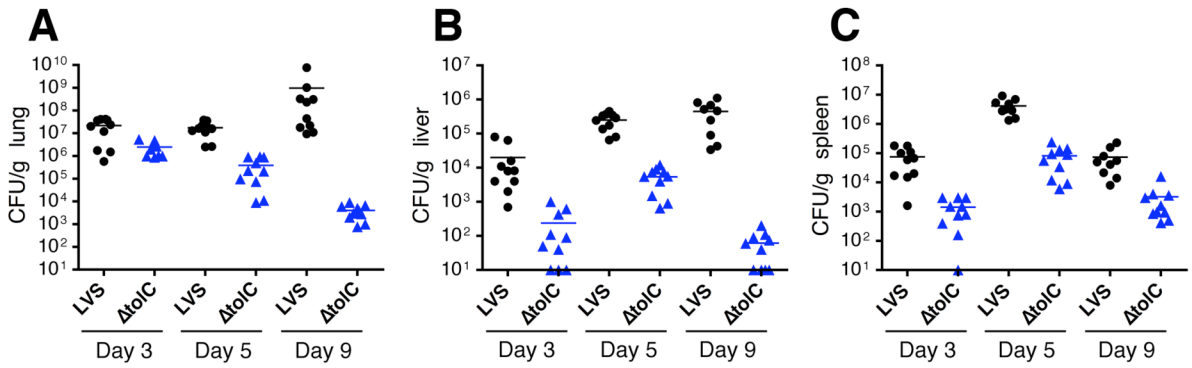

Figure 4.3 Intranasal ogan buden assay. C3H/HeN mice were intranasally infected with a sub-lethal dose ($5x10^3$ CFU) of the LVS or Δ*tolC* mutant. Organs were harvested on days 3, 5 and 9 PI, and CFU/g of organ weight were determined for the (A) lung, (B) liver and (C) spleen. The limit of detection per organ was 10 CFU. Two independent experiments with 5 mice per time point per bacterial strain were performed and the data combined. The bars indicate mean CFU values. Colonization by the Δ*tolC* mutant was significantly decreased compared to the wild-type LVS at each time point in each organ ($P < 0.05$ for lung day 3 PI; $P < 0.0001$ for all other comparisons).

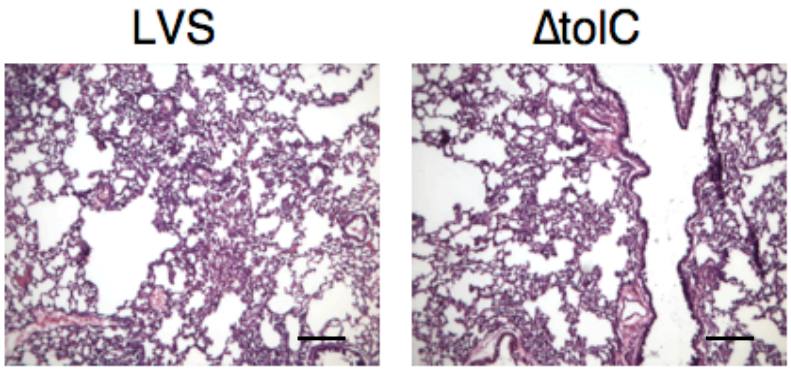

Figure 4.4 Intranasally infected lung hematoxylin- and eosin-stained sections. C3H/HeN mice were infected intranasally with a sub-lethal dose (5 x 10^5 CFU) of the LVS or Δ*tolC* mutant. Hematoxylin- and eosin-stained sections obtained from infected lungs harvested at day 5 PI show that the wild-type LVS and Δ*tolC* mutant cause very similar pathology.
Scale bars = 100 μm.

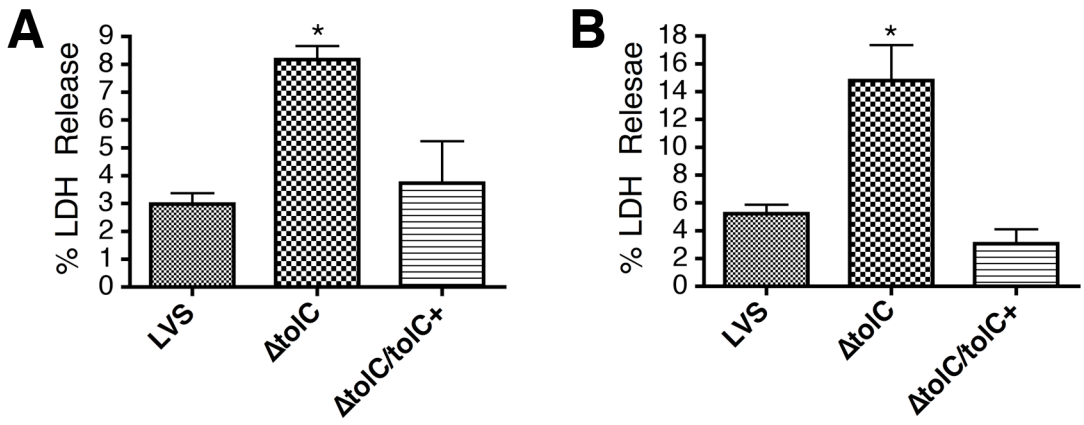

Figure 4.5 LVS induced cytotoxicity in muBMDM. MuBMDM cultured from C3H/HeN mice were infected with the LVS, Δ*tolC* mutant or complemented strain (Δ*tolC*/*tolC*$^{+}$) at MOI of 50. Cytotoxicity was quantified by measuring LDH release at (A) 17 or (B) 24 HPI. Bars represent means ± standard error of the mean (SEM) of three independent experiments. The Δ*tolC* mutant caused significantly increased LDH release compared to the wild-type LVS ($P < 0.05$).

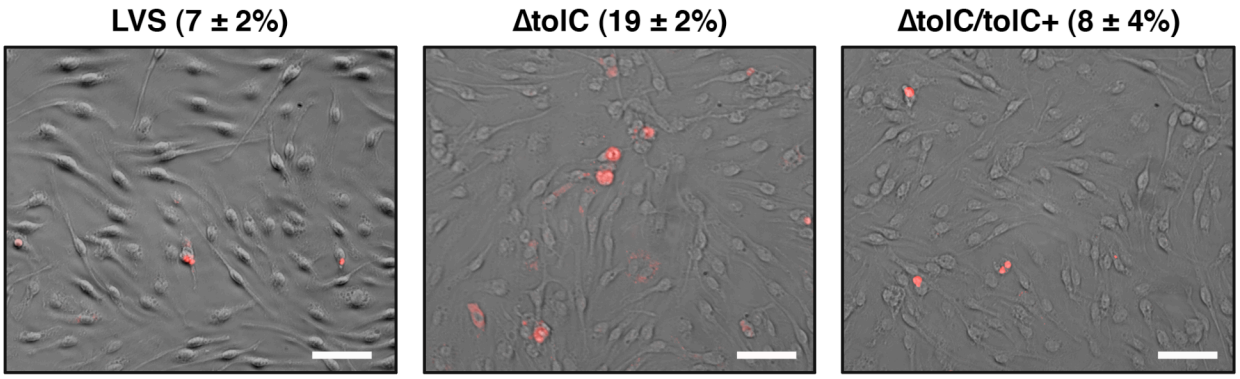

Figure 4.6 TUNEL staining of infected muBMDMs. MuBMDM infected as described above were assayed for apoptosis or pyroptosis at 17 HPI by TUNEL staining. The images show overlays of TUNEL-positive cells (red) and corresponding phase-contrast images. The percentages of TUNEL-positive cells ± SEM were calculated from ten separate fields and represent the average of three independent experiments. The Δ*tolC* mutant caused significantly increased TUNEL staining compared to the wild-type LVS ($P < 0.05$). Scale bars = 50 μm.

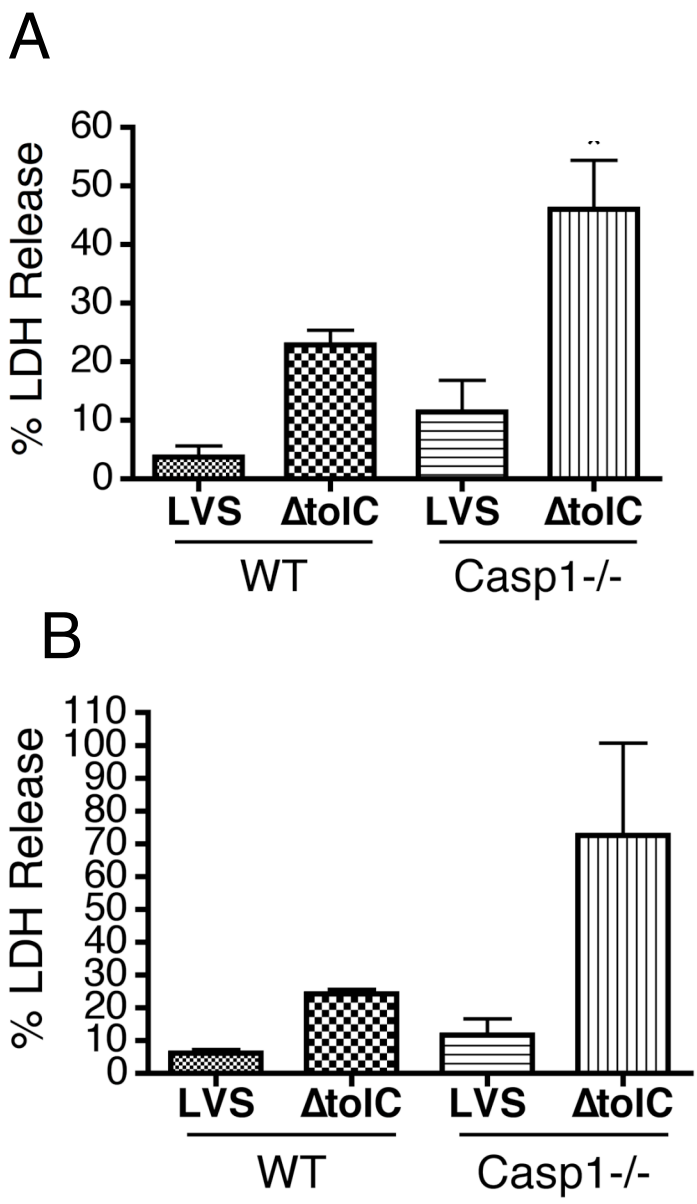

Figure 4.7 LVS induced cytotoxicity in caspase-1 deficient muBMDM. MuBMDM isolated from wild-type or caspase-1-deficient C57BL/6 mice were infected with the LVS or Δ*tolC* mutant at a MOI of 50. Cytotoxicity was quantified by measuring LDH release at 24 HPI. The Δ*tolC* mutant caused significantly increased LDH release compared to the wild-type LVS for the caspase-1-deficient muBMDM. (A) A representative experiment is shown. (B) A second representative experiment. Bars represent means ± SEM of three replicate samples.

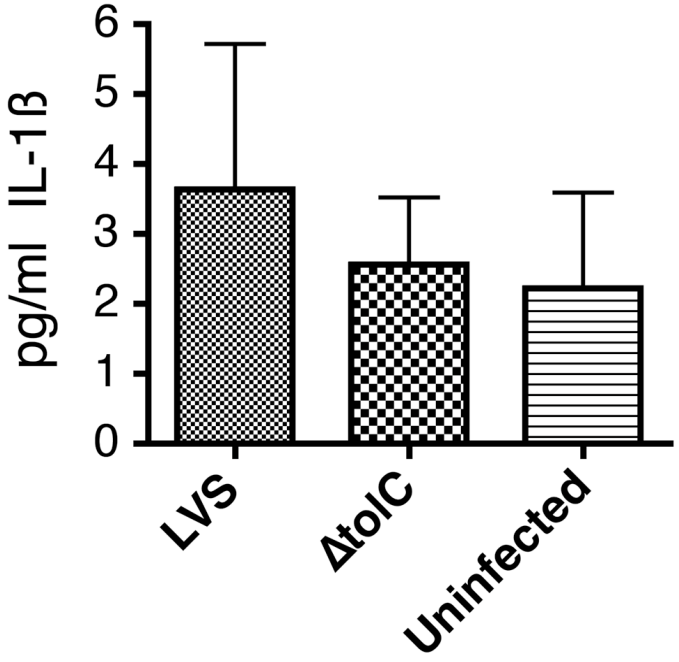

Figure 4.8 IL-1β release from LVS infected muBMDM. MuBMDM isolated from C3H/HeN mice were uninfected or infected with the LVS or Δ*tolC* mutant at a MOI of 50. ELISA of conditioned media at 24 HPI quantified IL-1β release. Bars represent means ± SEM of three independent experiments. IL-1ß secretion remained at background levels for all infections.

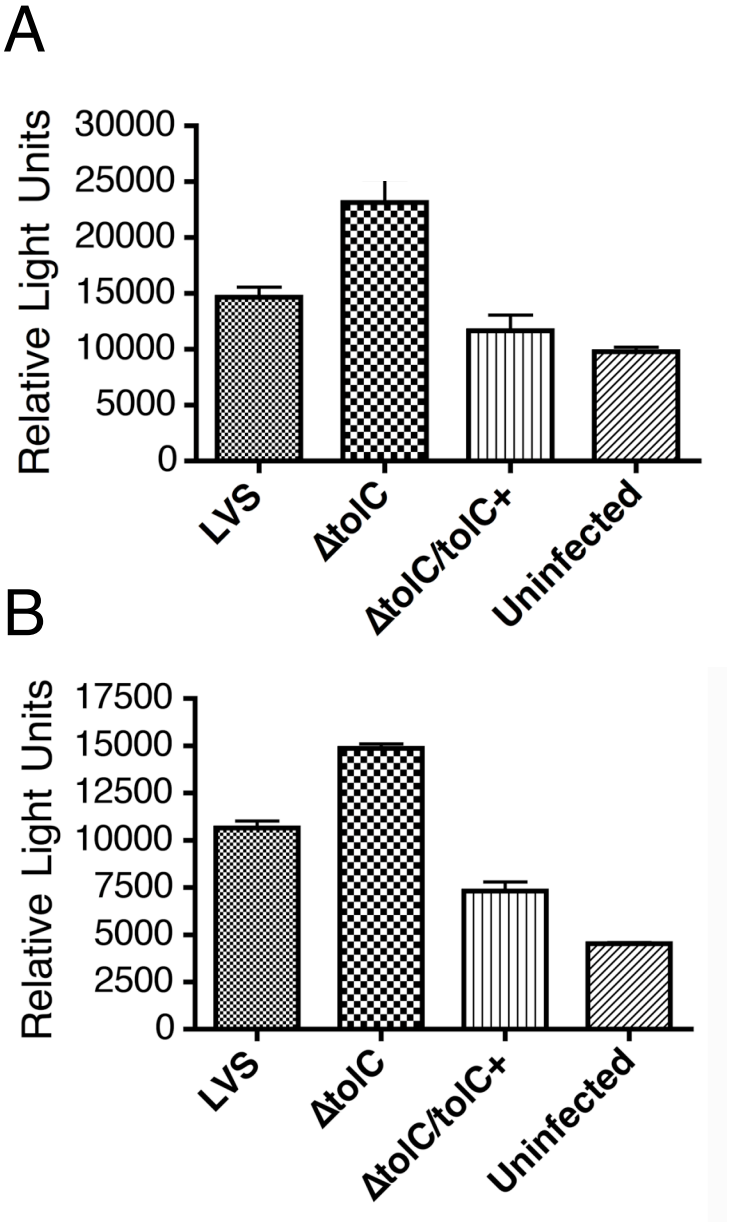

Figure 4.9 Activated caspase-3/7 from LVS infected muBMDM. MuBMDM isolated from C3H/HeN mice were uninfected or infected with the LVS, Δ*tolC* mutant or complemented strain (Δ*tolC*/*tolC*$^{+}$) at a MOI of 50. Activated caspase-3/7 was measured at 17 HPI using a luminescence-based assay. (A) A representative experiment is shown. (B) A second representative experiment. Bars represent means ± SEM of three replicate samples. Infection with the Δ*tolC* mutant caused a significant increase in caspase-3/7 activity compared to the wild-type LVS.

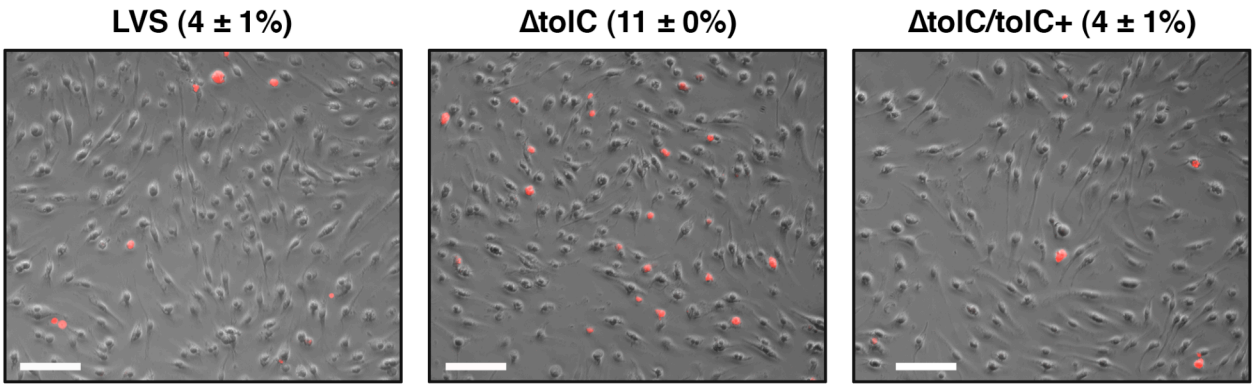

Figure 4.10 Caspase-3 staining of LVS infected muBMDM. MuBMDM isolated from C3H/HeN mice were uninfected or infected with the LVS, Δ*tolC* mutant or complemented strain (Δ*tolC*/*tolC*$^{+}$) at a MOI of 50 and probed with an antibody against mature caspase-3 followed by a TRITC-conjugated secondary antibody. The images show overlays of caspase-3-positive cells (red) and corresponding phase-contrast images. The percentages of caspase-3-positive cells ± SEM were calculated from ten separate fields and represent the average of three independent experiments. The Δ*tolC* mutant caused significantly increased staining compared to the wild-type LVS ($P < 0.05$). Bars = 50 µm.

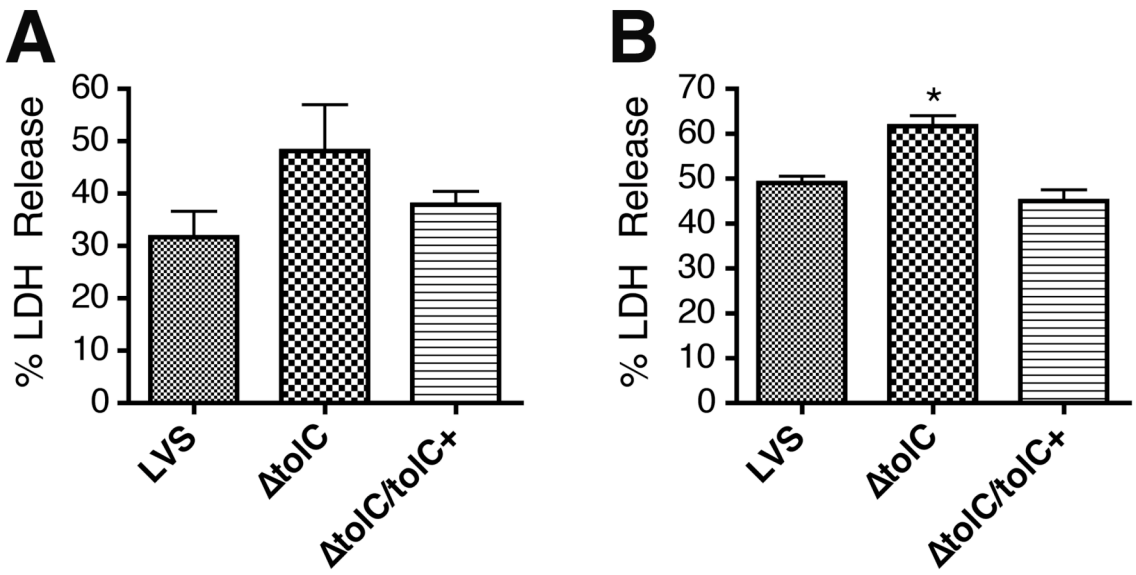

Figure 4.11 LVS induced cytotoxicity in HuMDM. HuMDM were infected with the LVS, Δ*tolC* mutant or complemented strain (Δ*tolC*/*tolC*$^{+}$) at a MOI of 50. Cytotoxicity was quantified by measuring LDH release at (A) 17 or (B) 24 HPI. Bars represent means ± SEM of three independent experiments. The Δ*tolC* mutant caused significantly increased LDH release compared to the wild-type LVS at 24 h PI ($P < 0.05$).

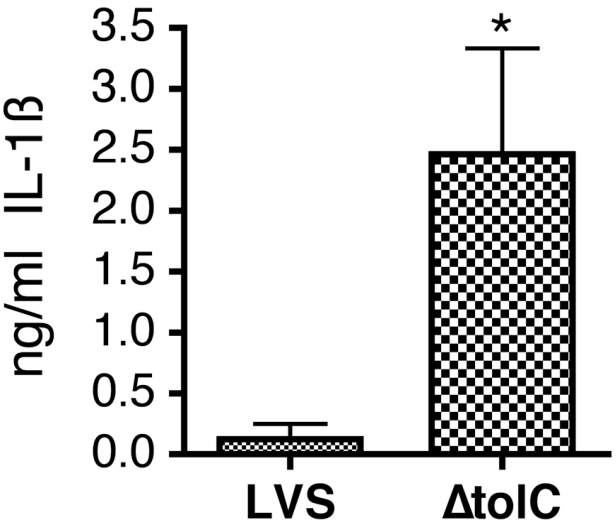

Figure 4.12 IL-1β release from LVS infected HuMDM. HuMDM were infected with the LVS or Δ*tolC* mutant at a MOI of 25. ELISA of conditioned media at 24 HPI quantified IL-1β release. Bars represent means ± SEM of three independent experiments. The Δ*tolC* mutant caused a significant increase in IL-1ß secretion compared to the wild-type LVS ($P < 0.05$).

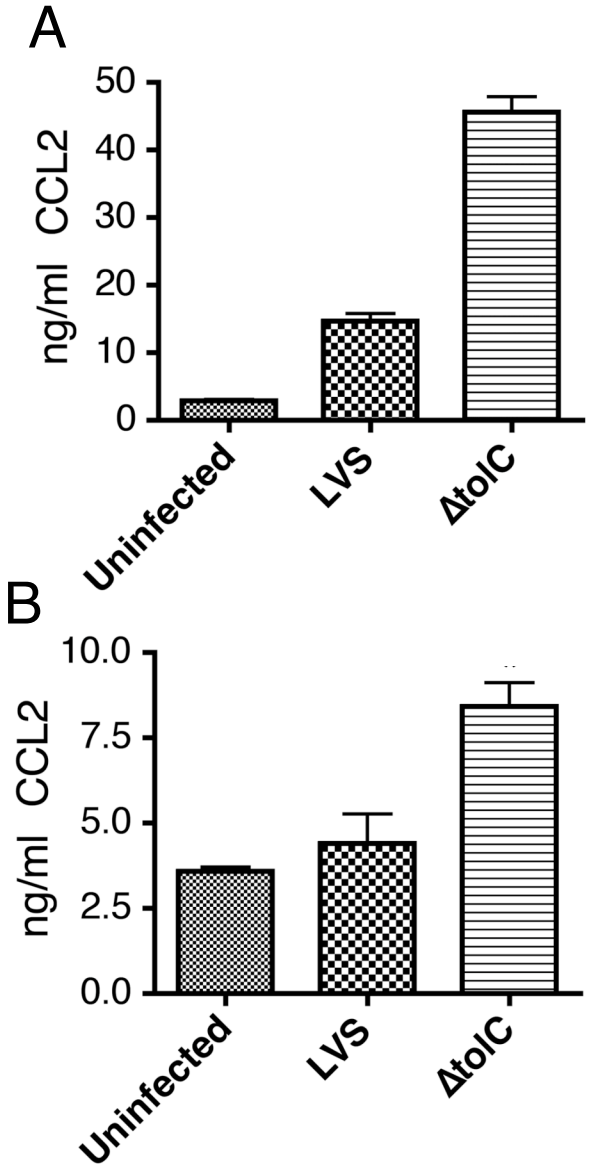

Figure 4.13 CCL2 release from LVS infected huMDM. HuMDM were uninfected or infected with the LVS or Δ*tolC* mutant at a MOI of 25. ELISA of conditioned media at 24 h PI quantified secretion of CCL2. (A) A representative experiment. (B) A second representative experiment. Bars represent means ± SEM of three replicate samples. The Δ*tolC* mutant caused significantly increased secretion of this proinflammatory chemokine compared to the wild-type LVS.

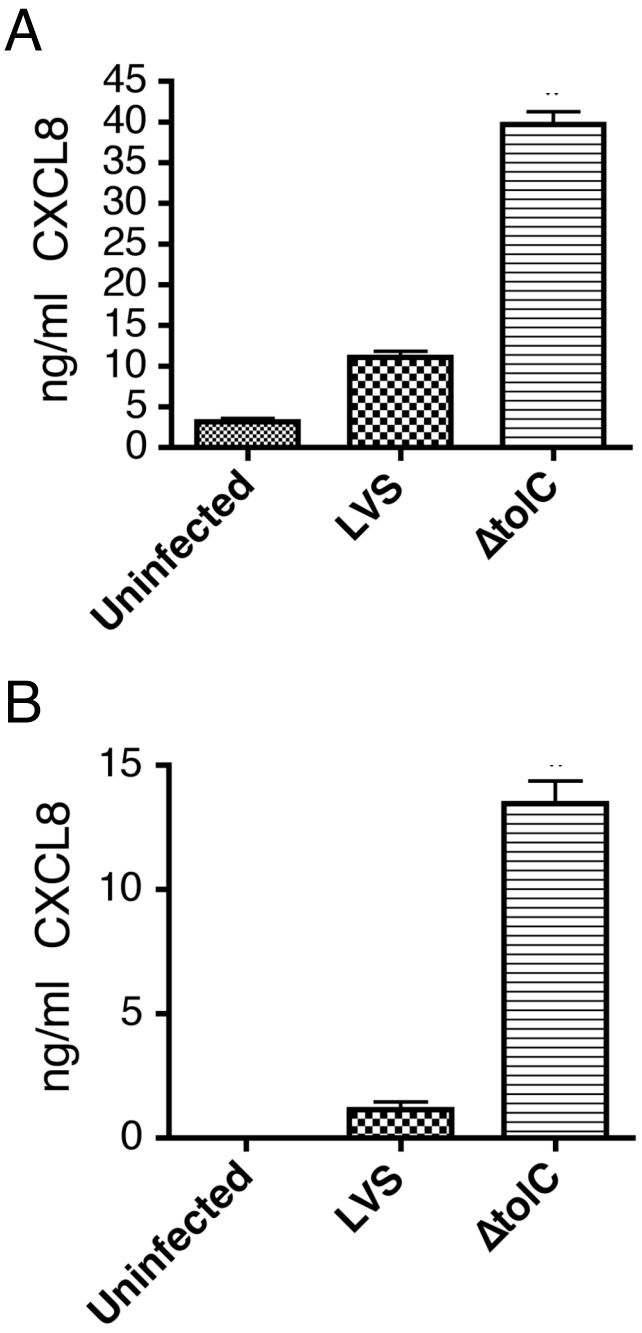

Figure 4.14 CXCL8 release from LVS infected huMDM. HuMDM were uninfected or infected with the LVS or Δ*tolC* mutant at aMOI of 25. ELISA of conditioned media at 24 HPI quantified secretion of CXCL8. (A) A representative experiment. (B) A second representative experiment. Bars represent means ± SEM of three replicate samples. The Δ*tolC* mutant caused significantly increased secretion of this proinflammatory chemokine compared to the wild-type LVS.

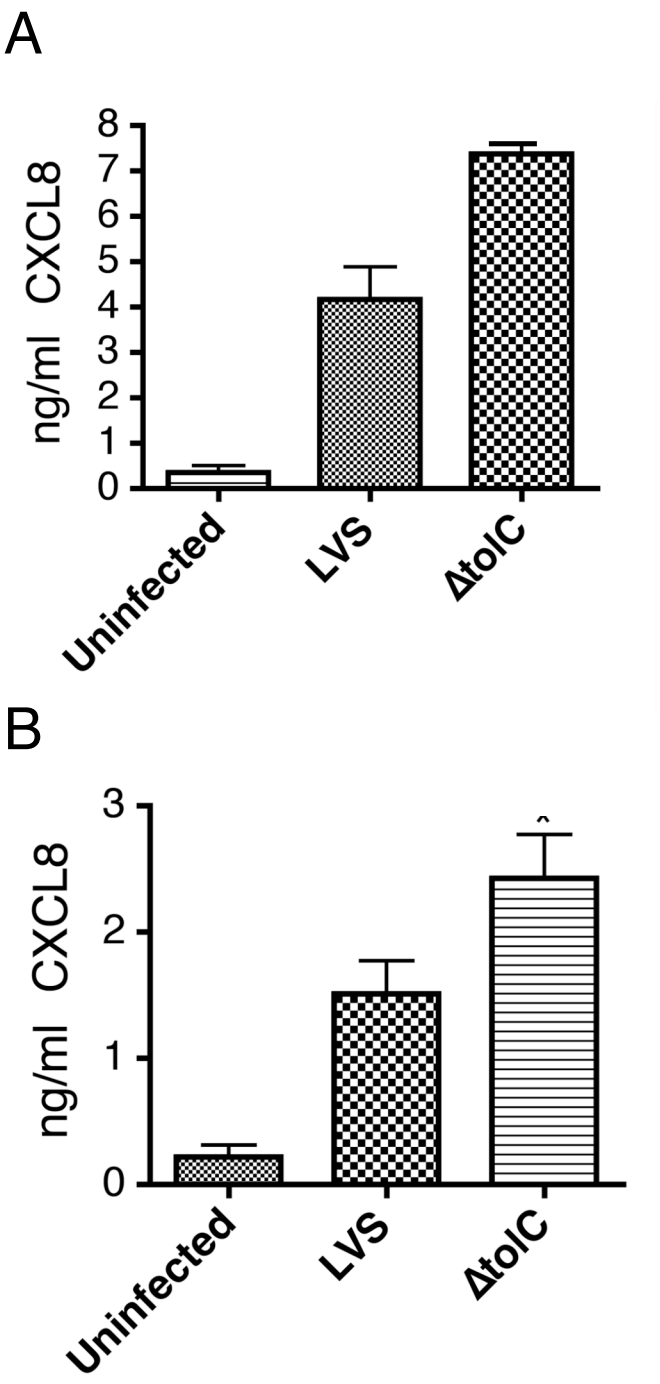

Figure 4.15 CXCL8 release from LVS infected HUVEC. HUVEC were incubated with medium alone or with the LVS or Δ*tolC* mutant at a MOI of 75. ELISA of conditioned media at 24 HPI quantified secretion of CXCL8. (A) A representative experiment. (B) A second representative experiment. Bars represent means ± SEM of three replicate samples. The Δ*tolC* mutant caused significantly increased secretion of this proinflammatory chemokine compared to the wild-type LVS.

Chapter Five
Investigation of TolC-Dependent Secreted Virulence Factors

I. Introduction

Based on our findings we hypothesize that *F. tularensis* TolC is functioning in the secretion of proteins, most likely a virulence factor, via a type I secretion apparatus. In addition to the three TolC homologs, the genome of *F. tularensis* provides further evidence to support the idea of a functioning type I secretion system. The type I secretion system is formed by the association of three separate proteins: the outer membrane channel protein (TolC), a periplasmic adaptor protein, and an inner membrane (IM) energy-providing protein (Koronakis et al., 2004). For multidrug efflux systems, the inner membrane component is more commonly a proton antiporter belonging to either the resistance-nodulation-division (RND) or major facilitator superfamily (MFS) (Koronakis et al., 2004; Koronakis et al., 1993). In protein secretion the inner membrane component is usually an ATP-binding cassette (ABC) transporter (Koronakis et al., 2004). Encoded within the genome of *F. tularensis* are fifteen potential ABC transporters, five to seven of which may be involved in efflux or secretion (Atkins et al., 2006). *F. tularensis* also contains several genes homologous to the *E. coli* periplasmic adaptor protein HlyD. Notably, when the *hlyD* sequence of *E. coli* was blasted against the genome of *F. tularensis,* Emr and Acr were identified in the genome of *F. tularensis* as being potential homologs. Emr and Acr systems work together with TolC in other bacteria to pump out a

broad range of antibiotics and harmful compounds (Koronakis et al., 2004; Zgurskaya and Nikaido, 1999).

E. coli TolC has been studied extensively since 1965, and as a result much is known about its structure and function in secretion. Hemolysin (HlyA) is the hallmark protein substrate studied to understand type I secretion in *E. coli* (Koronakis and Hughes, 1993). Hemolysin is a secreted toxin, which targets neighboring host cells, binds them and disrupts the integrity of the cell membrane. This causes the cells to lyse and release nutrients into the surrounding environment (Koronakis and Hughes, 1993). Colicin is a toxin produced by some species of *E. coli*, which inhibits the growth of similar or closely related bacterial species. *E. coli* colicin molecules are known to gain entry into bacteria via TolC (Davies and Reeves, 1975). In *E. coli* as well as *V. cholerae,* it is also known that TolC secretes bile salts (Bina and Mekalanos, 2001). Bile salts are detergent-like molecules found in the intestines and are harmful to bacteria if permitted to build up. MacConkey agar is a differential medium upon which only Gram-negative bacteria with a functional bile salt secretion apparatus grow (McCleery and Rowe, 1995).

The *E. coli* TolC is known to be involved in the efflux of enterobactin, a catecholate-type siderophore (Bleuel et al., 2005). Recently, the gene cluster *fslABCD,* responsible for synthesis of siderophore in *F. tularensis,* was characterized (Sullivan et al., 2006). Iron is one of the most limiting nutrients in the mammalian cell, and thus pathogenic bacteria have evolved means of acquiring iron from their hosts. Bacteria secrete siderophores, which are small molecules with a high affinity for binding iron. In fact, it has been shown that iron limitation affects the transcription of various genes in *F. tularensis,* such as *iglC* and *pdpB* (Deng et al., 2006).

In light of these findings we wanted to determine if the *F. tularensis tolC* or *ftlC* are involved in siderophore, hemolysin, bile salt or multidrug secretion/efflux, or if they confer sensitivity to colicin. Here, we report that the *F. tularensis tolC* homologs do not appear to be involved in the secretion of siderophore, they are not involved in the efflux of bile salts, and they do not confer sensitivity to colicin. In subspecies *novicida,* both *tolC* and *ftlC* form part of the multidrug resistance machinery, and *tolC* appears to be a virulence determinant of the subspecies. In vitro tissue culture infections showed that compared to the wild-type *F. novicida* U112, the *tolC* mutant is hypercytotoxic to muBMDM cells. Additionally, subspecies *novicida tolC* homologs are involved in secretion of hemolysin, a bona fide type 1 secretion system substrate.

II. Results

Complementation of *E. coli tolC* mutants with *F. tularensis tolC* or *ftlC*

We complemented an *E. coli tolC* mutant (kindly provided by Rajeev Misra at Arizona State University) with wild-type copies of LVS *tolC* or *ftlC* to determine whether or not the *F. tularensis* protein could restore the function of *tolC* in *E. coli.* The *E.coli tolC* and *ftlC* mutants were complemented with pGPTA, or pGPTB, respectively. We also transformed the mutant *E. coli* strains with the empty pFNLTP6gro-gfp vector and obtained gfp-expressing bacteria; thus, confirming that the native *F. tularensis* gro-EL promoter is functional in *E. coli.* Additionally, we complemented the mutant *E. coli* strains with pBAD-TA(His) and pBAD18-TB(His). Expression of these vectors was confirmed by Western blott analysis using anti-His-tag antibodies. The complemented *E. coli* strains were then tested for the ability to secret hemolysin, secrete bile salts, or act as a colicin receptor. To test for the ability to secrete hemolysin, the complemented *E. coli* mutants were plated as single colonies on LB plates containing 5% sheep erythrocytes. For strains with hemolytic secretion ability, the red blood cells within the agar surrounding the bacterial colonies would be lysed and a zone of clearing observed. We found that *tolC* and *ftlC* of the LVS were unable to complement the *E. coli tolC* mutant for hemolysin secretion (Table 5.1). In a separate assay, we tested the ability of *F. tularensis* TolC to bind colicin. Here, the complemented *E. coli* mutants were plated as a lawn on LB plates, paper discs containing varying concentrations of colicin were added

to the plates, and the following day sensitivity to the colicin was assessed by measuring the zone of clearing around the paper discs. The LVS *tolC* and *ftlC* did not complement the *E. coli tolC* mutant, to act as colicin receptors (Table 5.1). In addition to testing the complemented *E. coli* mutants for hemolysin secretion and colicin sensitivity, we tested for the ability to secrete bile salts. Here, we used MacConkey selectable medium. Growth on MacConkey medium requires that the bacteria secrete bile salts. The *F. tularensis* LVS TolC homologs were unable to complement the *E. coli tolC* mutants for bile salt secretion (Table 5.1).

Role of TolC homologs in the secretion of siderophore

The *E. coli* TolC is known to be involved in the efflux of siderophores (Bleuel et al., 2005). Additionally, we know that *F. tularensis* contains the gene cluster *fslABCD,* which is responsible for synthesis of siderophore (Sullivan et al., 2006). Therefore, we preformed a Chrome Azurol S (CAS) assay to determine if the *F. tularensis* TolC homologs are required for secretion of siderophore. The CAS assay is a method developed to detect siderophores (Schwyn and Neilands, 1987). CAS is mixed with iron to form a dye-Fe complex. When a strong chelator such as siderophore is present, it removes the iron from the dye, changing the solution color from blue to orange (Schwyn and Neilands, 1987). The presence of siderophore/CAS activity in the supernatants was determined by optical density measurements. Neither *tolC* nor *ftlC* appear to be involved in siderophore secretion, as the amount of CAS activity produced by the deletion strains mirrored that of the parental LVS (Figure 5.1).

Gaining insight into TolC Function using a transposon mutant library of subspecied *novicida*

To gain a better understanding of the function of the TolC and FtlC proteins, a transposon mutant library of *F. tularensis* subsp. *novicida* strain U112 was ordered from the University of Washington (Gallagher et al., 2007). Our initial analysis was conducted on strains U112_FTN1703::Tn18, which is mutated for the *tolC* homolog, and U112_FTN0079::Tn18, which is mutated for the *ftlC* homolog. We tested the ability of these mutants to cause disease in vivo, determined if either was hypercytotoxic to muBMDM cells when compared to the wild-type U112 strain, and lastly, analyzed the mutants for antibiotic sensitivity. Similar to intradermal infections using the LVS Δ*tolC* mutant, the subspecies *novicida* transposon mutant U112_FTN1703::Tn18 was attenuated for virulence, suggesting that the subspecies *novicida tolC* homolog is a virulence determinant (Figure 5.2). Again, as was seen in intradermal infections using the LVS Δ*ftlC* mutant, the subspecies *novicida* transposon mutant U112_FTN0079::Tn18 was only slightly attenuated for virulence, suggesting that the subspecies *novicida ftlC* homolog is not as important to virulence as the *tolC* homolog (Figure 5.2).

Tissue culture analysis using primary muBMDM cells revealed that the *tolC* homolog mutant U112_FTN1703::Tn18 is hypercytotoxic to murine macrophages. Cells infected with the U112_FTN1703::Tn18 strain released a greater amount of LDH into the medium when compared to cells infected with the wild-type U112 strain, U112_FTN0079::Tn18 or U112_FTN1277::Tn18 (Figure 5.3). Strain

U112_FTN1277::Tn18 has a transposon insertion in the gene homologous to *silC;* the *silC* gene shares more similarity with *E. coli* drug efflux proteins. Antibiotic sensitivity assays demonstrated that the U112_FTN1703::Tn18, U112_FTN0079::Tn18 and U112_FTN1277::Tn18 all participate as part of the multidrug resistance machinery in subspecies *novicida,* as all the transposon mutants exhibited an increase in sensitivity to a number of different antibiotics and dyes (Table 5.2).

To identify the type I secretion system proteins that partner together with TolC during multidrug efflux and protein secretion, analysis of additional subspecies *novicida* transposon mutants was conducted. In total, twelve transposon mutants homologous to type I secretion system partners in *E. coli* were analyzed (Figure 5.4). Three mutations were in homologs of the TolC, six transposon mutations were in homologs of the *E. coli* HlyD periplasmic adaptor protein, and three mutations were in homologs of the *E. coli* HlyB inner membrane protein. Of the inner membrane proteins, FTN1275 most closely resembles a drug efflux pump or H+ antiporter, FTN1693 resembles an ATP binding Cassette protein and FTN1610 resembles an RND efflux pump (Figure 5.4).

We conducted drug sensitivity assays on the remaining nine transposon mutants to determine if any of those protein are involved in multidrug efflux. Notably, strains U112 FTN_1609::Tn18 (periplasmic adaptor mutant) and U112 FTN_1610::Tn18 (IM protein mutant) displayed roughly the same increased sensitivity to various antibiotics, detergents, and dyes (Table 5.2). This data suggests that the *F. novicida* genes FTN1609 and FTN1610 may function as the periplasmic adaptor protein and inner membrane protein, respectively, for drug efflux. However, more analysis will have to be conducted

to determine conclusively if these proteins associate together in multidrug efflux and protein secretion.

Additional work with the subspecies *novicida* transposon mutants was performed to examine the role of the subspecies *novicida* TolC homologs in hemolysin (HlyA) secretion. Again, hemolysin (HlyA) is the hallmark protein substrate studied to understand type I secretion in *E. coli* (Koronakis and Hughes, 1993). The only species of *F. tularensis* known to have hemolytic abilities are subspecies *novicida* and *F. philomiragia.* We assessed hemolysin secretion over a period of time from the wild-type U112, U112 FTN1703::Tn18 (*tolC*), U112 FTN0079::Tn18 (*ftlC*), and U112 FTN1277::Tn18 (*silC*) strains. Cultures of these strains were incubated with horse blood erythrocytes, and lysis of the red blood cells was measured to determine hemolysin secretion. Lysis was measured by OD_{600} at 48 hours post incubation (PI). Our data shows that the subspecies *novicida tolC* homologs 1703, 0079, and 1277 all appear to be involved in the secretion of hemolysin, as each strain lysed a significantly lower amount of red blood cells compared to the lysis of red blood cells resultant from U112 co-incubation (Figure 5.5). The subspecies *novicida tolC* homolog, 1703, had the most significant decrease in hemolysin secretion compared to wild-type U112 (Figure 5.5). This is particularly interesting because it is the first evidence that the TolC of any *F. tularensis* species participates in type I protein secretion.

Production of a TolC polyclonal antibody

To further study and characterize the function of TolC and FtlC in vitro and in vivo, antibodies specific to these proteins were generated. To obtain purified protein, vectors for the expression and purification of TolC and FtlC from *E. coli* were constructed. His-tagged versions of the genes were constructed by PCR and cloned into Pet28-a vector for expression in *E. coli*. The *ftlC* gene contains an atypical TTG start codon, which results in very low expression of the protein. To express FtlC protein, a point mutation was made to the gene, mutating the TTG start codon to the more common ATG start codon. Additionally, we removed the signal sequences from the N-termini of the genes in order to purify the proteins from cytoplasmic inclusion bodies. The proteins were purified using fast protein liquid chromatography (FPLC). Once the purified protein was acquired we used it to raise rabbit polyclonal antibodies. The newly generated antibodies were tested for specificity by immunoblotting against LVS, Δ*tolC* and Δ*ftlC* whole cell lysates. The anti-TolC antibody was specific for TolC protein (Figure 5.6, panel A), but the anti-FtlC antibody appeared to cross react with TolC protein as well (Figure 5.6, panel B).

III. Discussion

To date, a secreted virulence factor for *F. tularensis* has failed to be identified. This is surprising considering the highly infectious nature of the organism. In this study we tested the ability of *F. tularensi*s to secrete a number of known *E. coli* TolC secretion substrates, including hemolysin, bile salts, and siderophores. Complementation of an *E. coli tolC* mutant incapable of secreting hemolysin with wild-type *F. tularensis tolC* did not restore hemolysin secretion to the *E. coli* mutant. In addition to testing the ability of *F. tularensis* TolC to secrete hemolysin, we tested its ability to secrete bile salts or to act as a colicin receptor. Neither TolC nor FtlC of *F. tularensis* is able to complement the *E. coli tolC* mutant for secretion of bile salt or confer sensitivity to colicin. This is not surprising, because the TolC proteins from different bacterial species are not always interchangeable (Vediyappan et al., 2006).

In *E. coli,* TolC is known to secrete siderophores, and recently the gene cluster *fslABCD* was identified as being responsible for synthesis of siderophore in *F. tularensis* (Bleuel et al., 2005; Sullivan et al., 2006). The first gene within the *fslABCD* gene cluster*, fslA,* was shown to be important to the survival of *F. tularensis* in tissue culture and in vivo (Sullivan et al., 2006). However, neither *F. tularensis tolC* nor *ftlC* appears to be involved in the release of siderophore, as there was no significant difference in the amount of siderophore present in the growth medium of the deletion strains when compared to the parental LVS.

Using the complete transposon mutant library of *F. tularensis* subsp. *novicida* (Gallagher et al., 2007) (http://www.francisella.org)*,* we were able to determine that *tolC*

and *ftlC* function the same way in both *F. tularensis* subspecies *novicida* and *holarctica.* Both *tolC* and *ftlC* mutants of subspecies *novicida* exhibited an increase in sensitivity to detergents, dyes and antibiotics, which suggests that both genes participate in multidrug efflux. In addition, the subspecies *novicida tolC* mutant was attenuated for virulence in the murine model via the intradermal route of infection. The subspecies *novicida ftlC* may be a virulence determinant in subspecies *novicida,* as the *ftlC* mutant strain was slightly attenuated for virulence in the murine model via the intradermal route of infection. The attenuation of the *F. novicida ftlC* mutant was significant when compared to infection with the wild-type U112 strain, but the most severe attenuation was observed in the subspecies *novocida tolC* mutant. Tissue culture analysis using primary muBMDM cells revealed that the subspecies *novicida tolC* mutant is hypercytotoxic to murine macrophages when compared to cells infected with the U112 strain. Reported in this dissertation and in previously published literature is the observation that the LVS induces apoptosis in murine macrophages based on an intrinsic apoptotic pathway (Lai et al., 2004). However, pyroptosis initiated by the activation of the inflammasome and caspase-1 has been reported in murine macrophages infected with subspecies *novicida*. We have not investigated the type of death observed in cells infected with subspecies *novicida*. It remains to be determined if cell death induced by subspecies *novicida* is apoptosis or pyroptosis, and the role of caspase in subspecies *novicida* induced cell death needs to be investigated. Our earlier findings demonstrate that the role of TolC in the activation or inhibition of caspases and proinflammatory responses differs between different host species. It would be interesting to determine if TolC mutants of different *F. tularensis* subspecies have the ability to activate different cell death pathways. In a separate analysis

using subspecies *novicida* transposon mutants, we determined that the subspecies *novicida* TolC, and to a lesser degree FtlC and SilC, function in the secretion of hemolysin. This is the first definitive evidence that TolC homologs of a *F. tularensis* subspecies actively participate in the secretion of protein.

In addition to characterizing the *tolC* and *ftlC* of *F. novicida,* we also investigated possible type I secretion system partners. We used the *E. coli hylD*, which is a periplasmic adaptor protein, and *hlyB,* which is an inner membrane energy providing protein, to search the genome of *F. novicida* by BLAST analysis. In total, six homologs of HlyD and three homologs of HlyB were identified. Using the complete *F. novicida* transposon library, we tested transposon mutants homologous to HlyD and HlyB in an antibiotic sensitivity screen. Noteworthy are two mutants, U112 FTN_1276::Tn18, a periplasmic adaptor homolog, and U112 FTN_1275::Tn18, a inner membrane protein homolog, because they displayed nearly identical sensitivity to the various drug panel compared to U112 FTN_1277::Tn18, which is the *silC* homolog. This is not surprising considering the location of these genes within the genomes; they all lie immediately next to one another. Therefore, it can be presumed that these genes are encoded and act within an operon. Additionally, two other transposon mutants, U112 FTN_1609::Tn18, a periplasmic adaptor protein homolog resembling an AcrA protein, and U112 FTN_1610::Tn18, an inner membrane protein homolog resembling an RND efflux pump, both displayed roughly the same sensitivity to the various antibiotics and dyes. The RND and AcrA are proton antiporters commonly used in multidrug efflux. This result suggests that the subspecies *novicida* genes FTN1609 and FTN1610 may function as the periplasmic adaptor protein and inner membrane protein, respectively, in multidrug

efflux. However, more analysis will have to be conducted to determine conclusively if these protein associate together in multidrug efflux and protein secretion.

Table 5.1 Attempted complementation of *Escherichia coli tolC* mutants with *Francisella tularensis tolC* or *ftlC*

Strains	Colicin Sensitivity	Hemolysin Activity	MacConkey Growth
RAM 958	No	No	No
RAM 960	Yes	No	Yes
RAM 970	No	No	No
RAM 972	Yes	Yes	Yes
958/pFNLTP6-tolC	No	Not Available	No
958/pFNLTP6-ftlC	No	Not Available	No
958/pFNLTP6-empty	No	Not Available	No
970/pFNLTP6-tolC	No	No	No
970/pFNLTP6-ftlC	No	No	No
970/pFNLTP6-empty	No	No	No
958/pBAD18-tolC	No	Not Available	No
958/pBAD18-ftlC	No	Not Available	No
958/pBAD18-empty	No	Not Available	No
970/pBAD18-tolC	No	No	No
970/pBAD18-ftlC	No	No	No
970/pBAD18-empty	No	No	No

RAM 958: Tn10:48 (*tolC*$^{-}$)
RAM 960: Strain 958 containing E. coli tolC rescue plasmid (pTrC/*tolC*$^{+}$
RAM 970: Strain 958 containing plasmid pHly (hemolysin operon)
RAM 972: Strain 960 containing pHly

Table 5.2 Drug sensitivity of *Francisella novicida* transposon mutants

Stains	Drug Class Detergent/ SDS (750µg)	Dyes/Ethidium Bromide (5µg)	Aminoglycosides/ Streptomycin (10µg)	Others/ Chloramphen (5µg)
LVS Deletion Mutants				
WT LVS	9 ± 1.0*	6 ± 0.0	20 ± 1.0	20 ± 1.0
LVS/Δ*tolC*	13 ± 1.0	18 ± 1.0	25 ± 1.0	24 ± 1.0
LVS/Δ*ftlC*	13 ±1.0	17 ± 1 .0	23 ± 1.0	26 ± 1.0
***F. novicida* Tn Mutants**				
WT U112	8 ± 0.5	15 ± 0.8	10 ± 0.0	16 ± 1.5
Outer Membrane Mutants				
U112:Tn1703 (TolC)	25 ± 1.6	18 ± 2.2	9 ± 2.3	20 ± 1.7
U112:Tn0779 (FtlC)	23 ± 1.3	19 ± 1.3	10 ± 2.0	20 ± 1.9
U112:Tn1277 (SilC)	11 ± 1.4	17 ± 0.0	11 ± 0.7	21 ± 0.0
Inner Membrane Mutants				
U112:Tn0029 (EmrA homolog)	10 ± 1.9	14 ± 0.8	8 ± 1.5	18 ± 1.9
U112:Tn1276 (EmrA homolog)	9 ± 0.6	17 ± 1.0	9 ± 0.6	19 ± 1.5
U112:Tn1609 (AcrA homolog)	22 ± 1.2	17 ± 1.0	10 ± 1.7	20 ± 1.7
U112:Tn1692 (AcrA homolog)	9 ± 1.3	14 ± 1.0	9 ± 1.2	16 ± 0.8
Adaptors Mutants				
U112:Tn1275 (H+ antipoorter)	8 ± 1.2	18 ± 0.8	8 ± 0.6	18 ± 1.4
U112:Tn1610 (RND efflux pump)	21 ± 1.7	17 ± 1.4	9 ± 1.2	19 ± 1.0
U112:Tn1693 (ATP binding Cassette	11 ± 2.0	14 ± 1.7	10 ± 1.5	17 ± 1.2

*Average diameter of the zone of inhibition (including filter disc) in mm ± standard deviation. The diameter of the filter disk is 6 mm.

IV. Figures

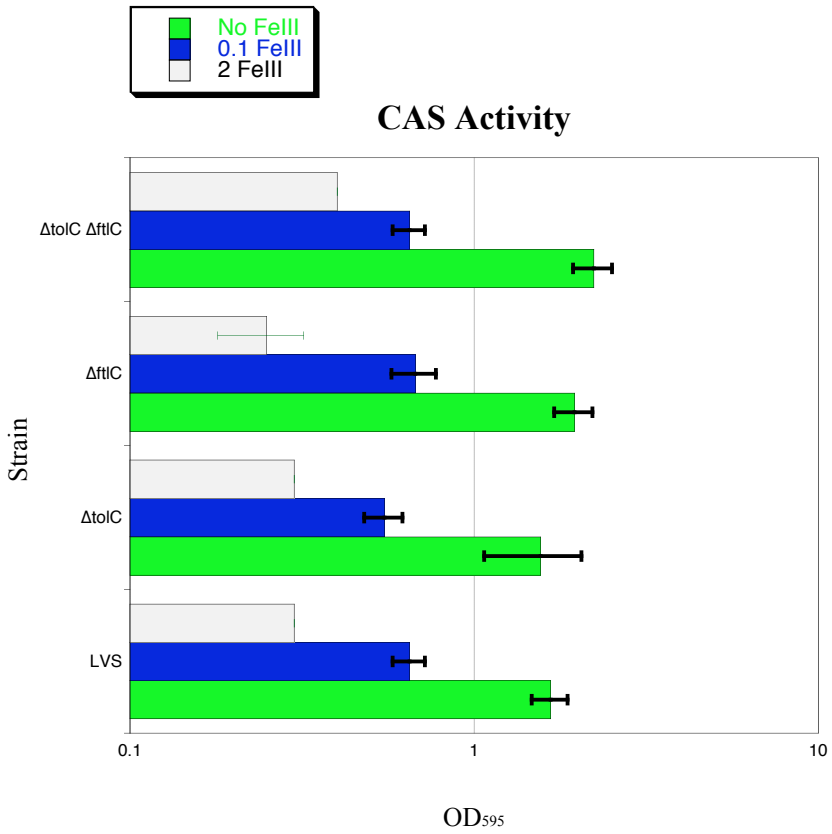

Figure 5.1 Chrome Azurol S (CAS) assay. LVS, Δ*tolC,* Δ*ftlC* and Δ*tolC* Δ*ftlC* were grown for 55 hours in CDM containing varying amounts of FeIII. After growth, OD_{630} measurments were taken to quantify siderophore secretion. The LVS, Δ*tolC,* Δ*ftlC* and Δ*tolC* Δ*ftlC* secreted comparable amounts of siderophore. Siderophore secretion in all cases was dependent upon the starting amount of iron present in the media either no FeIII, 0.1 μg/ml FeIII, or 2 μg/ml FeIII.

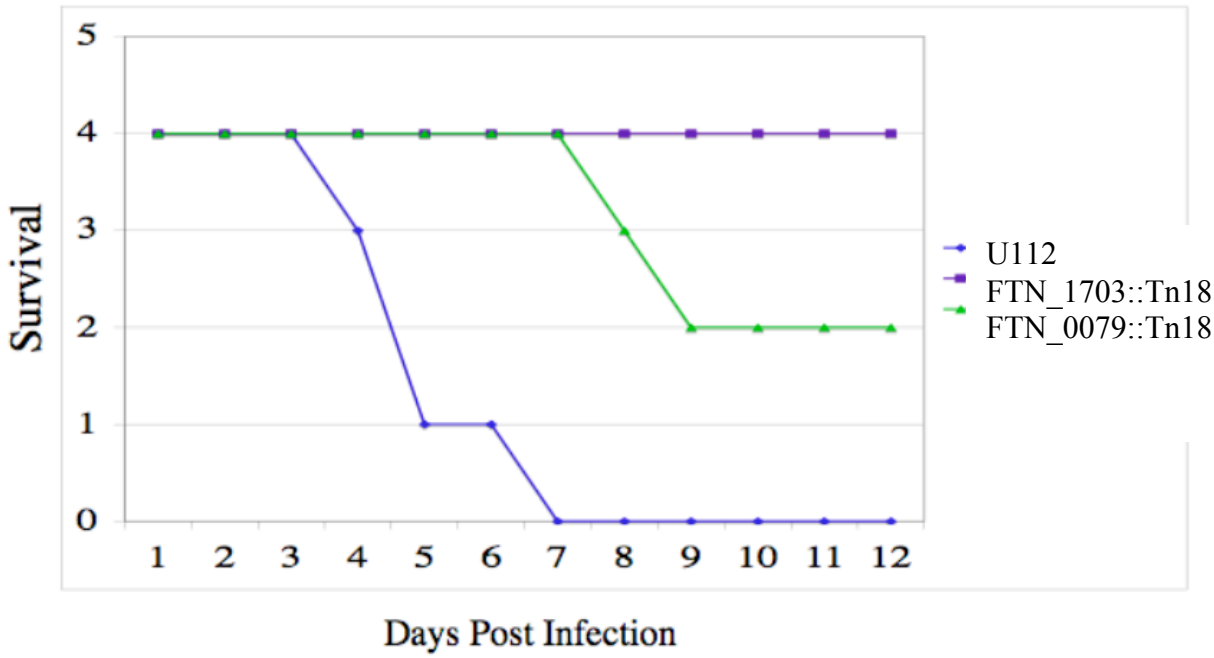

Figure 5.2 Lethal murine intradermal infection experiment. Groups of five Balb/C mice were intradermally inoculated with 1 x 10^6 CFU of U112, FTN_1703::Tn18 (*tolC* homolog) or FTN_0079::Tn18 (*ftlC* homolog) and monitored for survival for 12 days. The FTN_1703::Tn18 mutant was significantly attenuated compared to the parental U112 ($P < 0.02$). The FTN_0079::Tn18 mutant was significantly attenuated compared to the parental U112 ($P < 0.03$).

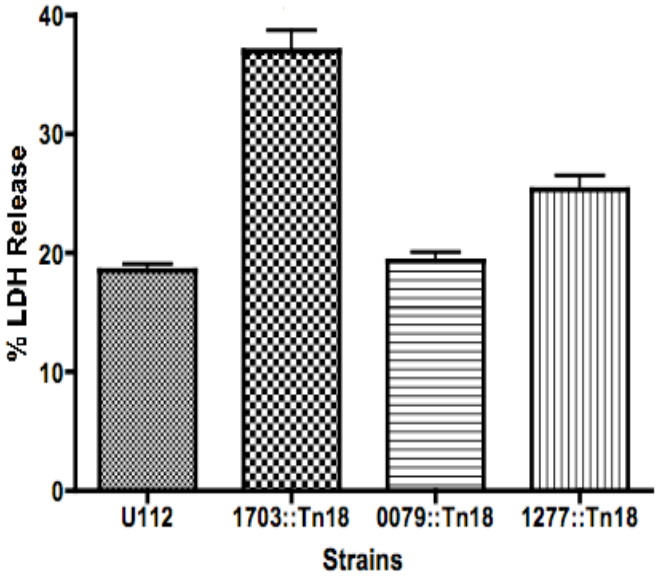

Figure 5.3 *Francisella novicida* induced cytotoxicity in MuBMDM. MuBMDM cultured from C3H/HeN mice were infected with U112, FTN_1703::Tn18 (*tolC* homolog), FTN_0079::Tn18 (*ftlC* homolog), or FTN_1277::Tn18 at a MOI of 50. Cytotoxicity was quantified by measuring LDH release at 24 HPI. A representative experiment is shown. Bars represent means ± SEM of three replicate samples. The FTN_1703::Tn18 mutant caused significantly increased LDH release compared to the wild-type U112.

A

TolC Homologs

FTN1703 = *F. novicida tolC*
FTN0779 = F. novicida *ftlC*
FTN1277 = F. novicida *silC*

B

Adaptors

FTN1692 (AcrA homolog), e=10-5
FTN1609 (AcrA homolog) e= 0.001
FTN0029 (EmrA homolog), low homology e= 0.018
FTN1276 (EmrA homolog)
FTN0718 (EmrA homolog)
FTN0454 (EmrA homolog)

C

ATPase Binding Cassettes

FTN1275 (Drug efflux pump, H+ antiporter)
FTN 1693 (ATP Binding Cassette)
FTN1610 (RND Efflux pump)

Figure 5.4 List of analyzed *Francisella tularensis,* subspecies *novicida* transposon mutants. (A) TolC homologs were identified using SchuS4 FTT1724 (*tolC*), SchuS4 FTT1095 (*ftlC*) and SchuS4 FTT1258 (*silC*) sequences, respectively, to search the genome of subspecies *novicida* by BLAST analysis. (B) Adaptor homologs were identified using *E. coli* HlyD (periplasmic adaptor protein) sequence to search the genome of subspecies *novicida* by BLAST analysis, three homologs were found to have significant homology to *E. coli* HlyD. Three additional EmrA homologs were identified using the FTN0029 (EmrA homolog) sequence to search the genome of subspecies *novicida* by BLAST analysis. (C) ATPase Binding Cassettes homologs were identified using *E. coli* HlyB (inner membrane protein) sequence to search the genome of subspecies *novicida* by BLAST analysis. Color codes indicate possible operons. All *Francisella novicida* transposon mutants were obtained from the University of Washington.

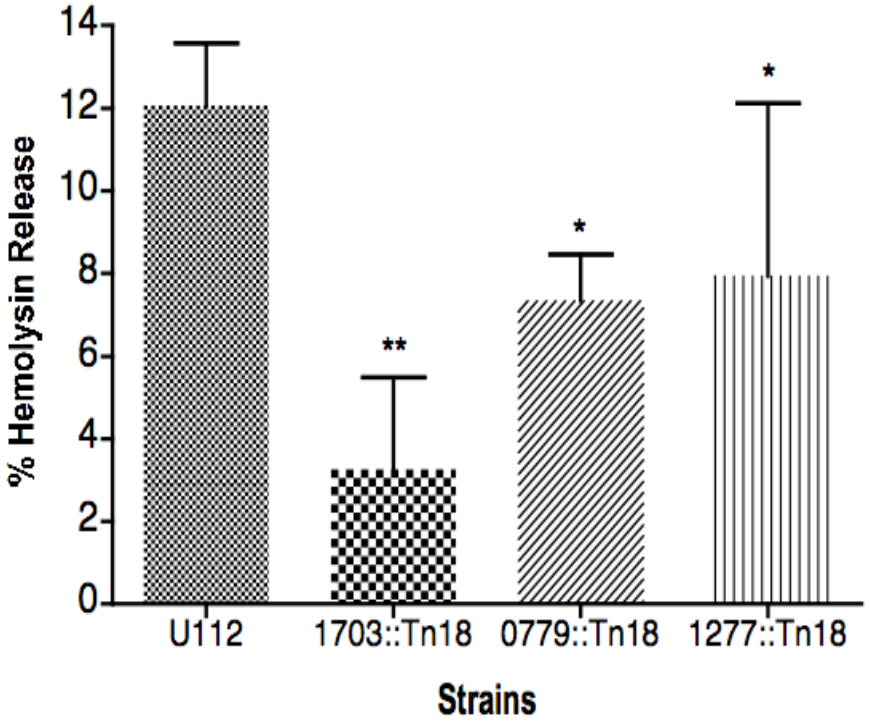

Figure 5.5 Hemolysin secretion assay. Cultures of U112, FTN_1703::Tn 18 (*tolC*), FTN_0079::Tn18 (*ftlC*), and FTN_1277::Tn18 (*silC*) were co-incubated with horse erythrocytes. At 48 hours post incubation lysis of red blood cells was measured by A_{540}. Bars represent means ± standard error of the mean (SEM) of three independent experiments. subspecies *novicida tolC* homologs FTN1703, FTN0079 and FTN1277 all appear to participate in secretion of hemolysin. FTN1703 has the most drastic reduction of hemolysin secretion when compared to U112 strain (**$P < 0.01$, *$P < 0.05$).

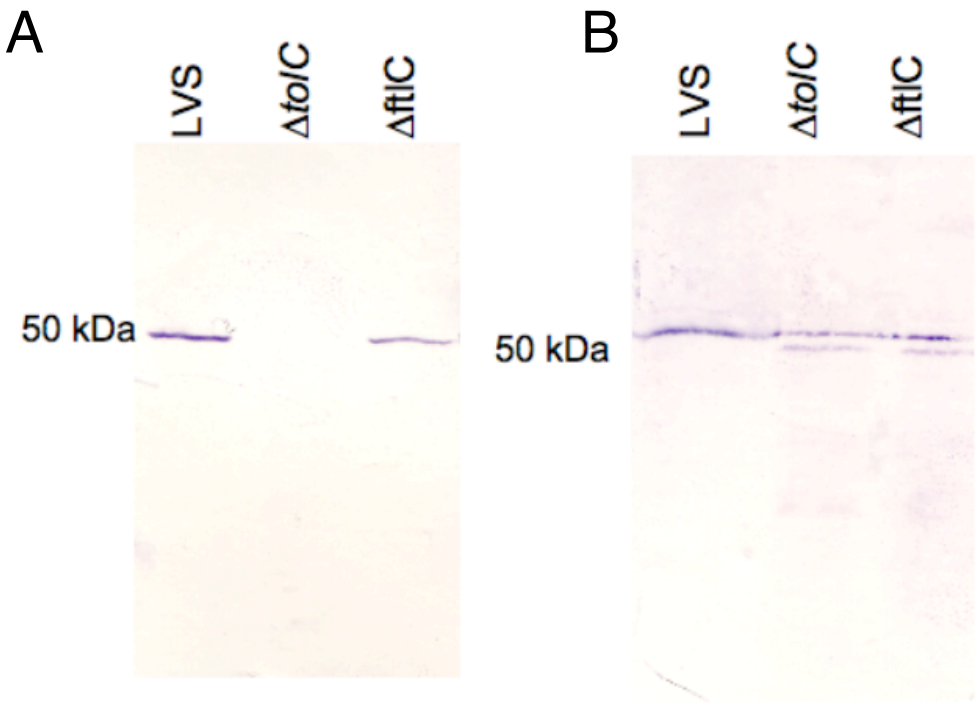

Figure 5.6 Specificity of Anti-TolC and anti-FtlC polyclonal antibodies. Anti-TolC and anti-FtlC polyclonal antibodies were tested against LVS, Δ*tolC* and Δ*ftlC* whole cell lysates to verify if the antibodies were specific to each respective protein. (A) Anti-TolC antibody against whole cell lysates shows that the α-TolC antibody is specific to the TolC protein. (B) Anti-FTLC antibody against whole cell lysates shows that the α-FtlC antibody cross-reacts with TolC.

Chapter 6

Conclusions and Future Directions

I. Conclusions

Gram-negative bacterial species have a complex cell envelope, containing an outer and inner membrane. Over millions of years of evolution these bacterial species have developed sophisticated secretion systems as a means to deliver bacterial toxins and virulence factors to the extracellular environment and into host cells. *F. tularensis* is devoid of any type III, IV or V secretion system (Larsson et al., 2005). This is very surprising when the pathogenic nature of *F. tularensis* is taken into consideration. There is some evidence supporting the idea that a type VI secretion system may be encoded in the FPI, but this notion has yet to be proven. In addition, within the genome of *F. tularensis* are 15 functional ATPases, which commonly function in type I secretion. The type I secretion system consists of three proteins: an outer membrane channel protein (OMP), a periplasmic adaptor protein and an inner membrane (IM) energy providing protein. The *E. coli* TolC protein, which is the OMP of its type I secretion system, was used to identify three orthologs of the TolC in *F. tularensis.* The three orthologs have been termed *tolC, ftlC* and *silC* (Gil et al., 2006; Huntley et al., 2007). The TolC and FtlC have the most homology to the *E. coli* TolC that participates in protein secretion, while the SilC resembles a protein utilized in drug efflux.

To verify the importance of these genes in *F. tularensis,* we used an allelic replacement technique to delete the *tolC* and *ftlC* genes from the genome of the LVS.

Through our characterization of the Δ*tolC* and Δ*ftlC* deletion mutants, we conclude that both the TolC and FtlC form part of the multidrug resistance machinery, while only the TolC appears to be a virulence determinant of *F. tularensis* as the Δ*tolC* strain was attenuated for virulence in the murine model of infection for both the intradermal and intranasal routes. Studies utilizing subspcies *novicida tolC* and *ftlC* transposon mutants obtained from the complete *F. novicida* transposon library (Gallagher et al., 2007) have brought us to the conclusion that both 1703 (*tolC*) and 0079 (*ftlC*) of *F. novicida* function similarly to the homologous genes in the LVS. In *F. novicida* both the TolC and FtlC function in multidrug efflux, while only TolC appears to be a major virulence determinant. We analyzed and compared the secretion of hemolysin from the wild-type U112, FTN_1703::Tn, FTN_0079::Tn, and FTN_1277::Tn and determined that all three TolC homologs of *F. novicida* do participate in hemolysin secretion. However, the TolC appears to be the most important for hemolysin secretion. This is the first evidence that TolC of *F. tularensis* participates in protein secretion.

In vivo organ burden assays with the LVS Δ*tolC* strain revealed that the deletion mutant is capable of systemic dissemination, as bacteria and pathology are observed in various reticuloendothelial organs. However, the deletion strain is defective for colonization of the organs, with CFU counts always 1 to 2 logs decreased when compared to the colonization of the wild-type LVS. The colonization defect of the Δ*tolC* mutant is most severe in the lungs of the infected animals, suggesting that the function of TolC may be more important in this particular organ. The aforementioned observations in regards to the *tolC* mutant hold true for both intradermal and intranasal murine infections.

In contrast to most other attenuated mutants of *F. tularensis* that have lost intracellular replication abilities, our tissue culture analysis shows that the Δ*tolC* mutant is able to replicate within murine and human macrophages, murine hepatocytes and human lung epithelial cells. Therefore, the role of the TolC in the pathogenesis of *F. tularensis* is not related to the ability to replicate intracellularly. In a previously published paper, the replication rate of *F. tularensis* was found to be directly proportional to the rate of LVS-induced host cell death (Lai and Sjostedt, 2003). In our studies, we found that induction of host cell death is not directly proportional to bacterial replication kinetics. The intracellular replication kinetics of the Δ*tolC* strain was consistently 1 to 2 logs less than the replication kinetics of the LVS inside murine macrophages and human lung epithelial cells and yet, the Δ*tolC* strain induced greater cell death in these cell types. In addition, we found that the Δ*tolC* mutant is hypercytotoxic to murine macrophages when compared to the toxicity of the LVS in murine macrophages. This data suggests that *F. tularensis* has the ability to inhibit induction of host cell death and that this ability is dependent upon TolC. A work previously published by Weiss et al., showed that two proteins produced by subspcies *novicida* function to inhibit or slow caspase-1 mediated cell death (Weiss et al., 2007a). In light of these observations, we analyzed if the induced cell death was apoptosis or pyroptosis. We concluded that the cell death induced by the LVS in murine macrophages is apoptosis, resulting in the activation of caspase-3. Thus, cell death was independent of caspase-1. Interestingly, when we infected human monocyte derived macrophages (huMDM), we again saw that the Δ*tolC* mutant was hypercytotoxic to these cells compared to cells infected with the LVS but this cell death was associated with the release of IL-1β, which signifies caspase-1 involvement. This

data suggests that the TolC of *F. tularensis* may function differently in different hosts. Additionally, we conclude that infection of huMDM with the Δ*tolC* strain elicits a significant increase in the amount of secreted chemokines CCL2 and CXCL8. This increased proimflammatory response elicited by the Δ*tolC* strain may contribute to the clearance of the pathogen in vivo.

Our hypothesis is that the intracellular replication of *F. tularensis* is essential to its overall pathogenesis. To ensure it has sufficient time to replicate intracellularly, *F. tularensis* actively inhibits or slows cell death. This inhibition of host cell death is dependent upon the OMP TolC, presumably by the secretion of a virulence factor(s). In addition, the LVS appears to actively suppress chemokine secretion and this suppression is dependent upon TolC. In the absence of TolC, the replicative niche of *F. tularensis* is lost, bacterial replication is hampered, and an increased proinflammatory response is mounted by the host. Ultimately, the host is able to successfully clear the pathogen.

II. Future Directions

Our data suggests that the TolC of *F. tularensis* is participating in the type I secretion of a virulence factor(s). Therefore, it is our goal to identify the secreted virulence factor(s). We have implemented a number of different strategies in our attempt to identify a TolC dependent secreted factor. Unfortunately, we have not yet identified any secreted factor, but our work thus far indicates that *F. tularensis* LVS is not secreting hemolysin, bile salts or siderophore via TolC nor is the TolC acting as the receptor for colicin. We would like to determine if the TolC is contributing to resistance to antimicrobial peptides by testing the *tolC* deletion mutants for sensitivity to peptides such as polymixin B. Our laboratory has been working hard to optimize *F. tularensis* secretion conditions. An effective secretion protocol will enable us to compare the secretion profile produced by wild-type LVS to the secretion profile produced by the Δ*tolC* mutant, with the hope of identifying a unique protein from the LVS profile that is missing from the Δ*tolC* profile. This protein can later be identified by mass spectrometry.

We believe the LVS is actively surpressing host cell death and expression of host proinflammatory chemokines. Therefore, it would be of intrest to determine if a co-infection of macrophages with LVS and Δ*tolC* could restore the induction of cell death or chemokines back to levels observed from infection with LVS alone. It would also be interesting to determine if conditioned media from macrophages infected with the LVS could reverse the phenotypes observed from macrophages infected with Δ*tolC* when added to the infection. Any reversal in phenotype would indicate that the virulence factor is indeed secreted via the TolC. In addition, we would like to assay infected murine and

human macrophages for secretion of IL-12, and IFN-γ since these cytokines are known to be crucial for host cell defense.

In *E. coli,* it is thought that the type I secretion machinery and TolC complex together only after initiation by the secreted substrate (Balakrishnan et al., 2001). Therefore, it is very important to identify the other protein that partners with TolC during type 1 secretion. Our work with the *F. novicida* transposon library has yielded some very promising results. We have identified both a periplasmic adaptor protein and an inner membrane protein that may associate with the TolC during multidrug efflux. This work is only in its preliminary stages, but we propose a coimmunoprecipitation (Co-IP) assay, using the polyclonal TolC and FtlC antibodies, described above, to isolate the entirely assembled type I secretion apparatus. Once the proteins are isolated they will be positively identified using mass spectrometry. This approach has been used in the past to identify protein secretion partners of the *E. coli* TolC (Letoffe et al., 1996). Additionally, we have isolated from the *F. novicida* transposon library the two mutants described by Weiss et al*.,* 2007, that are thought to actively inhibit host cell death. We are analyzing these mutants to determine if either of the proteins encoded by the respective genes are secreted via TolC.

It is important to note that, in addition to creating Δ*tolC* and Δ*ftlC* strains, a double deletion mutant strain, Δ*tolC*Δ*ftlC,* was created (data not shown). The Δ*tolC*Δ*ftlC* strain did not display heightened sensitivity to antibiotics above that of the single deletion mutants (data not shown). The *F. tularensis* genome contains a third TolC homolog. Based on the primary nucleotide sequence, this third TolC homolog is predicted to function as part of a multidrug efflux system. This would explain why the double mutant

does not exhibit an increase in drug sensitivity. Our data suggests that *tolC* and *ftlC* have in some instances overlapping substrate specificities, and they appear to compensate for each other when one is deleted or is non-functional. Thus, in regards to drug efflux, it is possible that the third TolC homolog *silC* functions as the major drug efflux pump and compensates for *tolC* and *ftlC* when they are absent from the genome. Further characterization of the double mutant is required; it would also be interesting to create and characterize a triple mutant.

Lastly, since an important goal of tularemia research is to identify and create a plausible vaccine candidate, we conducted an assay to see if the Δ*tolC* strain could provide protective immunity. Five C3H/Hen mice were intradermally infected with LVS, Δ*tolC*, or Δ*ftlC* at a dose of 2 x 10^5 CFU, or PBS was inoculated as a negative control; in previous publications this dose is shown to be sublethal (Conlan et al., 2003). The mice were monitored for a period of three months, during which time two of the five mice infected with the LVS died. All surviving mice were challenged by intradermal infection with the LVS at the lethal dose of 10^9 CFU. All mice challenged with the LVS survived with the exception of the control mice that received an initial inoculation of PBS. This experiment demonstrates that vaccination using the Δ*tolC* strain provides protective immunity against an intradermal LVS infection. Additional experiments will need to be conducted in collaboration with Public Health Research Institute (PHRI) to determine if the Δ*tolC* mutant provides protection against virulent type A strains. Based on these results and based on the fact that the LVS Δ*tolC* strain is able to replicate intracellularly, thus eliciting a strong cellular response from the host, the LVS Δ*tolC* strain is a compelling candidate for vaccine development.

Abd, H., Johansson, T., Golovliov, I., Sandstrom, G., and Forsman, M. (2003). Survival and growth of Francisella tularensis in Acanthamoeba castellanii. Appl Environ Microbiol *69*, 600-606.

Abu-Zant, A., Jones, S., Asare, R., Suttles, J., Price, C., Graham, J., and Kwaik, Y.A. (2007). Anti-apoptotic signalling by the Dot/Icm secretion system of L. pneumophila. Cell Microbiol *9*, 246-264.

Altschul, S.F., Gish, W., Miller, W., Myers, E.W., and Lipman, D.J. (1990). Basic local alignment search tool. J Mol Biol *215*, 403-410.

Andersen, C., Hughes, C., and Koronakis, V. (2000). Chunnel vision. Export and efflux through bacterial channel-tunnels. EMBO Rep *1*, 313-318.

Anthony, L.D., Burke, R.D., and Nano, F.E. (1991). Growth of Francisella spp. in rodent macrophages. Infect Immun *59*, 3291-3296.

Anthony, L.S., Ghadirian, E., Nestel, F.P., and Kongshavn, P.A. (1989). The requirement for gamma interferon in resistance of mice to experimental tularemia. Microb Pathog *7*, 421-428.

Atkins, H.S., Dassa, E., Walker, N.J., Griffin, K.F., Harland, D.N., Taylor, R.R., Duffield, M.L., and Titball, R.W. (2006). The identification and evaluation of ATP binding cassette systems in the intracellular bacterium Francisella tularensis. Res Microbiol *157*, 593-604.

Balagopal, A., MacFarlane, A.S., Mohapatra, N., Soni, S., Gunn, J.S., and Schlesinger, L.S. (2006). Characterization of the receptor-ligand pathways important for entry and survival of Francisella tularensis in human macrophages. Infect Immun *74*, 5114-5125.

Balakrishnan, L., Hughes, C., and Koronakis, V. (2001). Substrate-triggered recruitment of the TolC channel-tunnel during type I export of hemolysin by Escherichia coli. J Mol Biol *313*, 501-510.

Bar-Haim, E., Gat, O., Markel, G., Cohen, H., Shafferman, A., and Velan, B. (2008). Interrelationship between dendritic cell trafficking and Francisella tularensis dissemination following airway infection. PLoS Pathog *4*, e1000211.

Barker, J.H., Weiss, J., Apicella, M.A., and Nauseef, W.M. (2006). Basis for the failure of Francisella tularensis lipopolysaccharide to prime human polymorphonuclear leukocytes. Infect Immun *74*, 3277-3284.

Bazzocchi, C., Comazzi, S., Santoni, R., Bandi, C., Genchi, C., and Mortarino, M. (2007). Wolbachia surface protein (WSP) inhibits apoptosis in human neutrophils. Parasite Immunol *29*, 73-79.

Bendtsen, J.D., Nielsen, H., von Heijne, G., and Brunak, S. (2004). Improved prediction of signal peptides: SignalP 3.0. J Mol Biol *340*, 783-795.

Bergsbaken, T., Fink, S.L., and Cookson, B.T. (2009). Pyroptosis: host cell death and inflammation. Nat Rev Microbiol *7*, 99-109.

Bina, J.E., and Mekalanos, J.J. (2001). Vibrio cholerae tolC is required for bile resistance and colonization. Infect Immun *69*, 4681-4685.

Bingle, L.E., Bailey, C.M., and Pallen, M.J. (2008). Type VI secretion: a beginner's guide. Curr Opin Microbiol *11*, 3-8.

Bleuel, C., Grosse, C., Taudte, N., Scherer, J., Wesenberg, D., Krauss, G.J., Nies, D.H., and Grass, G. (2005). TolC is involved in enterobactin efflux across the outer membrane of Escherichia coli. J Bacteriol *187*, 6701-6707.

Bolger, C.E., Forestal, C.A., Italo, J.K., Benach, J.L., and Furie, M.B. (2005). The live vaccine strain of Francisella tularensis replicates in human and murine macrophages but induces only the human cells to secrete proinflammatory cytokines. J Leukoc Biol *77*, 893-897.

Bosio, C.M., Bielefeldt-Ohmann, H., and Belisle, J.T. (2007). Active suppression of the pulmonary immune response by Francisella tularensis Schu4. J Immunol *178*, 4538-4547.

Bosio, C.M., and Dow, S.W. (2005). Francisella tularensis induces aberrant activation of pulmonary dendritic cells. J Immunol *175*, 6792-6801.

Brotcke, A., and Monack, D.M. (2008). Identification of fevR, a novel regulator of virulence gene expression in Francisella novicida. Infect Immun *76*, 3473-3480.

Brotcke, A., Weiss, D.S., Kim, C.C., Chain, P., Malfatti, S., Garcia, E., and Monack, D.M. (2006). Identification of MglA-regulated genes reveals novel virulence factors in Francisella tularensis. Infect Immun *74*, 6642-6655.

Budihardjo, I., Oliver, H., Lutter, M., Luo, X., and Wang, X. (1999). Biochemical pathways of caspase activation during apoptosis. Annu Rev Cell Dev Biol *15*, 269-290.

Carr, M.W., Roth, S.J., Luther, E., Rose, S.S., and Springer, T.A. (1994). Monocyte chemoattractant protein 1 acts as a T-lymphocyte chemoattractant. Proc Natl Acad Sci U S A *91*, 3652-3656.

Celada, A., Gray, P.W., Rinderknecht, E., and Schreiber, R.D. (1984). Evidence for a gamma-interferon receptor that regulates macrophage tumoricidal activity. J Exp Med *160*, 55-74.

Chakraborty, S., Monfett, M., Maier, T.M., Benach, J.L., Frank, D.W., and Thanassi, D.G. (2008). Type IV pili in Francisella tularensis: roles of pilF and pilT in fiber assembly, host cell adherence, and virulence. Infect Immun *76*, 2852-2861.

Chamberlain, R.E. (1965). Evaluation of Live Tularemia Vaccine Prepared in a Chemically Defined Medium. Appl Microbiol *13*, 232-235.

Charity, J.C., Costante-Hamm, M.M., Balon, E.L., Boyd, D.H., Rubin, E.J., and Dove, S.L. (2007). Twin RNA polymerase-associated proteins control virulence gene expression in Francisella tularensis. PLoS Pathog *3*, e84.

Chase, J.C., Celli, J., and Bosio, C.M. (2009). Direct and indirect impairment of human dendritic cell function by virulent Francisella tularensis Schu S4. Infect Immun *77*, 180-195.

Cherwonogrodzky, J.W., Knodel, M.H., and Spence, M.R. (1994). Increased encapsulation and virulence of Francisella tularensis live vaccine strain (LVS) by subculturing on synthetic medium. Vaccine *12*, 773-775.

Chong, A., Wehrly, T.D., Nair, V., Fischer, E.R., Barker, J.R., Klose, K.E., and Celli, J. (2008). The early phagosomal stage of Francisella tularensis determines optimal phagosomal escape and Francisella pathogenicity island protein expression. Infect Immun *76*, 5488-5499.

Cianciotto, N.P. (2005). Type II secretion: a protein secretion system for all seasons. Trends Microbiol *13*, 581-588.

Clark, C.S., and Maurelli, A.T. (2007). Shigella flexneri inhibits staurosporine-induced apoptosis in epithelial cells. Infect Immun *75*, 2531-2539.

Clemens, D.L., Lee, B.Y., and Horwitz, M.A. (2004). Virulent and avirulent strains of Francisella tularensis prevent acidification and maturation of their phagosomes and escape into the cytoplasm in human macrophages. Infect Immun *72*, 3204-3217.

Clemens, D.L., Lee, B.Y., and Horwitz, M.A. (2005). Francisella tularensis enters macrophages via a novel process involving pseudopod loops. Infect Immun *73*, 5892-5902.

Cole, L.E., Elkins, K.L., Michalek, S.M., Qureshi, N., Eaton, L.J., Rallabhandi, P., Cuesta, N., and Vogel, S.N. (2006). Immunologic consequences of Francisella tularensis live vaccine strain infection: role of the innate immune response in infection and immunity. J Immunol *176*, 6888-6899.

Conlan, J.W., Chen, W., Shen, H., Webb, A., and KuoLee, R. (2003). Experimental tularemia in mice challenged by aerosol or intradermally with virulent strains of Francisella tularensis: bacteriologic and histopathologic studies. Microb Pathog *34*, 239-248.

Conlan, J.W., Shen, H., Webb, A., and Perry, M.B. (2002). Mice vaccinated with the O-antigen of Francisella tularensis LVS lipopolysaccharide conjugated to bovine serum albumin develop varying degrees of protective immunity against systemic or aerosol challenge with virulent type A and type B strains of the pathogen. Vaccine *20*, 3465-3471.

Conlan, J.W., Sjostedt, A., and North, R.J. (1994). CD4+ and CD8+ T-cell-dependent and -independent host defense mechanisms can operate to control and resolve primary and secondary Francisella tularensis LVS infection in mice. Infect Immun *62*, 5603-5607.

Davies, J.K., and Reeves, P. (1975). Genetics of resistance to colicins in Escherichia coli K-12: cross-resistance among colicins of group B. J Bacteriol *123*, 96-101.

de Bruin, O.M., Ludu, J.S., and Nano, F.E. (2007). The Francisella pathogenicity island protein IglA localizes to the bacterial cytoplasm and is needed for intracellular growth. BMC Microbiol *7*, 1.

Delepelaire, P. (2004). Type I secretion in gram-negative bacteria. Biochim Biophys Acta *1694*, 149-161.

Deng, K., Blick, R.J., Liu, W., and Hansen, E.J. (2006). Identification of Francisella tularensis genes affected by iron limitation. Infect Immun *74*, 4224-4236.

Dennis, D.T., Inglesby, T.V., Henderson, D.A., Bartlett, J.G., Ascher, M.S., Eitzen, E., Fine, A.D., Friedlander, A.M., Hauer, J., Layton, M.*, et al.* (2001). Tularemia as a biological weapon: medical and public health management. JAMA *285*, 2763-2773.

Elkins, K.L., Rhinehart-Jones, T.R., Culkin, S.J., Yee, D., and Winegar, R.K. (1996). Minimal requirements for murine resistance to infection with Francisella tularensis LVS. Infect Immun *64*, 3288-3293.

Ellis, J., Oyston, P.C., Green, M., and Titball, R.W. (2002). Tularemia. Clin Microbiol Rev *15*, 631-646.

Faherty, C.S., and Maurelli, A.T. (2008). Staying alive: bacterial inhibition of apoptosis during infection. Trends Microbiol *16*, 173-180.

Filloux, A. (2009). The type VI secretion system: a tubular story. EMBO J *28*, 309-310.

Forestal, C.A., Benach, J.L., Carbonara, C., Italo, J.K., Lisinski, T.J., and Furie, M.B. (2003). Francisella tularensis selectively induces proinflammatory changes in endothelial cells. J Immunol *171*, 2563-2570.

Forestal, C.A., Malik, M., Catlett, S.V., Savitt, A.G., Benach, J.L., Sellati, T.J., and Furie, M.B. (2007). Francisella tularensis has a significant extracellular phase in infected mice. J Infect Dis *196*, 134-137.

Forsman, M., Sandstrom, G., and Sjostedt, A. (1994). Analysis of 16S ribosomal DNA sequences of Francisella strains and utilization for determination of the phylogeny of the genus and for identification of strains by PCR. Int J Syst Bacteriol *44*, 38-46.

Fortier, A.H., Green, S.J., Polsinelli, T., Jones, T.R., Crawford, R.M., Leiby, D.A., Elkins, K.L., Meltzer, M.S., and Nacy, C.A. (1994). Life and death of an intracellular pathogen: Francisella tularensis and the macrophage. Immunol Ser *60*, 349-361.

Fortier, A.H., Polsinelli, T., Green, S.J., and Nacy, C.A. (1992). Activation of macrophages for destruction of Francisella tularensis: identification of cytokines, effector cells, and effector molecules. Infect Immun *60*, 817-825.

Foshay, L., Hesselbrock, W.H., Wittenberg, H.J., and Rodenberg, A.H. (1942). Vaccine Prophylaxis against Tularemia in Man. Am J Public Health Nations Health *32*, 1131-1145.

Fulop, M., Mastroeni, P., Green, M., and Titball, R.W. (2001). Role of antibody to lipopolysaccharide in protection against low- and high-virulence strains of Francisella tularensis. Vaccine *19*, 4465-4472.

Gallagher, L.A., Ramage, E., Jacobs, M.A., Kaul, R., Brittnacher, M., and Manoil, C. (2007). A comprehensive transposon mutant library of Francisella novicida, a bioweapon surrogate. Proc Natl Acad Sci U S A *104*, 1009-1014.

Gerlach, R.G., and Hensel, M. (2007). Protein secretion systems and adhesins: the molecular armory of Gram-negative pathogens. Int J Med Microbiol *297*, 401-415.

Gil, H., Benach, J.L., and Thanassi, D.G. (2004). Presence of pili on the surface of Francisella tularensis. Infect Immun *72*, 3042-3047.

Gil, H., Platz, G.J., Forestal, C.A., Monfett, M., Bakshi, C.S., Sellati, T.J., Furie, M.B., Benach, J.L., and Thanassi, D.G. (2006). Deletion of TolC orthologs in Francisella tularensis identifies roles in multidrug resistance and virulence. Proc Natl Acad Sci U S A *103*, 12897-12902.

Gioannini, T.L., Teghanemt, A., Zhang, D., Coussens, N.P., Dockstader, W., Ramaswamy, S., and Weiss, J.P. (2004). Isolation of an endotoxin-MD-2 complex that produces Toll-like receptor 4-dependent cell activation at picomolar concentrations. Proc Natl Acad Sci U S A *101*, 4186-4191.

Golovliov, I., Baranov, V., Krocova, Z., Kovarova, H., and Sjostedt, A. (2003a). An attenuated strain of the facultative intracellular bacterium Francisella tularensis can escape the phagosome of monocytic cells. Infect Immun *71*, 5940-5950.

Golovliov, I., Ericsson, M., Sandstrom, G., Tarnvik, A., and Sjostedt, A. (1997). Identification of proteins of Francisella tularensis induced during growth in macrophages and cloning of the gene encoding a prominently induced 23-kilodalton protein. Infect Immun *65*, 2183-2189.

Golovliov, I., Sjostedt, A., Mokrievich, A., and Pavlov, V. (2003b). A method for allelic replacement in Francisella tularensis. FEMS Microbiol Lett *222*, 273-280.

Grassme, H., Jendrossek, V., and Gulbins, E. (2001). Molecular mechanisms of bacteria induced apoptosis. Apoptosis *6*, 441-445.

Green, M., Choules, G., Rogers, D., and Titball, R.W. (2005). Efficacy of the live attenuated Francisella tularensis vaccine (LVS) in a murine model of disease. Vaccine *23*, 2680-2686.

Hager, A.J., Bolton, D.L., Pelletier, M.R., Brittnacher, M.J., Gallagher, L.A., Kaul, R., Skerrett, S.J., Miller, S.I., and Guina, T. (2006). Type IV pili-mediated secretion modulates Francisella virulence. Mol Microbiol *62*, 227-237.

Henry, T., Brotcke, A., Weiss, D.S., Thompson, L.J., and Monack, D.M. (2007). Type I interferon signaling is required for activation of the inflammasome during Francisella infection. J Exp Med *204*, 987-994.

Holland, I.B., Schmitt, L., and Young, J. (2005). Type 1 protein secretion in bacteria, the ABC-transporter dependent pathway (review). Mol Membr Biol *22*, 29-39.

Huang, A.J., Furie, M.B., Nicholson, S.C., Fischbarg, J., Liebovitch, L.S., and Silverstein, S.C. (1988). Effects of human neutrophil chemotaxis across human endothelial cell monolayers on the permeability of these monolayers to ions and macromolecules. J Cell Physiol *135*, 355-366.

Huntley, J.F., Conley, P.G., Hagman, K.E., and Norgard, M.V. (2007). Characterization of Francisella tularensis outer membrane proteins. J Bacteriol *189*, 561-574.

Huntley, J.F., Conley, P.G., Rasko, D.A., Hagman, K.E., Apicella, M.A., and Norgard, M.V. (2008). Native outer membrane proteins protect mice against pulmonary challenge with virulent type A Francisella tularensis. Infect Immun *76*, 3664-3671.

Knodler, L.A., Finlay, B.B., and Steele-Mortimer, O. (2005). The Salmonella effector protein SopB protects epithelial cells from apoptosis by sustained activation of Akt. J Biol Chem *280*, 9058-9064.

Koronakis, V., Eswaran, J., and Hughes, C. (2004). Structure and function of TolC: the bacterial exit duct for proteins and drugs. Annu Rev Biochem *73*, 467-489.

Koronakis, V., and Hughes, C. (1993). Bacterial signal peptide-independent protein export: HlyB-directed secretion of hemolysin. Semin Cell Biol *4*, 7-15.

Koronakis, V., Hughes, C., and Koronakis, E. (1993). ATPase activity and ATP/ADP-induced conformational change in the soluble domain of the bacterial protein translocator HlyB. Mol Microbiol *8*, 1163-1175.

Koronakis, V., Sharff, A., Koronakis, E., Luisi, B., and Hughes, C. (2000). Crystal structure of the bacterial membrane protein TolC central to multidrug efflux and protein export. Nature *405*, 914-919.

Lai, X.H., Golovliov, I., and Sjostedt, A. (2004). Expression of IglC is necessary for intracellular growth and induction of apoptosis in murine macrophages by Francisella tularensis. Microb Pathog *37*, 225-230.

Lai, X.H., and Sjostedt, A. (2003). Delineation of the molecular mechanisms of Francisella tularensis-induced apoptosis in murine macrophages. Infect Immun *71*, 4642-4646.

Lai, X.H., Wang, S.Y., Edebro, H., and Sjostedt, A. (2003). Francisella strains express hemolysins of distinct characteristics. FEMS Microbiol Lett *224*, 91-95.

Larsson, P., Oyston, P.C., Chain, P., Chu, M.C., Duffield, M., Fuxelius, H.H., Garcia, E., Halltorp, G., Johansson, D., Isherwood, K.E.*, et al.* (2005). The complete genome sequence of Francisella tularensis, the causative agent of tularemia. Nat Genet *37*, 153-159.

Lauriano, C.M., Barker, J.R., Nano, F.E., Arulanandam, B.P., and Klose, K.E. (2003). Allelic exchange in Francisella tularensis using PCR products. FEMS Microbiol Lett *229*, 195-202.

Lauriano, C.M., Barker, J.R., Yoon, S.S., Nano, F.E., Arulanandam, B.P., Hassett, D.J., and Klose, K.E. (2004). MglA regulates transcription of virulence factors necessary for

Francisella tularensis intraamoebae and intramacrophage survival. Proc Natl Acad Sci U S A *101*, 4246-4249.

Letoffe, S., Delepelaire, P., and Wandersman, C. (1996). Protein secretion in gram-negative bacteria: assembly of the three components of ABC protein-mediated exporters is ordered and promoted by substrate binding. EMBO J *15*, 5804-5811.

Lilo, S., Zheng, Y., and Bliska, J.B. (2008). Caspase-1 activation in macrophages infected with Yersinia pestis KIM requires the type III secretion system effector YopJ. Infect Immun *76*, 3911-3923.

LoVullo, E.D., Sherrill, L.A., Perez, L.L., and Pavelka, M.S., Jr. (2006). Genetic tools for highly pathogenic Francisella tularensis subsp. tularensis. Microbiology *152*, 3425-3435.

Ludu, J.S., de Bruin, O.M., Duplantis, B.N., Schmerk, C.L., Chou, A.Y., Elkins, K.L., and Nano, F.E. (2008). The Francisella pathogenicity island protein PdpD is required for full virulence and associates with homologues of the type VI secretion system. J Bacteriol *190*, 4584-4595.

Maier, T.M., Havig, A., Casey, M., Nano, F.E., Frank, D.W., and Zahrt, T.C. (2004). Construction and characterization of a highly efficient Francisella shuttle plasmid. Appl Environ Microbiol *70*, 7511-7519.

Malik, M., Bakshi, C.S., Sahay, B., Shah, A., Lotz, S.A., and Sellati, T.J. (2006). Toll-like receptor 2 is required for control of pulmonary infection with Francisella tularensis. Infect Immun *74*, 3657-3662.

Marchler-Bauer, A., and Bryant, S.H. (2004). CD-Search: protein domain annotations on the fly. Nucleic Acids Res *32*, W327-331.

Mariathasan, S., Weiss, D.S., Dixit, V.M., and Monack, D.M. (2005). Innate immunity against Francisella tularensis is dependent on the ASC/caspase-1 axis. J Exp Med *202*, 1043-1049.

Massari, P., Ho, Y., and Wetzler, L.M. (2000). Neisseria meningitidis porin PorB interacts with mitochondria and protects cells from apoptosis. Proc Natl Acad Sci U S A *97*, 9070-9075.

McCleery, D.R., and Rowe, M.T. (1995). Development of a selective plating technique for the recovery of Escherichia coli O157:H7 after heat stress. Lett Appl Microbiol *21*, 252-256.

McLendon, M.K., Apicella, M.A., and Allen, L.A. (2006). Francisella tularensis: taxonomy, genetics, and Immunopathogenesis of a potential agent of biowarfare. Annu Rev Microbiol *60*, 167-185.

Meibom, K.L., Forslund, A.L., Kuoppa, K., Alkhuder, K., Dubail, I., Dupuis, M., Forsberg, A., and Charbit, A. (2009). Hfq, a novel pleiotropic regulator of virulence-associated genes in Francisella tularensis. Infect Immun *77*, 1866-1880.

Milton, D.L., O'Toole, R., Horstedt, P., and Wolf-Watz, H. (1996). Flagellin A is essential for the virulence of Vibrio anguillarum. J Bacteriol *178*, 1310-1319.

Modi, W.S., Dean, M., Seuanez, H.N., Mukaida, N., Matsushima, K., and O'Brien, S.J. (1990). Monocyte-derived neutrophil chemotactic factor (MDNCF/IL-8) resides in a gene cluster along with several other members of the platelet factor 4 gene superfamily. Hum Genet *84*, 185-187.

Mohapatra, N.P., Soni, S., Bell, B.L., Warren, R., Ernst, R.K., Muszynski, A., Carlson, R.W., and Gunn, J.S. (2007). Identification of an orphan response regulator required for the virulence of Francisella spp. and transcription of pathogenicity island genes. Infect Immun *75*, 3305-3314.

Nano, F.E., and Schmerk, C. (2007). The Francisella pathogenicity island. Ann N Y Acad Sci *1105*, 122-137.

Nano, F.E., Zhang, N., Cowley, S.C., Klose, K.E., Cheung, K.K., Roberts, M.J., Ludu, J.S., Letendre, G.W., Meierovics, A.I., Stephens, G.*, et al.* (2004). A Francisella

tularensis pathogenicity island required for intramacrophage growth. J Bacteriol *186*, 6430-6436.

Ohara, Y., Sato, T., Fujita, H., Ueno, T., and Homma, M. (1991). Clinical manifestations of tularemia in Japan--analysis of 1,355 cases observed between 1924 and 1987. Infection *19*, 14-17.

Oyston, P.C., Sjostedt, A., and Titball, R.W. (2004). Tularaemia: bioterrorism defence renews interest in Francisella tularensis. Nat Rev Microbiol *2*, 967-978.

Pavlov, V.M., Mokrievich, A.N., and Volkovoy, K. (1996). Cryptic plasmid pFNL10 from Francisella novicida-like F6168: the base of plasmid vectors for Francisella tularensis. FEMS Immunol Med Microbiol *13*, 253-256.

Priefer, U.B., Simon, R., and Puhler, A. (1985). Extension of the host range of Escherichia coli vectors by incorporation of RSF1010 replication and mobilization functions. J Bacteriol *163*, 324-330.

Pukatzki, S., McAuley, S.B., and Miyata, S.T. (2009). The type VI secretion system: translocation of effectors and effector-domains. Curr Opin Microbiol *12*, 11-17.

Rasmussen, J.W., Cello, J., Gil, H., Forestal, C.A., Furie, M.B., Thanassi, D.G., and Benach, J.L. (2006). Mac-1+ cells are the predominant subset in the early hepatic lesions of mice infected with Francisella tularensis. Infect Immun *74*, 6590-6598.

Reilly, T.J., Baron, G.S., Nano, F.E., and Kuhlenschmidt, M.S. (1996). Characterization and sequencing of a respiratory burst-inhibiting acid phosphatase from Francisella tularensis. J Biol Chem *271*, 10973-10983.

Reyrat, J.M., Pelicic, V., Gicquel, B., and Rappuoli, R. (1998). Counterselectable markers: untapped tools for bacterial genetics and pathogenesis. Infect Immun *66*, 4011-4017.

Rodriguez, S.A., Davis, G., and Klose, K.E. (2009). Targeted gene disruption in Francisella tularensis by group II introns. Methods.

Sandstrom, G., Lofgren, S., and Tarnvik, A. (1988). A capsule-deficient mutant of Francisella tularensis LVS exhibits enhanced sensitivity to killing by serum but diminished sensitivity to killing by polymorphonuclear leukocytes. Infect Immun *56*, 1194-1202.

Sandstrom, G., Sjostedt, A., Johansson, T., Kuoppa, K., and Williams, J.C. (1992). Immunogenicity and toxicity of lipopolysaccharide from Francisella tularensis LVS. FEMS Microbiol Immunol *5*, 201-210.

Schwyn, B., and Neilands, J.B. (1987). Universal chemical assay for the detection and determination of siderophores. Anal Biochem *160*, 47-56.

Shrivastava, S., and Mande, S.S. (2008). Identification and functional characterization of gene components of Type VI Secretion system in bacterial genomes. PLoS One *3*, e2955.

Steinemann, T.L., Sheikholeslami, M.R., Brown, H.H., and Bradsher, R.W. (1999). Oculoglandular tularemia. Arch Ophthalmol *117*, 132-133.

Stewart, S.J. (1996). Tularemia: association with hunting and farming. FEMS Immunol Med Microbiol *13*, 197-199.

Sullivan, J.T., Jeffery, E.F., Shannon, J.D., and Ramakrishnan, G. (2006). Characterization of the siderophore of Francisella tularensis and role of fslA in siderophore production. J Bacteriol *188*, 3785-3795.

Svensson, K., Larsson, P., Johansson, D., Bystrom, M., Forsman, M., and Johansson, A. (2005). Evolution of subspecies of Francisella tularensis. J Bacteriol *187*, 3903-3908.

Tarnvik, A. (1989). Nature of protective immunity to Francisella tularensis. Rev Infect Dis *11*, 440-451.

Tarnvik, A., and Berglund, L. (2003). Tularaemia. Eur Respir J *21*, 361-373.

Tatusov, R.L., Galperin, M.Y., Natale, D.A., and Koonin, E.V. (2000). The COG database: a tool for genome-scale analysis of protein functions and evolution. Nucleic Acids Res *28*, 33-36.

Telepnev, M., Golovliov, I., Grundstrom, T., Tarnvik, A., and Sjostedt, A. (2003). Francisella tularensis inhibits Toll-like receptor-mediated activation of intracellular signalling and secretion of TNF-alpha and IL-1 from murine macrophages. Cell Microbiol *5*, 41-51.

Telepnev, M., Golovliov, I., and Sjostedt, A. (2005). Francisella tularensis LVS initially activates but subsequently down-regulates intracellular signaling and cytokine secretion in mouse monocytic and human peripheral blood mononuclear cells. Microb Pathog *38*, 239-247.

Thakran, S., Li, H., Lavine, C.L., Miller, M.A., Bina, J.E., Bina, X.R., and Re, F. (2008). Identification of Francisella tularensis lipoproteins that stimulate the toll-like receptor (TLR) 2/TLR1 heterodimer. J Biol Chem *283*, 3751-3760.

Thanabalu, T., Koronakis, E., Hughes, C., and Koronakis, V. (1998). Substrate-induced assembly of a contiguous channel for protein export from E.coli: reversible bridging of an inner-membrane translocase to an outer membrane exit pore. EMBO J *17*, 6487-6496.

Thanassi, D.G., and Hultgren, S.J. (2000). Multiple pathways allow protein secretion across the bacterial outer membrane. Curr Opin Cell Biol *12*, 420-430.

Thompson, J.D., Higgins, D.G., and Gibson, T.J. (1994). CLUSTAL W: improving the sensitivity of progressive multiple sequence alignment through sequence weighting, position-specific gap penalties and weight matrix choice. Nucleic Acids Res *22*, 4673-4680.

Tigertt, W.D. (1962). Soviet viable Pasteurella tularensis vaccines. A review of selected articles. Bacteriol Rev *26*, 354-373.

Vaara, M., and Nurminen, M. (1999). Outer membrane permeability barrier in Escherichia coli mutants that are defective in the late acyltransferases of lipid A biosynthesis. Antimicrob Agents Chemother *43*, 1459-1462.

Vediyappan, G., Borisova, T., and Fralick, J.A. (2006). Isolation and characterization of VceC gain-of-function mutants that can function with the AcrAB multiple-drug-resistant efflux pump of Escherichia coli. J Bacteriol *188*, 3757-3762.

Watanabe, T., Furuse, C., and Sakaizumi, S. (1968). Transduction of various R factors by phage P1 in Escherichia coli and by phage P22 in Salmonella typhimurium. J Bacteriol *96*, 1791-1795.

Weiss, D.S., Brotcke, A., Henry, T., Margolis, J.J., Chan, K., and Monack, D.M. (2007a). In vivo negative selection screen identifies genes required for Francisella virulence. Proc Natl Acad Sci U S A *104*, 6037-6042.

Weiss, D.S., Henry, T., and Monack, D.M. (2007b). Francisella tularensis: activation of the inflammasome. Ann N Y Acad Sci *1105*, 219-237.

Woolard, M.D., Hensley, L.L., Kawula, T.H., and Frelinger, J.A. (2008). Respiratory Francisella tularensis live vaccine strain infection induces Th17 cells and prostaglandin E2, which inhibits generation of gamma interferon-positive T cells. Infect Immun *76*, 2651-2659.

Yanisch-Perron, C., Vieira, J., and Messing, J. (1985). Improved M13 phage cloning vectors and host strains: nucleotide sequences of the M13mp18 and pUC19 vectors. Gene *33*, 103-119.

Zgurskaya, H.I., and Nikaido, H. (1999). Bypassing the periplasm: reconstitution of the AcrAB multidrug efflux pump of Escherichia coli. Proc Natl Acad Sci U S A *96*, 7190-7195.

Zogaj, X., Chakraborty, S., Liu, J., Thanassi, D.G., and Klose, K.E. (2008). Characterization of the Francisella tularensis subsp. novicida type IV pilus. Microbiology *154*, 2139-2150.